Université de Montréal

Assessing microvascular function with breathing maneuvers: an oxygenation-sensitive CMR study

par
Kady Fischer

Sciences Biomédicales
Faculté de Médicine

Thèse présentée à la Faculté de Médicine
en vue de l'obtention du grade de doctorat
en Sciences Biomédicales
option général

Juin, 2016

Résumé

Ce projet illustre cinq études, mettant l'emphase sur le développement d'une nouvelle approche diagnostique cardiovasculaire afin d'évaluer le niveau d'oxygène contenu dans le myocarde ainsi que sa fonction microvasculaire. En combinant une séquence de résonance magnétique cardiovasculaire (RMC) pouvant détecter le niveau d'oxygène (OS), des manœuvres respiratoires ainsi que des analyses de gaz artériels peuvent être utilisés comme procédure non invasive destinée à induire une réponse vasoactive afin d'évaluer la réserve d'oxygénation, une mesure clé de la fonction vasculaire.

Le nombre de tests diagnostiques cardiaques prescrits ainsi que les interventions, sont en pleine expansion[1]. L'imagerie et tests non invasifs sont souvent effectués avant l'utilisation de procédures invasives. L'imagerie cardiaque permet d'évaluer la présence ou absence de sténoses coronaires, un important facteur économique dans notre système de soins de santé [2]. Les techniques d'imagerie non invasives fournissent de l'information précise afin d'identifier la présence et l'emplacement du déficit de perfusion chez les patients présentant des symptômes d'ischémie myocardique. Néanmoins, plusieurs techniques actuelles requièrent la nécessité de radiation, d'agents de contraste ou traceurs, sans oublier des protocoles de stress pharmacologiques ou physiques. L'imagerie RMC peut identifier une sténose coronaire significative sans radiation. De nouvelles tendances d'utilisation de RMC visent à développer des techniques diagnostiques qui ne requièrent aucun facteur de stress pharmacologiques ou d'agents de contraste.

L'objectif principal de ce projet était de développer et tester une nouvelle technique diagnostique afin d'évaluer la fonction vasculaire coronarienne en utilisant l' OS-RMC, en combinaison avec des manœuvres respiratoires comme stimulus vasoactif. Ensuite, les objectifs, secondaires étaient d'utilisés l'OS-RMC pour évaluer l'oxygénation du myocarde et la réponse coronaire en présence de gaz artériels altérés. Suite aux manœuvres respiratoires la réponse vasculaire a été validée chez un modèle animal pour ensuite être utilisé chez deux volontaires sains et finalement dans une population de patients atteints de maladies cardiovasculaires.

Chez le modèle animal, les manœuvres respiratoires ont pu induire un changement significatif, mesuré intrusivement par débit sanguin coronaire. Il a été démontré qu'en présence d'une

sténose coronarienne hémodynamiquement significative, l'OS-RMC pouvait détecter un déficit en oxygène du myocarde. Chez l'homme sain, l'application de cette technique en comparaison avec l'adénosine (l'agent standard) pour induire une vasodilatation coronarienne et les manœuvres respiratoires ont pu induire une réponse plus significative en oxygénation dans un myocarde sain. Finalement, nous avons utilisé les manœuvres respiratoires parmi un groupe de patients atteint de maladies coronariennes. Leurs myocardes étant altérées par une sténose coronaire, en conséquence modifiant ainsi leur réponse en oxygénation. Par la suite nous avons évalué les effets des gaz artériels sanguins sur l'oxygénation du myocarde. Ils démontrent que la réponse coronarienne est atténuée au cours de l'hyperoxie, suite à un stimuli d'apnée. Ce phénomène provoque une réduction globale du débit sanguin coronaire et un déficit d'oxygénation dans le modèle animal ayant une sténose lorsqu'un supplément en oxygène est donné.

En conclusion, ce travail a permis d'améliorer notre compréhension des nouvelles techniques diagnostiques en imagerie cardiovasculaire. Par ailleurs, nous avons démontré que la combinaison de manœuvres respiratoires et l'imagerie OS-RMC peut fournir une méthode non-invasive et rentable pour évaluer la fonction vasculaire coronarienne régionale et globale.

Mots-clés : Oxygénation sensible ▪ RMC (résonance magnétique cardiovasculaire) ▪ BOLD (blood oxygen level-dependent) ▪ Adénosine ▪ Vasodilatation ▪ Vasoconstriction ▪ Hyperoxie

Abstract

This project encompasses five studies, which focus on developing a new cardiovascular diagnostic approach for assessing myocardial oxygenation and microvascular function. In combination with oxygenation-sensitive cardiovascular magnetic resonance (OS-CMR) imaging, breathing maneuvers and altered arterial blood gases can be used as a non-invasive method for inducing a vasoactive response to test the oxygenation reserve, a key measurement in vascular function.

The number of prescribed cardiac diagnostic tests and interventions is rapidly growing[1]. In particular, imaging and other non-invasive tests are frequently performed prior to invasive procedures. One of the most common uses of cardiac imaging is for the diagnosis of significant coronary artery stenosis, a critical cost factor in today's health care system[2]. Non-invasive imaging techniques provide the most reliable information for the presence and location of perfusion or oxygenation deficits in patients with symptoms suggestive of myocardial ischemia, yet many current techniques suffer from the need for radiation, contrast agents or tracers, and pharmacological or physical stress protocols. CMR imaging can identify significant coronary artery stenosis without radiation and new trends in CMR research aim to develop diagnostic techniques that do not require any pharmacological stressors or contrast agents.

For this project, the primary aim was to develop and test a new diagnostic technique to assess coronary vascular function using OS-CMR in combination with breathing maneuvers as the vasoactive stimulus. Secondary aims then used OS-CMR to assess myocardial oxygenation and the coronary response in the presence of altered arterial blood gases.

An animal model was used to validate the vascular response to breathing maneuvers before translating the technique to human subjects into both healthy volunteers, and a patient population with cardiac disease.

In the animal models, breathing maneuvers could induce a significant change in invasively measured coronary blood flow and it was demonstrated that in the presence of a

haemodynamically significant coronary stenosis, OS-CMR could detect a myocardial oxygen deficit. This technique was then applied in a human model, with healthy participants. In a direct comparison to the infusion of the coronary vasodilator adenosine, which is considered a standard agent for inducing vasodilation in cardiac imaging, breathing maneuvers induced a stronger response in oxygenation of healthy myocardium. The final study then implemented the breathing maneuvers in a patient population with coronary artery disease; in which myocardium compromised by a coronary stenosis had a compromised oxygenation response. Furthermore, the observed effects of arterial blood gases on myocardial oxygenation were assessed. This demonstrated that the coronary response to breath-hold stimuli is attenuated during hyperoxia, and this causes an overall reduction in coronary blood flow, and consequently an oxygenation deficit in a coronary stenosis animal model when supplemental oxygen is provided.

In conclusion, this work has improved our understanding of potential new diagnostic techniques for cardiovascular imaging. In particular, it demonstrated that combining breathing maneuvers with oxygenation-sensitive CMR can provide a non-invasive and cost-effective method for assessing global and regional coronary vascular function.

Keywords: Oxygenation-sensitive ▪ CMR (cardiovascular magnetic resonance) ▪ BOLD (blood oxygen level-dependent) ▪ Adenosine ▪ Vasodilation ▪ Vasoconstriction ▪ Hyperoxia

Table of Contents

List of Tables

List of Figures

List of Abbreviations & Acronyms

ACC	American College of Cardiology
ACE	Angiotensin-Converting Enzyme
AHA	American Heart Association
ANOVA	Analysis of Variance
AT2-R	Angiotensin-II Receptor
ATP	Adenosine Tri-Phosphate
AV	Atrioventricular
b-SSFP	Balanced Steady State Free Procession
BMI	Body Mass Index
BOLD	Blood Oxygen Level-Dependent
bpm	Beats Per Minute
BSA	Body Surface Area
BP	Blood Pressure
CAD	Coronary Artery Disease
caO_2	Arterial Oxygen Content
$ccsO_2$	Coronary Sinus Oxygen Content
CMR	Cardiovascular Magnetic Resonance (fr. *RMC*)
CMVD	Coronary Microvascular Disease
CO	Cardiac Output
CO_2	Carbon Dioxide
CROSB	Cardiovascular Response of Oxygenation in Swine Breathing
CT	Computed Tomography
dHb	Deoxyhaemoglobin
ECG	Electrocardiogram
EDV	End Diastolic Volume
EF	Ejection Fraction
ESV	End Systolic Volume
F	French
FA	Flip Angle
FAME	Fractional Flow Reserve versus Angiography for Guiding PCI in Patients with Multivessel Coronary Artery Disease trial
FiO_2	Inspiratory Fraction of Oxygen
FFR	Fractional Flow Reserve
GFR	Glomerular Filtration Rate
^1H	Hydrogen proton
Hb	Haemoglobin
HMR	Haemodynamic Microvascular Resistance
HR	Heart Rate
HV	Hyperventilation
HVBH	Hyperventilation Breath-Hold
ICU	Intensive Care Unit
i.m.	Intramuscular
IMR	Index of Microvascular Resistance
i.v.	Intravenous
K_{ATP}	Adenosine Triphosphate sensitive Potassium channel
LAD	Left Anterior Descending coronary artery
LAX	Long-Axis

LCx	Left Circumflex coronary artery
LBH	Long Breath-Hold
LOE	Level of Evidence
LV	Left Ventricle
MBG	Myocardial Blushing Grade
mmHg	Millimeter of Mercury
MOLLI	MOdified Look Locker Inversion
MPS	Myocardial Perfusion Scintigraphy
MRI	Magnetic Resonance Imaging
NMR	Nuclear Magnetic Resonance
NO	Nitrous Oxide
O_2	Oxygen
O_2er	Oxygen Extraction Rate
OS	Oxygenation-Sensitive (fr. *Oxygénation-Sensible*)
OSAS	Obstructive Sleep Apnea Syndrome
P50	Partial pressure at which 50% is desaturated
p	Partial Pressure
pA	Alveolar Partial Pressure
pa	Arterial Partial Pressure
PCI	Percutaneous Coronary Intervention
pcs	Coronary Sinus Partial Pressure
PET	Positron Emission Tomography
QCA	Quantitative Coronary Angiography
RCA	Right Coronary Artery
RF	Radiofrequency
RMC	Résonance Magnétique Cardiovasculaire (en. *CMR*)
ROSC	Return of Spontaneous Circulation
RPP	Rate Pressure Product
SA	Sinoatrial
SaO_2	Arterial Haemoglobin Saturation
SAX	Short-Axis
SD	Standard Deviation
SEM	Standard Error of Mean
SI	Signal Intensity
SI_{BP}[%]	Signal Intensity of the Blood Pool
SPECT	Single Photon Emission Computed Tomography
SpO_2	Peripheral Arterial Oxygen Saturation
SSFP	Steady State Free Procession
STIR	Short Tau Inversion Recovery
SV	Stroke Volume
T	Tesla
TE	Echo Time
TIMI	Thrombolysis in Myocardial Infarction score
TR	Temporal Resolution

Dedications and Acknowledgments

The work put into this thesis and all the studies composing it, is a result of many collaborations and could not have been done without the support of plenty of individuals.

Firstly I would like to thank my supervisor Dr. Matthias Friedrich, and Dr. Dominik Guensch for inviting me to take part in this exciting process. Both have spent many hours providing mentorship and support over the years, guiding me through my studies and into becoming a researcher. Ich bedanke mich für die Geduld, die sie mit mir hatten und für die Jahre der Zusammenarbeit, die man mir ermöglichte, obwohl ich die meiste Zeit nur von Eishockey geredet habe. Ihre Führung und Leitung hat mir nicht nur bei meiner wissenschaftlichen Arbeit geholfen, sondern mich auch für meine berufliche Weiterentwicklung vorbereitet.

Thank you to all the research partners and co-authors, who have been essential in the success of these studies, starting in Calgary with all of those who initially helped to develop the idea used in the thesis, and introduced me to research during my undergrad degree. The majority of studies could not have been done without the many people of the Philippa and Marvin Carsley CMR Research Centre at the Montreal Heart Institute. Particular thanks to the surgical skills of Julie Lebel who was vital for the animal studies, and to those people who had a major participating role in the studies, Nancy Shie, Stefan Huettenmoser, Gobinath Nadeshalingham, Janelle Yu and Camilo Molina. For providing mentorship, I would like to acknowledge Tiago Teixeira, Tarik Hafyane, and my graduate committee. Additionally, these projects were made possible by the collaborations with Siemens developers who developed the MRI sequences.

One of my favourite experiences was being able to live in Switzerland and conduct my studies in this very beautiful country. So I am very grateful to the people at the Inselspital in Bern Switzerland, in particular to Dr. Dominik Guensch, and Prof. Balthasar Eberle of the anaesthesia department who made this possible. And for the great experiences, I thank all the other people in the many departments I unofficially belonged to, especially the DIPR office.

Furthermore, on a personal note, during these in the stressful times I thank the Dennis Wideman Shootout Fail youtube clip for providing great stress relief through the years. And I am also very appreciative of the Canadian National Hockey teams for retaining the Olympic gold medal throughout my degree; this has brought me so much joy to fall back on.

And finally, I would like to acknowledge my family, my mother, grandparents and others, for all their support during my many years of schooling. This is especially true for Gage, Rudi and Bri, who have been very patient, even though I have been far away from home.

Objectives

Overall Objective: Investigate the utility of breathing maneuvers as a technique to assess coronary vascular function and myocardial oxygenation in combination with cardiovascular magnetic resonance.

This project has been organized into three parts:

Part 1: Animal Model

Chapter 1: Validate if breathing maneuvers can identify myocardial oxygenation deficits in the presence of a haemodynamically significant coronary artery stenosis, in relationship to coronary blood flow and blood gas measurements

Chapter 2: Evaluate the breath-hold stimulus on coronary flow in the presence of altered arterial blood gases

Chapter 3: Assess the effects of hyperoxia on myocardial oxygenation

Part 2: Translation to Healthy Humans

Chapter 4: Test the effect of breathing maneuvers on myocardial oxygenation in comparison to a standard pharmacological vasodilation protocol

Part 3: Validation in a Cardiac Patient Population

Chapter 5: Assessing the feasibility of using breathing maneuvers to detect ischemia in coronary artery disease

0 Introduction

In Canada, cardiovascular diseases account for more than 30% of deaths, with coronary artery disease (CAD) accounting for more than half of them[3]. This trend is not unique for Canada, as European nations report that more than 40% of deaths are due to cardiovascular diseases, in particular due to coronary artery disease[4]. As a result, most cardiac exams look for the presence of coronary artery disease. Coronary artery disease is often diagnosed through anatomical or functional assessment in the setting of an invasive coronary angiography. Quantitative coronary angiography (QCA) visually assesses the anatomical appearance of coronary arteries and quantifies the degree of luminal narrowing, while fractional flow reserve (FFR) assesses the haemodynamic impact of a given stenosis. FFR determines the effect of a stenosis on the coronary flow by assessing the pressure difference distal and proximal to the stenosis, independent of the degree of the blockage. FFR is currently considered the gold standard for assessing the severity of coronary disease and its suitability for mechanical revascularisation. However, both these exams only address the patency of coronary epicardial vessels, and do not allow for assessing the impact on the actual oxygenation status of the myocardial tissue. Thus imaging modalities such as cardiovascular magnetic resonance (CMR), positron emission tomography (PET), and single photon emission computed tomography (SPECT) have developed techniques to look at coronary vascular function in relation to the myocardial tissue. A recent cost analysis in the United Kingdom reported the most cost-efficient method was to perform contrast enhanced CMR prior to any revascularization[5]. It is essential to keep developing this pathway to better understand ischemic cardiomyopathies, and to improve diagnostic testing.

0.1 Introduction to CMR

Magnetic resonance for clinical application in the heart was introduced in the early 1980's[6]. While initially, CMR was used to visualize anatomical features, advances of the modality have resulted in many ways to assess myocardial tissue characteristics, flow, and contractile function. Multiple clinical issues can be addressed in one exam, reducing the need

for multiple testing. These images are obtained using specific software settings defining the precise execution of the MR during a scan. These are MRI sequences, with specific settings called parameters.

The Basics of the MRI Signal

The source of the MR signals that eventually form the images, stems from the magnetic properties of protons and their movements in the strong external magnetic field. Because the hydrogen protons (^{1}H) are very abundant in the human body, ^{1}H is typically used for in vivo MR imaging. Due to its unpaired proton, the hydrogen nucleus behaves as a tiny spinning magnet, producing its own magnetic field, called spins. At equilibrium, these spins are in random direction, but when exposed to the magnetic field of the scanner, the spins align in parallel and anti-parallel formation in the direction to the field (z-axis, Figure 1B). While aligned, the protons precess like a spinning top around the longitudinal axis of the main magnetic field. The rotation of each proton is in phase with each other, and with a frequency proportional to the magnetic field strength (Larmor Frequency; 128MHz at 3T). A slight imbalance between the numbers of protons aligning in each direction results in a local net magnetization (Figure 1). This alignment occurs by entering the static magnetic field of the MRI.

To acquire specific images, MR scanner systems will generate a secondary magnetic field, using magnetic field gradients and radiofrequency (RF) electromagnetic pulses matching the Larmor Frequency of the proton spins so a tissue volume can be selectively excited. These processes work together to alter the local magnetization. The gradient systems induce small variations of the magnetic field and hence the frequency, which allows for localizing the signal in the large field. When exposed to the RF pulses, and the net magnetization is tipped in a different angle away from the direction of the primary magnetic field away from z-axis (Figure 1C) and the atoms exhibit a resonant behaviour. After these pulses are turned off, the MRI signal is then acquired from the release of energy or the rate of relaxation as the protons move out of phase with one another and come back to equilibrium. This relaxation can be separated into two major relaxation components, the longitudinal relaxation time, T1 (Figure

1E, along the z-axis), and transverse relaxation time, T2 (Figure 1D, x-y direction). The transverse relaxation is also highly dependent on local inhomogeneities. The resulting time is called T2*. The combination of these three processes (T1, T2 and T2*) forms the basis of the majority of CMR sequences, and MR protocols can be fine-tuned to exploit the differences of relaxation properties in tissue.

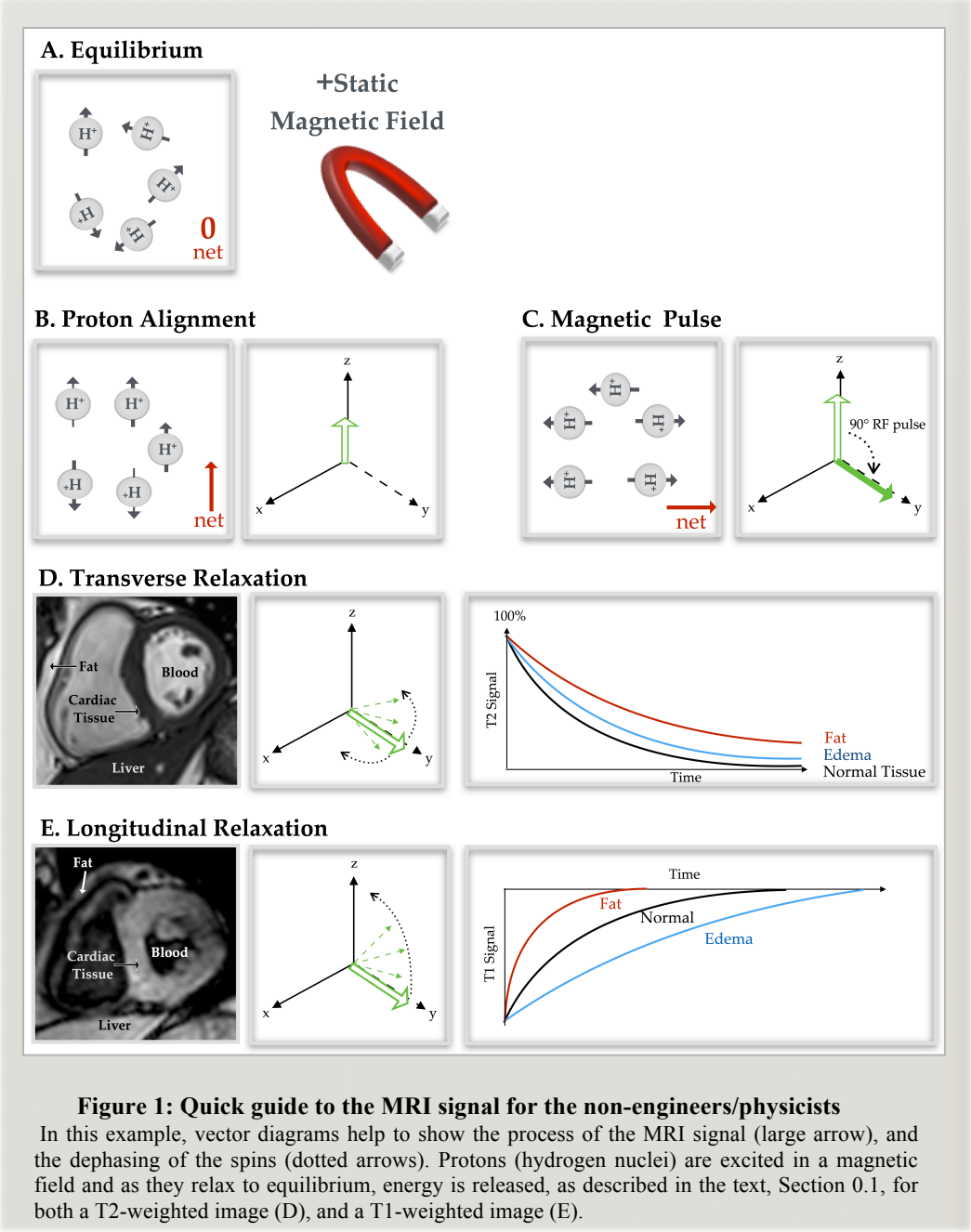

Figure 1: Quick guide to the MRI signal for the non-engineers/physicists
In this example, vector diagrams help to show the process of the MRI signal (large arrow), and the dephasing of the spins (dotted arrows). Protons (hydrogen nuclei) are excited in a magnetic field and as they relax to equilibrium, energy is released, as described in the text, Section 0.1, for both a T2-weighted image (D), and a T1-weighted image (E).

Figure 1D is an example of T2 relaxation, and tissues with higher proton or water content, for example fat or edematous tissue, will have a longer relaxation time, and consequently a greater T2 signal than normal myocardial tissue. Furthermore, T2* relaxation can be measured from this process as well, reflecting the local inhomogeneities that disturb the local magnetic field, such as iron and deoxyhaemoglobin, (described in more detail in section 0.3). Standard T1-weighted imaging is different from T2-weighted imaging, in that tissues with faster T1 relaxation times will appear brighter. As fat has the fastest T1 relaxation time, it appears brighter in the images, while edematous tissue and blood will be darker (Figure 1E), Thus the signal acquired in images is affected by the type and angle of pulse given, the amount of protons in the imaging plane, the molecular environment of the protons, and other factors that may accelerate or decelerate the proton relaxation.

Common Imaging Planes

CMR images are thin (typically 6 to 10mm) slices of a defined spatial angulation. The most common orientations for cardiac imaging are long-axis (LAX) views which are para-coronal and parasagittal views oriented to the anatomical axis of the heart (Figure 2A), and short axis (SAX) views orientated parallel to the axial plane of the heart and perpendicular to the LAX (Figure 2B). In the presented studies, the LAX view is primarily used to help localize the short axis slices and to visualize any morphological abnormalities, for example, abnormal valve function or chamber size.

The majority of analysis presented in this thesis is performed from the SAX views. They are advantageous as there are often large amounts of tissue in the imaging plane for analysis, and most anatomical regions of the myocardium can be visualized in a perpendicular or near-perpendicular relationship to the plane. This reduces so-called partial volume effects, where the visualised region contains for example blood and myocardium. Furthermore, a single slice cutting through the left ventricle (LV) contains tissue perfused by each of the three coronary arteries, starting at the basal slices closest to the valves down to the apical slices. With SAX views, the analysis can be designated for well-defined regions, also referred to as segments.

Specifically, when analyzing coronary artery diseases, regional deficits can point to a problem with the feeding coronary artery (Figure 2C).

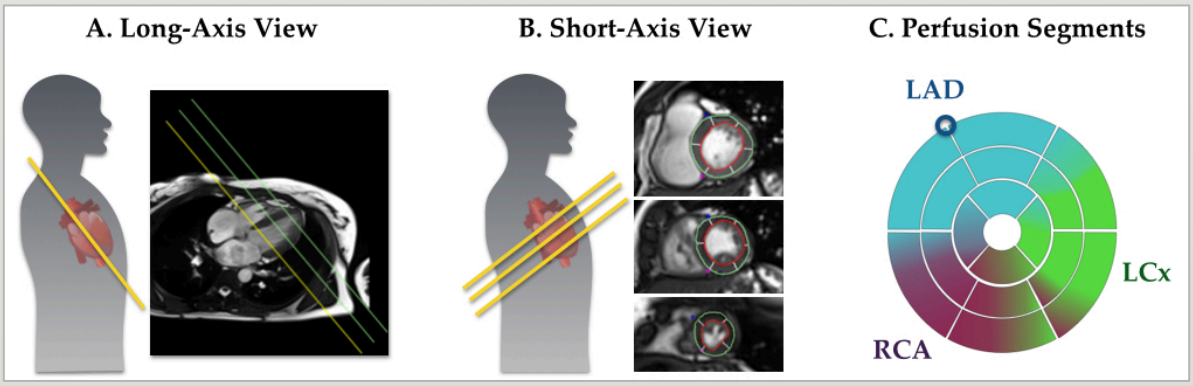

Figure 2: CMR imaging slices
A. A four-chamber view can be made of a long-axis (LAX) image displaying the left and right ventricle and the atria. B. Short-axis (SAX) views can be localized off the LAX, and displayed from the top to bottom are the basal, mid-ventricular and apical slice, with the contours marking the left-ventricular wall. C. The left ventricle of each SAX slice can be segmented following the AHA model (Outer ring; basal slice, middle ring; mid slice, inner ring; apical slice) showing the perfusion of the three coronary arteries, the left-anterior descending artery (LAD, blue), the left circumflex artery (LCx, green), and the right coronary artery (RCA, purple). Depending on the anatomy, two coronary arteries can supply blood to the same segments leading to a mixed perfusion bed. Adapted from the Mayo Clinic Guide to Cardiac Magnetic Resonance, Donato et al 2012, and Cerquiera et al, 2002[7–9].

0.2 CMR Sequences

CMR is a rapidly evolving, versatile imaging modality, which uses numerous sequences and several contrast mechanisms for various research and clinical applications. This project incorporates both clinically used sequences that measure ventricular function, and edema for standard data measurements, as well as newly developed sequences for measuring changes of myocardial oxygenation. These oxygenation-sensitive sequences are the focus of the research studies presented in this thesis, using an MRI with a magnetic field strength of 3 Tesla (T). Because of the strong magnetic field, some patients may be contraindicated for exams if they have non-MR-compatible metallic implants in their body.

Function Imaging

CMR is widely accepted as the gold standard for visualizing the heart and for quantitative assessment of morphology, flow, contractile function and tissue characteristics. For function and morphology imaging, cine sequences are used. These sequences acquire multiple images over a few heartbeats, with data obtained within just tens of milliseconds. Such images are obtained during different phases of the cardiac contraction and relaxation and then assembled to make a dynamic series, essentially reconstructing a video of the entire cardiac cycle. The sequence, as can be seen in Figure 3, can display the anatomical features of the heart, with a clear delineation between tissue, blood and fat. Cine function imaging is incorporated into almost all clinical CMR scans as one of the pillars of clinical diagnosis[10]. It is also incorporated as a measurement into each chapter that includes CMR imaging (chapter 1, 3, 4 and 5). New analysis software can supply even additional information beyond the standard measurements from the same set of images. Very recently, a novel technique became available, allowing for analyzing myocardial strain and strain rate from regular cine CMR images[11]. Furthermore, these cine sequences also form the base for the oxygenation-sensitive imaging (Section 0.3). Consequently, a variety of data can be extracted from this single acquisition.

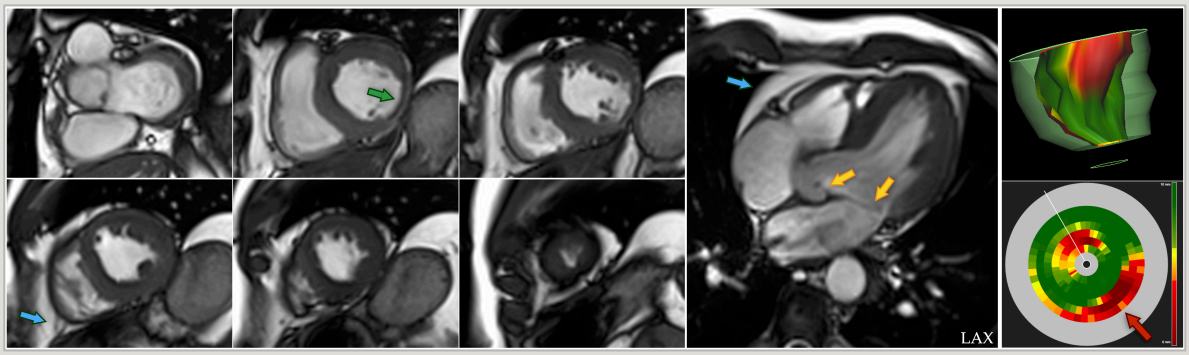

Figure 3: Function cine
By taking cine images of multiple slices throughout the heart, the overall function and morphology of the heart can be both visualized and quantified from a single set of images, which are obtained in about 5 minutes. CMR is the gold standard for morphological assessment, as the ventricle walls (green arrow), valves (yellow arrow), and pericardial fat (blue arrow, white layer) can be easily observed. In this patient example, a thin wall caused by a myocardial infarction can be seen in the basal slices of the left ventricle (green arrow) in the SAX images, which corresponds to poor regional wall motion, quantified by CMR analysis software (red arrow), and shown as a 3D-model (top right).

Edema Imaging

Myocardial edema is a marker for acute injury, and is included as a criterion when diagnosing acute cardiac diseases, such as myocardial infarction, severe ischemia, and myocarditis[12]. Edema imaging does not require an external contrast agent. Sequences that are T2-weighted are effective in assessing myocardial edema because protons bound to free water have a longer T2 relaxation time, thus lead to a higher signal intensity in areas with an increased content of free water. The current clinical standard sequence used for cardiac edema imaging is a T2-weighted triple-inversion recovery spin echo sequence (Short Tau Inversion Recovery, STIR). When the myocardial signal is normalized to skeletal muscle, both regional and global edema can be quantified, while suppressing the signal from fat that would otherwise be high in a T2-image to reduce misinterpretation with possible edema (Figure 4). Newer sequences now involve the use of myocardial mapping. Most signal intensity measurements are on an arbitrary scale and can only be used as relative measurements in comparison to other measurements. Mapping sequences use a colourful display to show the absolute relaxation times, without the need for a normalizing muscle. Thus absolute quantification can be performed, which is useful for assessing diffuse edema, and for comparing to other exams. Besides T2 maps, T1 maps can also be used for measuring edema as free water also prolongs T1, visualized as a brighter signal[13]. Similar to the STIR, T1-maps will also null the signal from fat tissue.

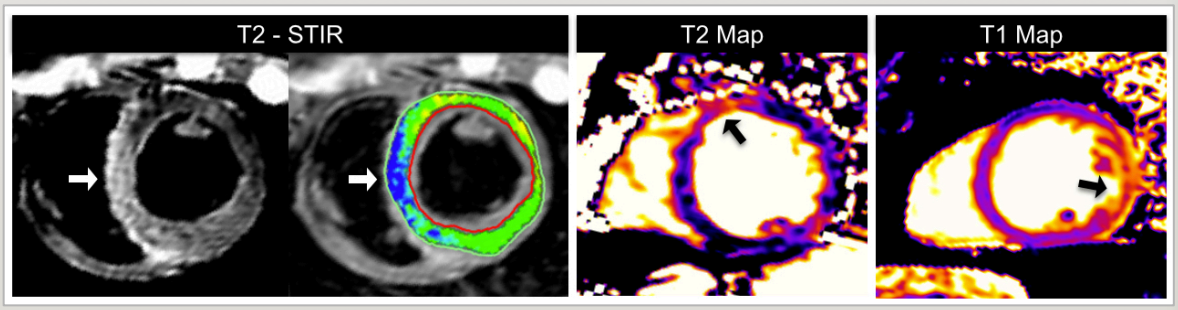

Figure 4: Common CMR methods of measuring edema
Inflammation can be both visualized (arrows) and quantified by the amount of hyper-enhancement in different CMR images (each technique is of a different patient). T2-STIR (left) represents the established semi-quantitative technique commonly used in clinical exams that demonstrate relative edema, while new developments have led to mapping techniques that provide colourful displays of edema with absolute measurements.

Contrast Enhanced MRI exams

Contrast agents are mainly used to identify structures which otherwise cannot be specified in non-contrast (native) MR images. Clinically used contrast agents alter proton relaxation properties and thus allow for selectively highlighting regions with increased contrast agent accumulation. This commonly occurs in tissue with increased relative volume of blood vessels, or in regions with increased interstitial volume of distribution, which delays the washout from these regions. Early CMR studies used ionized substances such as manganese[14] yet nowadays, gadolinium-based compounds are the primary contrast agent in imaging exams[15]. Gadolinium agents create a contrast because they markedly reduce T1 time. This translates into a regional signal variation that can display areas with increased extracellular space such as fibrosis, because gadolinium compounds typically show a fast distribution into interstitial space[16]. As irreversible tissue injuries such as necrosis or fibrotic scar or infiltration from amyloid or sarcoid lead to a marked proportional increase of the interstitial space, gadolinium-enhanced images may be used to identify and quantify the pathological tissue characteristics, which can be associated with specific diagnoses or expected left ventricular remodelling[17,18]. Contrast agents however add cost, require a physician to be available due to the risk for allergic reactions, and cannot be used in patients with acute or severe renal failure, as poor renal clearance can increase the possibility of side-effects from gadolinium accumulation and may lead to the rare yet serious nephrogenic systemic fibrosis[19]. This presents a limitation for cardiac patients, as renal failure is a common ailment presenting with cardiac disease. In particular with coronary artery disease, the prevalence of kidney failure (glomerular filtration rate, GFR<60ml/min/1.73m^2) has been reported to be more than 12% in a Canadian study[20] and as high as 22% in a large international trial including more than 22,000 patients[21]. Consequently, these patients may not be able to undergo contrast-enhanced MR imaging, and without viable alternatives, there may not be all the information available to make a proper diagnosis. In addition, recent evidence indicated that gadolinium may accumulate in brain tissue even in the absence of kidney failure[22]. Despite the fact that contrast-enhanced CMR is routinely performed, myocardial imaging is not an official indication for gadolinium contrast agents, meaning its use is considered off-label.

Thus it is desirable to be able to image cardiac tissue pathology using the native MRI signal only, without exogenous contrast agents. As a novel approach, oxygenation-sensitive (OS)-CMR may offer a non-pharmacological method to measure myocardial vascular function.

0.3 Oxygenation-Sensitive CMR

Oxygenation-sensitive (OS)-CMR is a technique that non-invasively measures changes in myocardial tissue oxygenation without using pharmacologic contrast agents. The majority of myocardial functional imaging is performed to detect inducible ischemia or vascular dysfunction, with a relative or absolute oxygen deficit in the myocardium caused by a mismatch of blood supply and demand. Oxygenation-sensitive imaging is a more direct marker for assessing ischemia or regional dysfunction because it goes beyond the standard perfusion techniques that just focus on blood supply, but it also adds the secondary component of assessing oxygenation. This is important as it gives a clearer picture if myocardial oxygenation is compromised or not, independent of changes in blood supply. OS imaging, also known as Blood Oxygen Level-Dependent (BOLD) MRI, has been used in brain imaging prior to its first application for cardiac imaging about 15 years ago.

History of Oxygenation-Sensitive or BOLD Imaging

BOLD-MRI was introduced in functional brain imaging studies in the early 1990's, when it was used for mapping neuronal activity[23,24]. Assessing pixel-wise changes in signal, the activation of certain brain areas could be visualized through small SI changes in BOLD-sensitive MR images caused by the minute decrease of de-oxygenated hemoglobin, induced by vasodilation. This led to direct mapping of cerebral blood flow. The latter feature is more related to what cardiac OS imaging tries to achieve. Subsequently, brain-imaging studies used BOLD as a measure of cerebrovascular reactivity. This had been used to assess cerebral lesions, and it was shown that in post-stroke patients BOLD responses were regionally attenuated despite intact anatomy[25], suggesting limited cerebral perfusion to these regions. Additionally, another study used BOLD imaging to demonstrate that cerebrovascular

reactivity was reduced in the presence of an intracranial stenosis, but showed improvement after extra-intra cranial bypass surgery[26]. While cerebrovascular lesions may be the brain's counterpart to coronary artery lesions, BOLD-fMRI has also been used to show abnormalities in cerebrovascular reactivity that occur without significant lesions, such as in neurodegeneration like Alzheimer's, and with brain injury studies where abnormal BOLD responses were found in sports-related post-concussion syndrome[27]. Because BOLD fMRI has been utilized for more than 25 years, many clinical studies have assessed its utility in a wide range of neural disorders, with plenty of reviews describing the clinical applications[28].

OS/BOLD imaging is not strictly limited to the heart and brain, but has also been used in the kidneys[29]. However, it should be noted that while all these sequences used for different parts of the body rely on the same principles of the BOLD effect, the sequences are significantly different in order target the imaging requirements of the specific organ. BOLD fMRI in the brain is often voxel-based analysis, so this means signal is obtained from a very small area. In cardiac imaging, the spatial resolution is not as high, and often analysis is performed across a greater area including a wide mix of vascular and muscular components.

OS-CMR studies lagged about a decade behind the brain studies. A primary reason for the delay was developing a sequence that can obtain images very rapidly in order to deal with the movement of a beating heart, while still producing decent image quality and useful results. The first applications of OS-CMR started to be published in the late 1990's, with data in cardiovascular patients occurring at the beginning of the millennium[30–34]. Using pharmacological stress agents, myocardial oxygenation deficits were detected in patients with coronary artery disease (CAD) who had also undergone coronary angiography[31,34]. More than half of the current OS-CMR publications use CAD patient groups. This is likely because CAD is one of the most common causes of myocardial ischemia, and significant coronary lesions can be detected visually by angiography and fractional flow reserve[35–38]. Furthermore, the myocardial oxygenation responses during pharmacological stimuli have been compared to perfusion deficits assessed by established cardiac imaging modalities such as SPECT, PET and first pass perfusion CMR[34,39–41]. These papers have shown there is a relationship with these validated imaging modalities, yet this relationship is not entirely linear. These other modalities measure just the blood supply, but not the oxygenation of the heart. These are two

related but different mechanisms, which result in a non-linear relationship. Newer publications are assessing other cardiovascular diseases as well that lead to ischemia in the absence of coronary artery lesions, such as hypertrophic cardiomyopathy, obstructive sleep apnea syndrome, syndrome X, type 2 diabetes, and patients with renal disease[33,42–46]. This will be described in more depth in section 0.7, but these studies used OS-CMR to detect microvascular dysfunction, which can cause ischemia despite normal coronary arteries.

As MRI rapidly advances, so do the sequences, thus even within a group, the OS sequence may be different between publications a few years apart. Consequently, the results obtained in one centre, cannot be directly compared to other publications, nor is there currently a global cut-off value, which determines healthy from abnormal myocardium. To highlight this point Table 1, shows that in using the same magnetic field (3T), and same hyperaemic stress (adenosine infusion at 140 µg/kg/min), the results are not completely relatable to each other. Additionally, all 5 publications were published within a period of 4 years and thus should not have been too significantly affected by advances in sequence technology.

	OS-CMR	Tesla	Sequence	FA / TR	Voxel Size (mm)
Arnold 2012	2.3%	3	T2-prep ECG gated bSSFP	44° / 2.86 ms	8mm (matrix:168z192)
Fischer 2014	3.9%	3	T2-prep ECG gated bSSFP	35°/ 3.4ms	2.0x2.0x10.0
Karamitsos 2010	7.0%	3	T2-prep ECG gated bSSFP	44° / 2.86 ms	8mm (matrix:168z192)
Jahnke 2010	7.1%	3	T2-prep GRE, free breathing	30° / 5.0 ms	1.3x1.3x8.0
*Manka 2010	16.1% (+5ms)	3	T2* GRE	35° / 13ms	1.2x1.2.8,0

Table 1: OS-CMR during adenosine hyperaemic stress

Average OS-CMR response at 3T in healthy volunteers or healthy segments for the Arnold paper during pharmacological hyperaemic stress (Adenosine 140ug/kg/min). *Manka et al reported an absolute difference in T2* time. FA: flip angle, TR: repetition time[35,39,40,47,48].

In conclusion, OS-CMR has been validated by multiple studies in patients, healthy volunteers and animals. The goal of this thesis is to develop the application of breathing maneuvers as a non-pharmacological method of assessing myocardial oxygenation to use in combination with oxygenation-sensitive imaging.

Foundation of the OS Signal

This field of imaging started off using standard T2*-weighted sequences, and then developed to also incorporate T2 effects, resulting in a sequence dependent on both processes[30,32,34,49]. OS sequences exploit the dephasing of the MRI signal (Figure 1), relying on changes to the T2* signal decay rate by local inhomogeneities and to the T2 component that is affected by changes in proton count (Figure 5). In myocardial tissue, these inhomogeneities are primarily caused by the magnetic properties of the ferrous iron component of haemoglobin (Hb), found in the blood. Hb has paramagnetic properties when deoxygenated, and influences the phase evolution of water protons in the tissue leading to a loss in magnetic field homogeneity. This accelerates the relaxation of the signal, causing an MR signal decrease[24]. Otherwise, oxygenated haemoglobin has diamagnetic properties, which has a small stabilizing effect on the surrounding water proton relaxation times[24]. Subsequently, the basis of the endogenous contrast is due to the field distortion related to deoxyhaemoglobin (dHb), and OS signal response can be an inverse reflection of changes in the dHb fraction in the imaging plane[50]. Additionally, because OS sequences are also T2-weighted, a greater localized blood volume could theoretically increase the signal. However, this effect is fairly negligible as the majority of the signal increase is believed to be due to the effect of increased blood supply improving oxygenation and the "washing-out" of dHb[51].

A similar molecule to Hb is myoglobin in the cardiac muscle cells, which when deoxygenated can also have paramagnetic effects, yet no BOLD/OS study has assessed this the impact of this molecule. How myoglobin changes may affect OS-CMR is unknown, but the involvement of myoglobin oxygen delivery in the heart is still controversial[52]. This is because the partial pressure of oxygen (P50) of myoglobin at which 50% of the myoglobin molecules are saturated is very low (2.7mmHg). Therefore, myoglobin is only desaturated at extremely low oxygen levels, thus likely providing a stable background signal. While it has been suggested, that myoglobin may take part in oxygen delivery to the heart at very high cardiac workloads, this has only been shown in a theoretic model based on Krogh cylinder-like distributions of capillaries. A myoglobin deficient mouse model showed that mice lacking myoglobin had adapted to maintain sufficient normal myocardial oxygen consumption, even during physical stress[53]. Reviewing the available published data, the impact of myoglobin on

changes of tissue oxygenation and thus SI during non-critical states is likely negligible in comparison to the oxygen delivery by Hb, and is not factored into other OS-CMR publications[54,55].

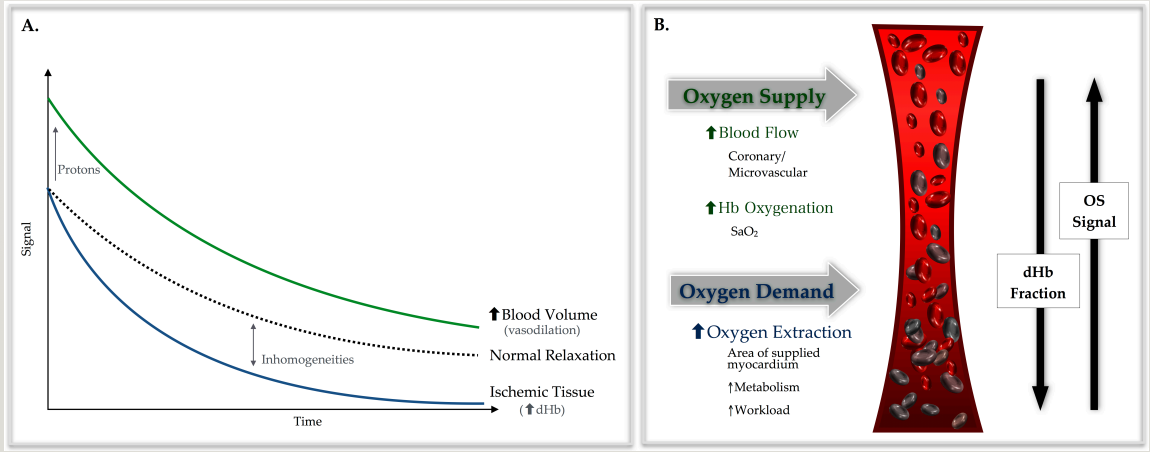

Figure 5: Factors of the OS signal

Oxygenation-Sensitive (OS) signal is based on a balance of proton density and the deoxyhaemoglobin fraction. Inhomogeneities such as deoxyhaemoglobin (dHb) accelerate the relaxation of the T2 signal (A). Thus tissues with greater deoxyhaemoglobin fractions such as ischemic tissue will have a lower signal. On the other hand, tissues that have an increase in blood volume have a greater number of protons present and start with a higher signal. Thus factors that affect the balance of oxygen demand and oxygen supply influence a change in oxygenation signal (B).

The absolute value of the signal intensity in OS-CMR images also is subject to confounders such as distance of the assessed tissue to the surface coil, other magnetic field homogeneities, field strength and other factors. Therefore, current methods are more suited for measuring changes of the signal intensity during dynamic conditions, such as during induced variations of blood flow. As a result, these static factors will be cancelled out and the OS measurement will just reflect the factors that changed during the stimulus.

Confounders for the Signal Intensity in OS-CMR

The average dimensions of the voxels in OS-CMR range from a diameter of about 0.9-2.0mm with a depth of 10mm (Figure 6). Furthermore, during image analysis, the reader will define large regions in which the signals of multiple voxels are averaged, often based on

perfusion territories. Thus for the measurements, one single value will incorporate effects from across a large area of the heart, and mixes the vascular and tissue components together into one value. One voxel can be composed of thousands of microvessels. Capillaries constitute the majority of the microvasculature, as the capillary density is reported to be about 2000 capillaries per mm^2, with about 8 arterioles/mm^2[256,57].

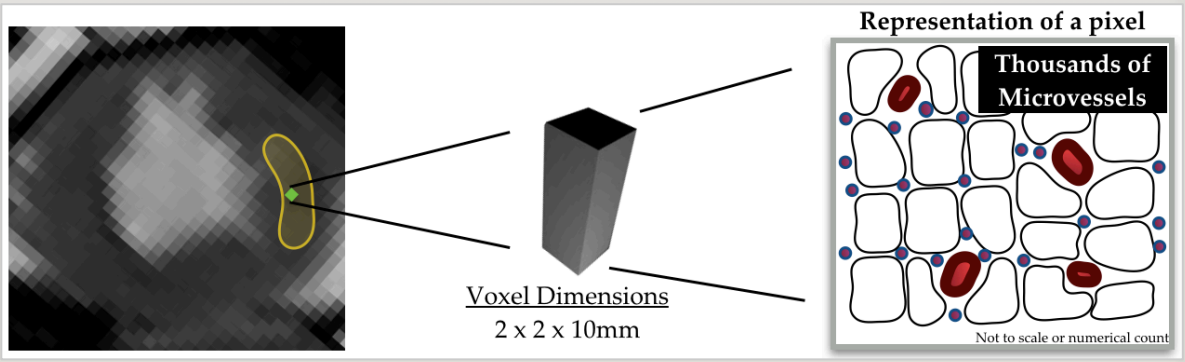

Figure 6: Dimensions and components of an OS-CMR voxel
This representation shows that with CMR analysis, a region of interest (yellow) is made averaging the values of many voxels (green square), which themselves average the effects of many myocardial components including thousands of microvessels (capillaries are blue, arterioles are red, and cardiomyocytes are white, picture is not to scale, nor does it include many other structures found in the myocardium).

Specifically, as the majority of the T2* component of the OS signal comes from the capillaries, the density and dHb content in these vessels will have a significant effect[32]. As stated in section 0.6, the arterioles control the majority of the blood supply which will end up controlling oxygenation and the washout of the dHb. Thus, territories that have greater density of these vessels will have greater OS changes. However, the density of the microvessels is not similar throughout the heart, especially between the subepicardium and subendocardium. Regions with greater density of these functioning vessels will have a greater OS response. In healthy human hearts, the subepicardial capillary density is 21% greater than the endocardial capillary density and this will have a greater effect on the OS signal[56]. The subendocardial tissue is more prone to ischemia especially downstream to a coronary stenosis because it has a higher metabolic demand and the regional vasodilatory reserve is closer to capacity[58,59], whereas at rest the subepicardium has a higher availability of arterioles ready to increase

perfusion, leading to redirection in blood flow away from the subendocardium in certain situations[60]. Furthermore, the subendocardium is most vulnerable to increased extravascular pressure and wall stress, which will increase the vascular resistance of the microvessels as well.

On the other hand, this distribution and function can be affected by myocardial injury. For example, patients with cardiovascular disease can have greater volumes of fibrosis in the subendocardial myocardium[61], and in these areas there is an even lower capillary density[57], which would cause lesser OS changes. In summary, the spatial resolution of OS-CMR is insufficient to separate effects on vasculature and other tissue components. This is consistent with other validated modalities such as cerebral near infrared spectroscopy, which is an accepted tool for detecting changes in the cerebral oxygenation balance based on hemoglobin oxygen saturation. This technique is also affected by the strong venous component and a weak arterial influence, yet is a valid technique for monitoring cerebral oxygenation during surgery or intensive care[62]. Thus, the OS response is generally accepted as a measure of the general status of oxygenation reserve during a stimulus, incorporating the overall effects of the oxygen supply and demand balance,

OS Signal and the Balance Between Oxygen Supply and Demand

Changes in the dHb fraction occur when the balance between oxygen supply and demand shifts, resulting in a relative change of myocardial oxygenation (Figure 5). Myocardial OS signal rises also by increasing Hb oxygenation through decoupling oxygen supply from demand, by either reducing the oxygen demand of the heart while maintaining the blood supply, or increasing myocardial blood flow without a matching increase in demand[30,63]. A reduction in signal occurs when the oxygen consumption is increased to a level greater than the oxygenation supply, such as during periods of high cardiac workload or restricted blood supply.

The heart already has a high oxygen extraction at resting/baseline conditions, and because of this narrow extraction reserve, it cannot increase oxygen extraction as much as other tissues such as the skeletal muscle. Consequently, the increased oxygen requirement of the myocardium is primarily met by increasing the blood flow rather than significantly

increasing the extraction of the current blood volume. During strenuous exercise however, humans can increase myocardial oxygen extraction[64], and in a dog model this could be increased by nearly a factor of 2[65]. The oxygen extraction reserve for swine is not available, but this animal model does have a higher basal rate than humans[66]. Nevertheless, in healthy vasculature, any increase in oxygen extraction should be compensated for by a blood supply increase, and this would either maintain the balance between oxygen demand and supply, or shift it towards higher oxygen supply because of an overcompensating increase in perfusion. In CAD patients, this balance cannot be maintained during vasoactive stress, such as during exercise or diagnostic testing. This balance could be affected by an increased myocardial oxygen demand and a higher extraction but with no reciprocating increase in blood supply, possibly in the cases where the coronary vasculature is chronically vasodilated to maintain blood supply even at rest situations, thus without vasodilatory capacity. Or this balance can be compromised even with unchanged demand, but reduced blood supply, which can occur during coronary steal where healthy vessels have less resistance and end up directing more blood away from the affected regions. Although oxygen extraction is one of the significant cofactors that affect OS signal, the signal is not specifically a measure of oxygen extraction, as described above.

This concept of uncoupling the oxygen demand versus oxygen supply is the basis for applying OS-CMR to investigate vascular function and myocardial ischemia.

Application of OS-CMR to Assess Vascular Function

The "oxygenation response" is the physiologic endpoint and marker for the responsiveness of the coronary vasculature to vasoactive stimuli. In the presence of a vasodilating stimulus, healthy vessels will react with an increase of their diameter and a subsequent rise in blood flow, thus increasing the OS signal. However, the OS signal response will be attenuated if a dysfunctional vessel cannot respond to a vasodilatory stimulus or increased myocardial demands, which may result in overt tissue ischemia.

In the presence of severe coronary artery stenosis and inadequate blood flow, the vessels may be already maximally dilated to maximize blood flow, even during resting

conditions. Thus even during a vasodilatory stimulus, throughput of the blood cannot be increased further. This could be due to a lack of additional vasodilation, or to pooling of the blood caused by blockages elsewhere. To compound this effect, in the presence of a stenosis, downstream vessels may still have the capacity to dilate, or there may be a greater amount of capillary recruitment, resulting in more blood volume distal to the blockage[30]. Because of the bottleneck effect caused by the stenosis, the majority of blood distal to this stenosis will be deoxygenated, as fresh oxygenated blood is not being replenished. Subsequently, with the downstream vasodilation, there will be a greater volume of dHb resulting in a decrease in signal, which is opposite of the effect seen in healthy vessels[30]. Thus, OS-CMR imaging in the presence of a vasoactive stimulus can be used to differentiate healthy versus dysfunctional vessels. By measuring the response of the myocardium rather than specific vessels, OS-CMR can be a measure of the responsiveness of the entire vascular tree, including the epicardial coronary artery and the microvascular system (Section 0.7).

Standard Pharmacological Techniques

In the last 15 years the majority of OS-CMR studies have used pharmacological agents as a vasodilating stimulus[30,34,35,37–40,48,67]. Besides dipyridamole and regadenosone, adenosine infusion is commonly used for pharmacological vasodilation. Under regular circumstances, adenosine does not significantly affect cardiac output but increases blood flow through coronary vasodilation. Typical protocols in cardiac imaging induce hyperaemia by a systemic infusion of adenosine at a rate of >140μg/kg/min for less than 5 minutes. The impact of such hyperaemia can be monitored by OS-CMR, as the myocardial oxygenation response has been positively correlated with blood flow[68]. However, there are significant drawbacks to using adenosine. First, adenosine increases the cost of a CMR exam, as in Canada the product alone costs more than $100 per patient, and because of possible arrhythmia or bronchospasm, requires a specifically trained physician to be present for the administration. More importantly, in some cases adenosine can cause patient discomfort and health risks including dyspnea, flushing, chest pain, palpitations, light-headedness, sweating, nausea, headache and anxiety [69]. This prompted a 2013 federal drug authority warning about the use of adenosine and regadenosone in cardiac imaging [70]. Consequently, alternative techniques that remove the need

for adenosine would improve patient comfort, safety and the cost burden of myocardial ischemia imaging.

0.4 Breathing Maneuvers

Rather than relying on external agents, methods that use intrinsic factors to manipulate vascular function have been investigated. Our studies have looked into using breathing maneuvers as a vasoactive stimulus. Breathing maneuvers involve any participant initiated methods of paced breathing and breath-holds.

History and Summary of Breathing Maneuvers

As blood-oxygen-level-dependent (BOLD) imaging originated in functional MRI of the brain, the use of breathing protocols and inhalation of gas mixtures have already been used to manipulate cerebral blood flow. Breath-holding and other choreographed breathing protocols had been employed as a simple technique for causing short epochs of mild hypercapnia[71–74]. Additionally, brain imaging studies have looked at having participants inhale gas mixtures with different levels of carbon dioxide and oxygen in order to systemically alter the arterial blood gas partial pressures[75–78]. While mostly studied in younger healthy volunteers, this field has also looked into the BOLD signal responses during breathing maneuvers of children and aging populations as well as different neurological disorders such as brain tumours, intracranial stenosis, cerebral infarcts and progressive disorders like Alzheimer's Disease[26,79–81]. Additionally, these studies may use different techniques, for example using long and repetitively paced breathing blocks in which breathing patterns are repeated over a period of minutes, or combining breathing protocols with other tasks simultaneously. Brain imaging studies have more options available than CMR when it comes to breathing maneuver protocols, as the majority of CMR imaging requires images to be obtained during a breath-hold anyway, in order to reduce chest motion whereas brain imaging can occur during free-breathing. Thus CMR protocols must be short. Our groups in Calgary had performed pilot studies in animals and healthy volunteers to assess the use of simple breathing maneuvers that could be performed with CMR. This involved a breath-hold or

hyperventilation performed independently to manipulate myocardial oxygenation in swine and a small cohort of healthy volunteers [82,83].

Introduction to the Suggested Breathing Maneuvers.

In this project we mostly focus on a combined maneuver of hyperventilation followed by a breath-hold. In our pilot study and other publications, it is suggested that the average breath-hold following a normal breathing pattern is about 30s in healthy volunteers[83,84]. However, it is unlikely that patients can maintain a breath-hold as long. Furthermore, while a breath-hold would likely increase blood flow, hyperventilation precedes hypocapnia, which is known to reduce blood flow. A hyperventilation-induced relative vasoconstriction followed by a voluntary apnea with its vasodilatory impact would therefore exploit a greater range of vascular function. Thus, we suggested using a combined maneuver in which participants would hyperventilate by breathing deeply at a rapid pace for some time and then perform an end-expiratory breath-hold. With CO_2 being the strongest breathing stimulus, preceding a breath-hold with hyperventilation can not only extend the breath-hold duration by reducing the CO_2 content and thus shifting the starting level farther from the threshold at which the breakpoint of a breath-hold occurs[85,86], but also increases the total range of observable changes. With the extended breath-hold, the participant undergoes a greater range in CO_2 and coronary vasomotion. The other maneuver investigated is a standard maximal breath-hold from a normal breathing rate that assessed just the vasodilatory stimulus.

Breathing Maneuver Protocol

For this project, the breathing maneuver technique has been refined for efficiency and reproducibility. Prior to the imaging exam, all participants undergo a brief training on how to conduct the breathing maneuvers. This includes reading an information pamphlet, watching an instruction video, and practicing the maneuver with a study nurse, research team member or MRI technician. The detailed protocol for MRI technicians including both breathing maneuver and scanning instructions is included as appendix 1. In these presented studies, the breath-holds are performed at end-expiration. The primary reason for this is for image quality

purposes, and this is standard for most cardiac imaging. The actual variability of the thorax position is reduced by using an expiratory breath-hold and thus the heart will remain in a very similar position between different image acquisitions. Additionally, during an inspiratory breath-hold, study participants tend to slowly exhale throughout the breath-hold, impairing image quality. Finally, an end-expiration breath-hold reduces lung volume differences between participants, in comparison to an inhalation breath-hold.

Combined Hyperventilation Breath-Hold Maneuver (HVBH)

The primary breathing maneuver investigates is the combined hyperventilation breath-hold maneuver (HVBH). Prior to performing any breathing maneuvers, a single baseline image has been obtained (Figure 7). The participant breathes at a normal rate, and for the image makes an end-expiration breath-hold of 3-10s, depending on the number of slices required. Afterwards the participant hyperventilates for 60s, breathing at a deep and rapid pace. To ensure a reproducible breathing pattern, we implemented a metronome with a click rate of 60 beats/min, instructing the patient to breathe in and breathe out in sync with two consecutive click sounds. Thus, participants following these instructions breathed at 30 breaths/min. The breathing motion can be tracked using a breathing monitor belt, although the precise depth of the breath can't be measured in the MRI. Moreover, there is a camera that displays the participant's chest movements to the staff in the control room. The technicians can instruct the participant to change their breathing pattern if it does not appear sufficient. At 60s into the hyperventilation, the participant is guided by the technician to take one breath, after which they conduct an end-expiration breath-hold that is maintained for as long as comfortable. CMR images are acquired continuously throughout the breath-hold. Once the participant needs to breathe, s/he indicates to the technician that they ended the breath-hold using an indicator ball. Furthermore, the technician can observe the MRI images and the patients' chest movement to visually note the end of the breath-hold.

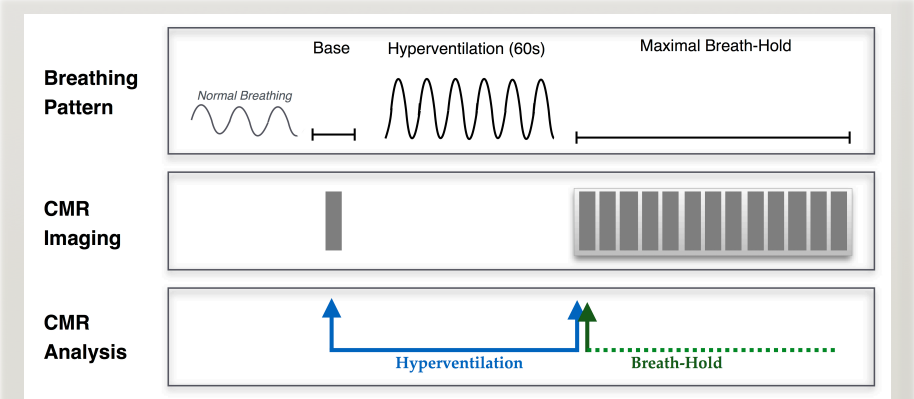

Figure 7: The combined Hyperventilation Breath-Hold (HVBH) Maneuver
The acquisition of a CMR measurement is represented by the grey boxes, and breath-holds are indicated by a flat line. For the analysis, hyperventilation is always compared between the baseline image and first image of the breath-hold, while for the breath-hold, any image is compared to the first acquisition.

For the analysis of the maneuver, the effect of hyperventilation is determined by a two-point assessment only, similar to adenosine. The response is calculated by the percent change in signal between the baseline image prior to hyperventilation, and the first image of the breath-hold. Because the breath-hold can be continuously imaged, the response throughout the maneuver can be assessed by comparing the signal of any time-point to the first image.

Long Breath-Hold (LBH)

The other maneuver investigated in this project is the long breath-hold (Figure 8), which is a maximal breath-hold conducted following normal breathing, without a preceding hyperventilation. This maneuver is performed in a similar method to the second part of the HVBH, where a patient holds an end-expiration breath-hold for as long as comfortable. The intent of this maneuver is to observe just the vasodilation effects of a breath-hold, and if the response is different when the vasodilatory stimuli does not follow the vasoconstriction of hyperventilation.

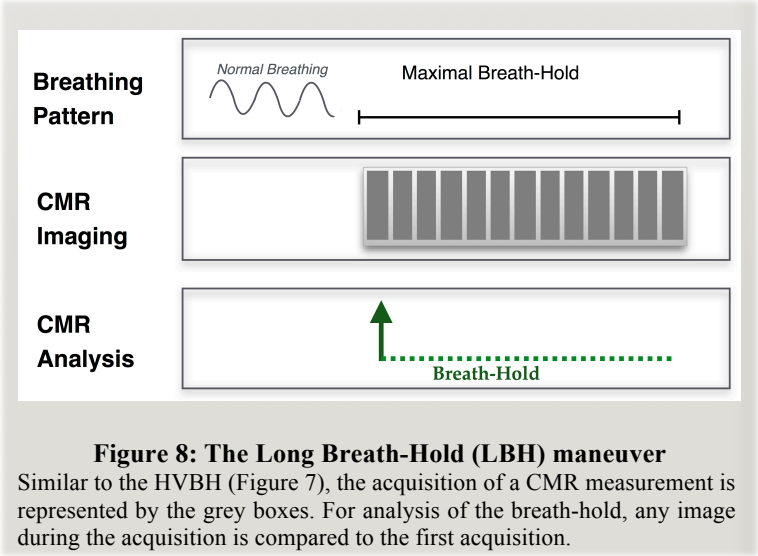

Figure 8: The Long Breath-Hold (LBH) maneuver
Similar to the HVBH (Figure 7), the acquisition of a CMR measurement is represented by the grey boxes. For analysis of the breath-hold, any image during the acquisition is compared to the first acquisition.

Standardization, limitations and safety aspects of breathing maneuvers

Compared to other vasodilatory triggers, breath-holding has many advantages; the greatest being that no specialized equipment is needed. Breathing exercise tests however require subject compliance which may affect interindividual reproducibility[87]. As described above, we aimed to standardize hyperventilation between participants by using a metronome to control the breathing pace, and controlled for the breathing depth by visual observation. However, hyperventilation is still reliant on subject compliance and capability, and some patients may not be able to conduct the breathing tests as efficiently. A period of 60s was chosen because a pilot study in healthy volunteers showed that it still induced a change in myocardial oxygenation that matched the effects of 120s of hyperventilation, but had less side effects[83]. Currently, acquisition of good images requires a breath-hold, thus the effects throughout the hyperventilation period cannot be assessed. However, future research is aiming to develop navigator based imaging, which account for chest motion and allows for image acquisition during breathing.

The breath-holds can be monitored more easily. All breath-holds are performed at end-expiration and the main variability between participants comes from the individual breath-hold breakpoints, when the participant feels the need to breathe. The duration of a voluntary breath-

hold may be influenced by many factors such as initial gas content, lung volume, chemoreceptor sensitivity, secondary diseases, tolerance, and patient compliance[86]. While the animal and volunteer studies analyze the entire breath-hold, in patient studies analysis has been refined to the first 30s. This is because following proper hyperventilation, more than 90% of patients assessed so far could reach that time-point (Table 2).

	Failed Hyperventilation	Breath-Hold Time		
		0 – 14s	15 – 29s	≥30s
Healthy	0	0	3	89
Coronary Artery Disease	0	0	1	6
Heart Failure	0	0	1	5
Heart Transplant	0	0	0	28
Obstructive Sleep Apnea Syndrome	0	0	5	24
TOTAL	**0**	**0**	**10**	**152**

Table 2: Success of the Hyperventilation Breath-hold maneuver

All human participants of the published and ongoing studies[47,88–90] as of January 2016, were able to hyperventilate successfully and maintain a breath-hold for at least 15s at rest conditions (ie. without supplemental oxygen, or haemodilution). Patients are grouped by their primary diagnosis of the study they participated in, and may have had co-presenting cardiac disorders. Of note, participants were allowed to repeat the breathing maneuver if they experienced a problem.

0.5 Arterial blood gas manipulation

In a related subject, this study also looks at the effect of stable arterial blood gases on coronary flow and myocardial oxygenation. This differs slightly from breathing maneuvers, which induce an acute and intermediate change in arterial blood gases. In particular, the impact of targeted arterial tension of oxygen (paO_2), and carbon dioxide ($paCO_2$) were assessed, with a focus on how blood gas levels themselves alter the baseline and how they affect the coronary response to a breathing maneuver.

Impact of Oxygen

In response to the myocardial demand for oxygen, it has been known for decades that both arterial and tissue hypoxia will increase the coronary blood supply to compensate for the

lower oxygen content. In 1957, it was shown the inhalation of a hypoxic mixture (10% oxygen) led to a doubling in coronary flow as the coronary arterial oxygen content was reduced[91], and this effect is still shown true with advanced flow measurement technologies[92]. Additionally, previous publications by our group showed that despite arterial hypoxaemia, myocardial oxygenation could be maintained in an anaesthetized swine model, demonstrating a regulatory mechanism. This was likely due to an increase in blood supply to counteract the low blood oxygenation, but this was not specifically measured in that study[93].

Parts of this project also look at the effect of supra-normal oxygen tensions. Despite the general belief that supplemental oxygen is beneficial for cardiac patients, hyperoxia is known to decrease coronary blood flow[94], and can lead to worse prognosis in the case of survival after sudden cardiac arrests a well as during ST-segment elevation myocardial infarctions[95,96]. Thus Chapter 3 looked at the impact of hyperoxia on myocardial oxygenation in animals with experimentally induced coronary stenosis.

Impact of Carbon Dioxide

A systemic increase in CO_2 tension leads to an increase of cerebral and myocardial blood flow[7-9]. Independent from local metabolic demand, an increase in systemic $paCO_2$ modulates tissue blood flow and will consequently lead to an excess perfusion similar to pharmacologic vasodilators. Non-metabolic increases in CO_2 can be modulated through breathing maneuvers, such as breath-holds or paced breathing patterns[82,83], and through the inhalation of CO_2 rich gas mixtures[99,100]. Low tension of CO_2 has an opposing effect, triggering vasoconstriction and a subsequent reduction in perfusion. This state of hypocapnia can be induced by hyperventilation. Furthermore, there is an interaction between CO_2 and O_2 as the vasodilatory effects of hypercapnia are potentiated by hypoxia[101]. Chapter 2 investigates these combinations by targeting the specific arterial blood gas levels, but a mild form of this combination can also occur with the breathing exercises at the end of a long breath-hold.

Impact of Arterial Blood Gases on the Response to Vasoactive Stimuli

Since abnormal arterial blood gas levels may occur in various clinical situations, it is important to assess how they may affect responses to vasoactive stimuli. Cardiac diagnostic tests using vasoactive stimuli could be confounded by blood gas levels and breathing patterns. While a poor response is considered evidence for coronary artery stenosis or a microvascular perfusion abnormality, other factors that may attenuate or falsely augment the signal could lead to false conclusions. In particular, with cardiac patients, the oxygen content of the blood can be abnormal as some cardiac patients can experience chronic hypoxaemia, while others may receive supplemental oxygen during exams creating a state of hyperoxia, all affecting the baseline of such procedures for assessing vascular function. Therefore, in the experiments described in chapter 2, we measured how paO_2 and $paCO_2$ levels affect the coronary flow response to a short breath-hold stimulus.

0.6 Vascular Function

Functioning vasomotor reaction is essential for maintaining and tightly regulating blood and oxygen supply to the myocardium, responding to changing tissue demands. During the evolution of atherosclerosis, microvascular function may be altered long before overt morphological changes develop such as coronary artery stenosis. A healthy coronary vascular system can markedly increase blood flow, also known as the coronary flow reserve. If this function is compromised, the adaptation to changes of workflow or blood oxygenation is impaired, and, in more severe cases, myocardial ischemia can result. Consequently, the majority of diagnostic techniques that assess vascular function specifically target the vasodilatory reserve.

The vascular response is based on the ability to modify vascular resistance, which is the primary determinant of myocardial blood supply. This resistance is regulated mostly by the coronary anatomy and the ability of the vessels to dilate through vascular smooth muscle contraction. The coronary artery bed is composed of two major zones: the “conduit vessels”, which includes the coronary arteries and pre-arterioles, and the microvasculature, composed of

arterioles and capillaries[102]. Many techniques such as the fractional flow reserve (FFR), look specifically at the response of the large coronary arteries. In a healthy anatomy however, these vessels are not major components of actual coronary resistance. Rather it is the microvasculature that is considered responsible for matching coronary blood flow to myocardial oxygen demand[103]. Thus, to induce the greatest change in coronary flow, vasodilators will target the microvasculature, specifically the endogenous vasodilators.

Mechanisms of Vasomotion

Vascular resistance is regulated by multiple mechanisms that are still not fully understood. Current theories about coronary vascular function control focus on neural, endothelial, metabolic and myogenic regulation, which can act on cardiac myocytes, endothelial cells, or smooth muscle cells. The goal of diagnostic vasodilators is to induce a short-acting but maximal effect. This project focuses on a comparative analysis of the impact of adenosine and breathing maneuvers, and partial pressures of CO_2 and O_2 in the blood.

Metabolic Control

The arterioles maintain a controlled balance between myocardial oxygen supply and demand. As the consumption of oxygen is often correlated with cardiac workload, many metabolic products associated with cardiac workload have vasodilative properties to transiently increase blood supply. Thus, increased adenosine production, high pCO_2, low pO_2 and acidosis are all positively correlated with coronary blood flow, with the strongest effect on microvessels of less than 200μm in diameter[104]. Adenosine is also an endogenous metabolite of cardiac myocytes that is assumed to be released when myocardial pO_2 drops[105]. However, for the purpose of clinical imaging, a much higher dose is required than can be produced naturally, thus an intravenous dose of pharmaceutically isolated adenosine is needed so a sufficiently large dose can be administered. Adenosine has many actions, but the most important in the case of coronary dilation is its role in smooth muscle relaxation, blocking the calcium-channels that would normally induce smooth muscle constriction[106].

Independent of adenosine effects, coronary arterial pO_2 and pCO_2 have been known for decades to be correlated with coronary vascular resistance [107,108]. There is a profound synergistic effect on coronary blood flow when low pO_2 is combined with high pCO_2. Vice versa, high O_2 tensions and low CO_2 tensions can attenuate dilation and even have vasoconstrictive properties[94,109,110]. The effects of pCO_2 and pO_2 are attributed to induce 30-40% of the coronary flow response[101], yet this is only a portion of the response, supporting the idea of multiple regulating mechanisms. Both brain and heart imaging studies have investigated administering these gases through inhalation[75,78,93,100], and altering the local amounts endogenously through the breathing maneuvers [71,72,111,112]. The exact role of metabolites on the coronary vasomotor response is not fully known. Especially with the blood gases pCO_2 and pO_2, metabolites can also impact the microvasculature through vagal-mediated pathways activated by both peripheral and central chemoreceptors. Despite different sensory pathways, stimulation of both responses, either hypercapnia or hypoxemia, will cause vagal cholinergic coronary vasodilation[113]. For example, arterial chemoreceptors detect both hypoxemia and hypercapnia, and redirect more flow to the heart through sympathetic activation in order to compensate for the drop in perfusion pressure caused when the coronary vessels dilate through direct effects[114]. Thus, vasodilation requires the cooperation of both direct and vagal regulation by metabolites.

On the other hand, high O_2 tensions can lead to vasoconstriction, with multiple mechanisms suggested. This can be mediated by endothelium dependent mechanisms, leading to inhibition of K_{ATP} channels[115]. Other studies have shown that high oxygen tensions are related to the production of reactive oxygen species[116], which are directly involved in the destruction of nitric oxide released from the endothelium[94]. The vasoconstriction has also been shown to be both dependent and independent of the autonomic nervous control[117,118]. Despite the uncertainty about the specific mechanism, it is known that hyperoxia leads to a decrease in coronary artery blood flow[94,119], however studies in the last 25 years have not used modern techniques to assess the impact on the microvasculature.

	Stimulus	Vaso-	Suggested Causes and Mechanisms	Location
Metabolic	↓O_2 ↑CO_2 ↓H+	dilator	Can be induced by hypoxia, altitude, exercise, breath-holds/poor ventilation, ++ Unclear mechanisms, can include activation of peripheral and central chemoreceptors, adenosine release	Micro-vasculature
	Adenosine	dilator	Naturally released during hypoxia Injected pharmacological dose Suggested mechanisms is by blocking calcium channels and blocking smooth muscle contraction	
	NO	dilator	Can be triggered by many mechanisms, and is a by-product of other vasomotor pathways	
	↑O_2	constrictor	Induced by supplemental oxygen Inhibit K_{ATP} channels, produce reactive oxygen species, endothelium dependent and independent, autonomic control	
	↓CO_2	constrictor	Induced by hyperventilation, altitude	
	Endothelins	constrictor	Can be released by cardiovascular diseases, diabetes, changes in blood pressure , ++ Causes smooth muscle contraction – strongest physiological vasoconstrictor in humans	
Hormonal	Atrial Natiuretic peptie	dilator	Minimal effect with physiological concentrations	
	Angiotensin II Antidiuretic H Epinephrine Nor-epinephrine	constrictor	Work to maintain higher blood pressure Angiotensin II leads to endothelin release*	
Nervous	Sympathetic tone	dilator	β-adrenergic receptors are activated, and stimulates metabolic production* More predominant in subendocardium	
		constrictor	α-adrenergic – can restrict metabolic dilation, can help protect against coronary steal More predominant in epicardium	
	Parasympathetic tone	dilator	Minor and weak effects Can be induced by cold pressor tests, acetylcholine	
Myogenic	↑Coronary blood pressure	dilator	Designed to maintain perfusion Dependent on the coronary autoregulation response	Coronary tree
	↓Coronary blood pressure	constrictor	Can activate stretch receptors (Ca+) leading to muscle contraction (Bayliss effect) and lead to metabolite production*	
Endothelial	Pressure / Flow	dilator	Caused by shear stress on the vessel wall Can lead to NO release*	Pre-arterioles

Table 3: Examples of coronary control

While the mechanisms of coronary vasomotion are still not well understood, this table highlights some of the primary pathways for controlling vasodilation and vasoconstriction. Specifically, the mechanisms of metabolites, oxygen and carbon dioxide, that are key factors during the breathing maneuvers. This table does not discuss the use of pharmacological agents. *Non-metabolic processes can still trigger metabolite production and the subsequent pathways of vasomotor control[102,120–122].

Non-metabolic Control of the Coronary System

While CO_2 and O_2 are considered to be a significant factor in the control of coronary flow, the full effects of breathing maneuvers are unknown. In chapter 2, the impacts of short breath-holds that are not long enough to induce a change in blood gases on coronary blood flow are assessed. In conscious humans, Sasse et al. showed that changes of paO_2 and $paCO_2$ occur only after 10s of breath-holding, although the time needed for blood distribution to the artery measured may account for this delay, and a similarly there would be a delay in blood distribution to the myocardium as well from the lungs[84]. Thus, activation of other responses that manipulate the coronary flow may occur early in the breath-hold before arterial blood gases change. Pulmonary stretch receptors and redirection of blood flow to the heart by sympathetically activated peripheral vasoconstriction have been suggested as other mechanisms of coronary flow change, not specifically related to the blood gases[123–125].

0.7 Coronary Artery Disease Versus Microvascular Disease

Although coronary artery disease is traditionally thought of as a disease with significant stenoses in the epicardial coronary arteries, more than a third of patients who have chest pain and suspected CAD do not have detectable culprit lesions in their coronary angiogram [126]. As such symptoms reflect a mismatch between oxygen demand and supply due to inadequate regulation of blood flow, microvascular dysfunction has become an important diagnostic target, especially in women[127].

Coronary Microvascular Disease (CMVD)

CMVD can correspond with a limited vasodilatory capacity or an increased vasoconstrictor response. Both of these aspects can be assessed with the combined breathing maneuver, HVBH, which uses hyperventilation as a vasoconstrictor, and a long breath-hold, to trigger a vasodilatory response. As described in section 0.6, the microvasculature controls the blood supply to the heart, and thus even in the absence of coronary artery stenosis, microvascular dysfunction can cause myocardial ischemia (Figure 10B).

Isolated CMVD has also been called cardiac syndrome X, defined by the presence of chest pain without associated significant coronary stenosis[128]. In a long-term follow-up study, these patients still showed a significantly increased mortality and serious cardiac events[129]. Traditionally, a pitfall of diagnosing microvascular disease was the lack of methods able to directly assess the microvascular component. Rather, CMVD was often diagnosed if a patient had cardiac symptoms with no other observable reasons for these symptoms. Modern imaging modalities are now able to assess microvascular dysfunction, although standard strategies often use nuclear cardiology techniques and require an injection of pharmacological agents. Research using such technologies has provided evidence that CMVD can present alone as primary coronary microvascular dysfunction[58], but is commonly found along with CAD, diabetes, hypertension, and cardiac transplants. Due to the heterogeneity of CMVD, 5 major classifications were proposed (Table 4,[102]). Although CMVD is still not well understood due to the diversity of the disease and previous inability to measure microvascular function, newer imaging modalities are rapidly advancing the knowledge of the disease. By being able to detect and classify CMVD, treatment strategies can be better targeted, creating the potential for more cost-effective and successful treatments.

	CMVD Type	Causes	Specific Diseases
1	In the absence of obstructive CAD and myocardial diseases	Caused by traditional risk factors, smoking, diabetes, hypertension, etc., Partly reversible	Microvascular angina,
2	In the presence of myocardial diseases	Adverse remodelling of intramural coronary arterioles	Found in genetic and secondary cardiomyopathies Hypertrophic cardiomyopathy, congestive cardiomyopathy, myocarditis, aortic stenosis
3	In the presence of CAD	In CAD and acute coronary syndrome	Coronary syndrome, stable angina,
4	Iatrogeneic	After recanalization, caused by vasoconstriction or distal embolization,	Percutaneous coronary intervention Coronary aortic bypass graft
5	Post-heart transplant	Alterations in autonomic tone, inflammation and immune mechanisms	Specific to Heart Transplant

Table 4: Clinical classifications of CMVD,
Adapted from Camici, 2007[102].

Coronary Artery Disease in the Absence of CMVD

On the other hand, it is also possible that even obstructive CAD can be non-symptomatic because of a preserved microvascular function (Figure 10C)[130]. Thus even in the presence of a pathologic FFR or QCA result, tissue assessment of perfusion or oxygenation can show normal results. Consequently, there is debate on whether stenosed vessels should always be revascularized, or if patients who are stable with a clean microvascular function should avoid the procedure, highlighting the clinical importance of assessing coronary vascular function[130,131].

Imaging Coronary Microvasculature

The ability to image microvascular disease has not always been feasible, and thus diagnosis of CMVD relied on the more traditional methods for imaging ischemia (Figure 9). In addition to symptoms and electrocardiography, imaging modalities focused on the epicardial arteries and the microvascular function was indirectly predicted from these results. While the primary intent of angiography is to visualize the size and location of coronary lesions, some aspects of microvascular function can be observed by the tracking the passage of the contrast agent through the heart (TIMI frame count/myocardial perfusion grade)[132]. Other methods assess the haemodynamic function of the coronary arteries, as these large vessels could are fairly easy to access with intracoronary measurement tools. Fractional flow reserve (FFR) is the primary technique used to assess the functional relevance of a stenosis and if blood supply is significantly hindered during hyperaemia. From this response an indirect assessment of the microvascular resistance during hyperaemia (HMR) can be calculated[133]. Similarly, coronary thermodilution also involves the placement of a measurement device in the coronary arteries. Based on the diffusion time of contrast agent, thermodilution can be used to assess coronary flow and calculate the index of microcirculatory resistance (IMR) based on the measurements in the coronary arteries[133]. These calculations about the microvasculature are based on the theory that epicardial coronary flow reserve is ultimately affected by the microvascular resistance (section 0.6). Yet, these tests require invasive

measurements to place devices inside the heart, and they are not a functional assessment on the effects to the myocardium nor do they directly assess ischemia.

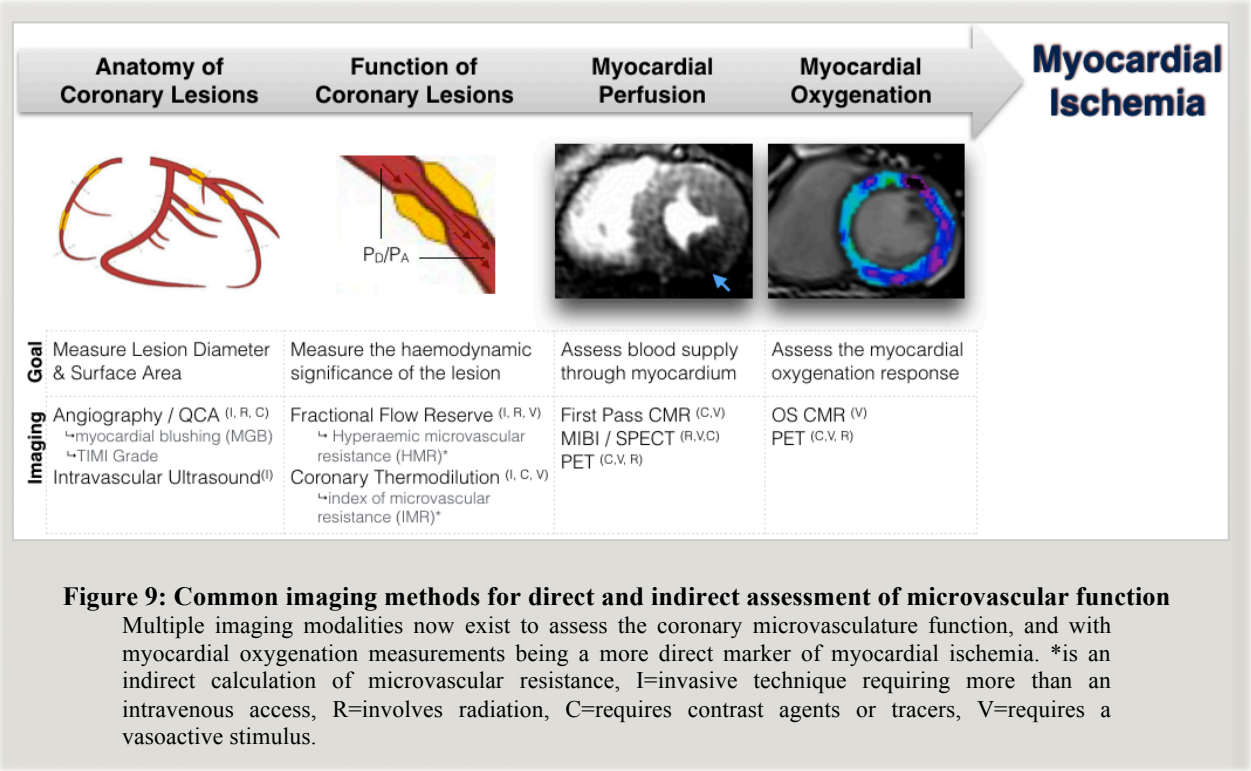

Figure 9: Common imaging methods for direct and indirect assessment of microvascular function
Multiple imaging modalities now exist to assess the coronary microvasculature function, and with myocardial oxygenation measurements being a more direct marker of myocardial ischemia. *is an indirect calculation of microvascular resistance, I=invasive technique requiring more than an intravenous access, R=involves radiation, C=requires contrast agents or tracers, V=requires a vasoactive stimulus.

As stated above, microvascular dysfunction can occur in the presence or absence of coronary lesions. While the microvasculature can't be directly measured *in vivo*, non-invasive measurements can reflect the microvascular function by measuring the myocardial response. MRI and nuclear imaging both developed methods to assess the perfusion of the myocardium during a vasoactive stimulus, using the surrogate markers for blood supply (mainly cumulative tracer uptake or first-pass contrast agent inflow) as a marker of microvascular function. However, first-pass perfusion CMR requires contrast agents and vasodilators (section 0.6), while nuclear imaging (PET, SPECT) requires vasodilators, specialized tracers, and involves exposure to radioactivity.

While ischemia is caused by inadequate blood supply, the actual direct marker would be tissue oxygenation as the cellular mismatch is the direct effector on cellular function and injury. Thus new techniques such as oxygen based PET imaging and oxygenation-sensitive

CMR are the most direct measurement of myocardial vascular dysfunction or ischemia. And with the development of vasoactive breathing maneuvers instead of infused pharmacological vasodilators, OS-CMR has the potential to be a fully non-invasive as well as stress- and radiation-free technique to assess for regional microvascular function or inducible ischemia.

Territorial Assessments

In CAD with significant proximal stenosis (which are also the most important for interventional therapy), oxygenation deficits typically show a rather uniform regional distribution within a coronary territory[38,39]. On the other hand, with microvascular disease, it can be more difficult to localize and classify ischemia, as the deficits are often more diffuse and dysfunctional arterioles are more globally distributed[103]. In addition to different distribution patterns, the inner myocardial layer consumes more oxygen, and is exposed to a lower perfusion pressure (competing with the intraventricular pressure) and thus more likely to develop ischemia[103]. It is therefore important to have sensitive techniques to detect minor changes in oxygenation of the tissue, as well as detect small regional abnormalities.

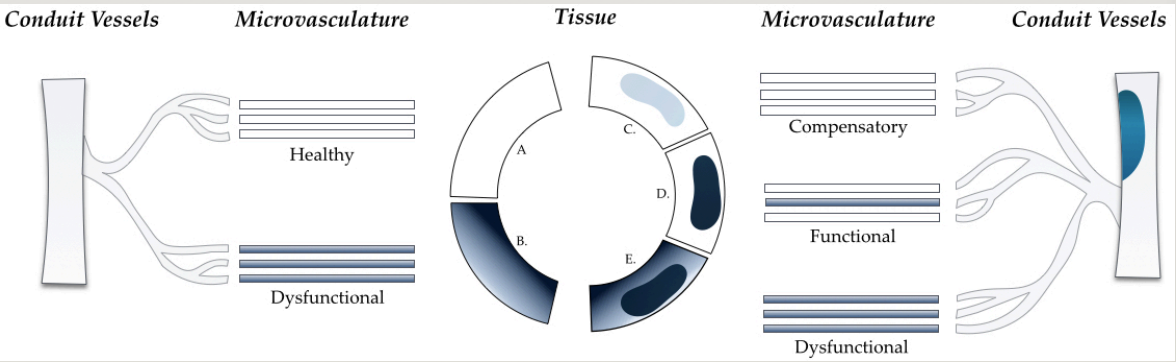

Figure 10: Balance between epicardial and microvessel function on myocardial ischemia
Perfusion of the myocardium relies on both the function of the micro- and conduit vessels (i.e. coronary arteries), with healthy shown as white, and dysfunction as dark. In the presence of healthy coronary arteries (left), healthy microvasculature will result in normally perfused tissue (A), whereas dysfunctional microvessels may cause a diffuse ischemia (B). On the right, microvascular dysfunction can be both present and absent in the presence of a coronary stenosis. Fully functioning microvasculature may actually compensate for the coronary stenosis, and there may be little damage to the tissue (C.). Common presentation is for some microvascular dysfunction, in with there is a defined region of ischemia due to the stenosis (D), or a combination of both can lead to an overall ischemia (E). Adapted from Lanza 2010, and Crea 2014[58,130].

In this project, coronary artery stenosis is assessed both in the presence and absence of microvascular dysfunction. Part 1 (chapters 1-3) involves a controlled animal model, in which a severe coronary artery stenosis was created in an otherwise healthy animal, resulting in a simulated acute coronary stenosis without any microvascular dysfunction (Figure 10C). Part 3 (chapter 5) assesses a clinical scenario, where cardiac patients have verified coronary artery stenosis with a possibility of with microvascular dysfunction.

Part 1: Assessing breathing maneuvers and the effect of arterial blood gases in an experimental animal model

Foreword

Part 1 describes the three articles that have been produced from the single animal study "Cardiovascular Response of Oxygenation during Swine Breathing (CROSB)", performed at the Montreal Heart Institute.

Chapter 1 and 2 pertain to the primary objective of the project, which is to investigate the use of breathing maneuvers as a vasoactive stimulus, and how this can be used to assess myocardial oxygenation deficits. With the animal model, invasive measurements such as coronary sinus blood gases and coronary flow of the LAD coronary artery can be reliably performed in a very controlled experimental; environment and compared with OS-CMR results. As a result, we can more precisely define how the OS-CMR results relate to the physiological changes in the heart.

Chapter 3 has a more clinical intent. OS-CMR is used as a measurement to evaluate myocardial oxygenation in the presence of coronary artery stenosis, and how oxygenation is compromised when supplemental oxygen is administered.

Funding was provided by the Montreal Heart Institute Foundation, the Canadian Foundation for Innovation, and the Fonds de Recherche Santé Québec.

Acknowledgements

In addition to the author list, I would like to acknowledge the help of Gobinath Nadeshalingham, Janelle Yu, Stefan Huettenmoser, Camilo Molina, and the members of the Philippa and Marvin Carsley CMR Research Centre for assisting with the experiments. In addition, to Radiometer Canada for providing an ABL 780 blood gas analyzer and St. Jude Medical Canada for providing a Fractional Flow Reserve Machine.

1 Chapter 1 - Breathing Manoeuvres as a Vasoactive Stimulus for Detecting Inducible Myocardial Ischemia – an Experimental Cardiovascular Magnetic Resonance Study

Foreword

This study provides the foundation of the experimental assessment of the utility of breathing maneuver. In an animal model we could directly compare the results from the CMR images to invasively measured parameters such as blood flow of the coronary artery, and blood gas levels of both the arterial blood and in the coronary sinus to determine which parameters are affecting the myocardial oxygenation during the breathing maneuvers. Additionally, this study compares multiple breathing maneuvers directly to the current clinical standard of pharmacological-induced vasodilation, to help determine the best breathing maneuver protocol for subsequent studies. This is the first project to show that in the presence of significant coronary stenosis, there is an abnormal oxygenation response during the vasoactive breathing maneuver.

Data from this chapter was presented at the 2014 European Society of Cardiovascular Magnetic Resonance (EuroCMR) congress in Vienna, Austria, and was the best oral presentation of the congress.

Breathing Maneuvers as a Vasoactive Stimulus for Detecting Inducible Myocardial Ischemia – an Experimental Cardiovascular Magnetic Resonance Study

Kady Fischer, BHSc;[a,b] Dominik P Guensch, MD;[a,b] Nancy Shie, BSc;[a] Julie Lebel, RLAT;[a, c] Matthias G Friedrich, MD[a,d,e,f,g]

[a]Philippa & Marvin Carsley CMR Centre at the Montreal Heart Institute, Université de Montréal, Montreal, Canada,

[b]Bern University Hospital, Department Anaesthesiology and Pain Therapy, Bern, Switzerland,

[c]McGill University Health Centre Research Institute, Montreal, Canada;

[d]Departments of Radiology, Université de Montréal, Montreal, Canada;

[e]Departments of Medicine and Diagnostic Radiology, McGill University, Montreal, Canada

[f]Department of Cardiology, Heidelberg University Hospital, Heidelberg, Germany

[g]Departments of Cardiac Sciences and Radiology, University of Calgary, Calgary, Canada

Short Title: Blunted Oxygenation in Coronary Artery Stenosis

All authors have read and approved the manuscript. The presented version dates from January 2016 and is currently in the process of being submitted to peer-reviewed journals.

1.1 Abstract

Background: Breathing maneuvers can elicit a similar vascular response as vasodilatory agents like adenosine; yet, their potential diagnostic utility in the presence of coronary artery stenosis is unknown. We hypothesized that breathing maneuvers can non-invasively detect inducible ischemia when combined with oxygenation-sensitive cardiovascular magnetic resonance (OS-CMR).

Methods and Results: In 11 swine with experimentally induced significant stenosis (fractional flow reserve <0.75) of the left anterior descending coronary artery (LAD) and 9 control animals, OS-CMR at 3T was performed during two different breathing maneuvers, a long breath-hold; and a long breath-hold following 60s hyperventilation. The resulting change of coronary blood flow and myocardial oxygenation was compared to that induced by iv adenosine infusion. In control animals, hyperventilation decreased coronary blood flow (-34±23%), while flow increased with adenosine infusion (15±16%), a long breath-hold (97±88%), and with a long breath-hold following hyperventilation (346±327%). In animals with stenosis, breathing maneuvers attenuated the flow response significantly more than adenosine. Breath-holds following hyperventilation consistently yielded a significant difference in the observed oxygenation response between the perfusion territory of the stenosed LAD and remote myocardium (-3.9±5.3% vs. +2.5±4.2% by end of breath-hold, P=0.001), while this response was uniform in control.

Conclusion: The myocardial oxygenation response to hyperventilation with subsequent breath-holding is blunted in myocardium subtended by a severely stenotic coronary artery. Breathing maneuvers may be useful for diagnostic testing in patients with suspected coronary artery disease.

Keywords: Magnetic Resonance Imaging ▪ Oxygen ▪ Myocardial Ischemia ▪ Breathing Exercises ▪ Adenosine ▪ Experimental Model

1.2 Translational Prospective

We present here the first findings of using oxygenation-sensitive cardiovascular magnetic resonance (OS-CMR) imaging and breathing maneuvers to detect haemodynamically relevant coronary artery stenosis. Recent studies have verified that breathing maneuvers induce a myocardial oxygenation response in healthy humans, providing a possible alternative to pharmacological agents such as intravenous adenosine. Our study provides invasive findings of coronary blood flow and blood gases confirming the effects on the cardiac system during breathing maneuvers, and how these data relate to the detection of myocardial oxygenation deficits with CMR. This study is of importance in regard to both the clinical translation of OS-CMR for the assessment of suspected myocardial ischemia in patients. This technique may allow for a physiologic stress test for microvascular and microvascular disease without using any stress agents or contrast media.

1.3 Introduction

The numbers for prescribed cardiac diagnostic tests and interventions are rapidly growing[1]. Notably, imaging for inducible myocardial ischemia or coronary artery stenosis has become on of the of the most critical cost factors in today's health care systems [2]. While imaging techniques such as stress echocardiography and nuclear cardiology are generally very useful for identifying ischemia-producing coronary artery stenosis, they require pharmacological or physical stress protocols. Nuclear techniques are also limited by radioactivity of tracers. Cardiovascular magnetic resonance imaging (CMR) can identify significant coronary artery stenosis without radiation, commonly using either dobutamine stress or first-pass perfusion protocols[134,135]. Yet again, infusion of pharmacological stress agents is required.

As a newer technique, oxygenation-sensitive CMR (OS-CMR) imaging allows for monitoring changes of myocardial oxygenation, based on the so-called blood oxygen level-dependent (BOLD) effect: A reduction of tissue oxygenation leads to a relative decrease of oxyhaemoglobin and a relative increase of deoxyhaemoglobin, which in turn causes a signal

intensity (SI) drop in CMR images sensitive to this effect[23]. In the presence of a stenosis, this effect can be augmented further by post-stenotic capillary recruitment[31]. OS-CMR differs from perfusion imaging techniques in that it directly reflects the oxygenation status of the tissue instead of using surrogate markers such as perfusion or blood flow.

In functional MRI studies of the brain and, more recently, the heart, alterations of blood gases by breathing maneuvers or inhalation of gas mixtures were identified as an alternative to pharmacologic vasodilation[71,100,112]. In particular, a combination of hyperventilation and breath-holds with OS-CMR yielded promising results in monitoring changes of myocardial oxygenation induced by vasoactivity[82,83,111], yet its clinical potential to identify myocardium exposed to a severely stenotic coronary artery has not been explored. As the vascular response to breathing maneuvers is also dependent on the presence of a patent coronary artery, OS-CMR with breathing maneuvers appears to have a very strong potential to identify severe coronary artery stenosis. We therefore hypothesized that breathing maneuvers, especially a long breath-hold following hyperventilation, lead to a blunted oxygenation response in myocardium exposed to severe coronary artery stenosis in comparison to normally perfused tissue.

1.4 Methods

Animal Preparation

This study was conducted in accordance with the Guide to the Care and Use of Experimental Animals by the Canadian Council on Animal Care and approved by the local Animal Care and Use Board. Twenty healthy swine (33±1kg, Yorkshire-Landrace) were included. Another study performed in the same animals group was recently published[136]. The swine were pre-medicated by intramuscular injection of 4ml Telazol (200mg tiletamine, 200mg zolazepam) and 0.8mg atropine. Anaesthesia was induced with propofol (2-4mg/kg, i.v.) prior to intubation, and maintained with continuous propofol (4-36 mg/kg/hr, i.v.) and remifentanil (0-3.5µg/kg/min, i.v.) infusion as required. Amiodarone (75mg i.v.) was infused, and serum electrolytes were corrected to normal values to prevent arrhythmia[137]. The femoral

vein was cannulated for drug and fluid administration, while the femoral artery was used for haemodynamic monitoring and arterial blood gas analyses. A right jugular vein sheath was placed to provide access to the coronary sinus for venous blood gas analyses. A left-sided thoracotomy was performed for the placement of an MR-compatible perivascular flow probe on the proximal left anterior descending (LAD) coronary artery (Transonic Systems, Ithica, NY, USA). Nine animals served as controls, while eleven animals were allocated to undergo a LAD stenosis protocol. After instrumentation, a bolus of 5000U Heparin was administered to prevent clotting.

Stenosis Protocol

A perivascular hydraulic occluder (In Vivo Metric, CA, USA) was used to constrict the LAD adjacent to the flow probe (Figure 11). Vasodilation was induced with 140µg/kg/min adenosine administered through a central vein. FFR was measured with a coronary pressure guidewire (St. Jude Medical, MN, USA). Concurrently, the occluder was inflated to constrict the vessel until a stable FFR reading of <0.75 was reached. This occlusion was maintained throughout the study. Control animals were considered to have an FFR of 1.0.

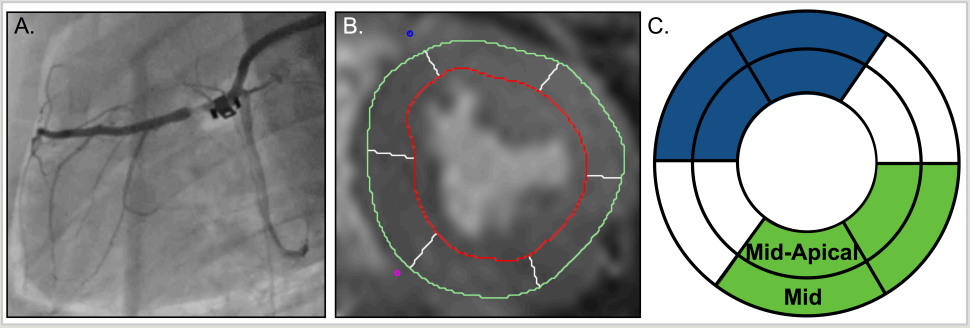

Figure 11: Experimental Set-up.
A. Fluoroscopy image of the left anterior descending (LAD) coronary artery with the perivascular occluder the flow probe in place. B. Example of OS-CMR image with AHA automatic segmentation. C. Assignment of segments to LAD territory (blue) and remote myocardium (green), excluding the segments with possible mixed perfusion.

Quantitative Coronary Angiography

Quantitative coronary angiography (QCA) was performed prior to CMR imaging using a standard protocol[138]. Minimal LAD diameters were measured in the occluder-obstructed area, for the stenosis group, or distal to the flow probe for the control animals using the online single-plane view imaging system (model 1.2.3; Electromed International, QC, Canada).

Experimental Protocol

Animals were transferred to an MRI suite and were continuously monitored for invasive blood pressure, heart rate, peripheral saturation (SpO_2) and end-tidal carbon dioxide ($EtCO_2$). Unless specified, arterial blood gases were maintained at a baseline normoxic (paO_2=100mmHg) and normocapnic ($paCO_2$=40mmHg) levels, targeted through ventilation adjustments. CMR images were acquired with a clinical 3T MRI system (MAGNETOM Skyra 3T; Siemens Healthcare, Erlangen, Germany) using an 18-channel cardiac phased array coil. All images were obtained during breath-holds, created by a pause in ventilation at end-expiration, after a passive exhalation. Left ventricular (LV) function was imaged with standard balanced steady-state free precession (SSFP) cine in a short-axis stack. Then, OS-CMR imaging was performed for two short axis slices, mid-ventricular and mid-apical distal to the blood flow probe, using a previously published ECG triggered SSFP sequence[47] with each of the three maneuvers conducted in random order:

- HV/HVBH: a combined hyperventilation and breath-hold. After baseline OS-CMR images were obtained, animals were manually hyperventilated (HV) for 60s, at a rate of 30-40 breaths/min with a ventilator bag and an additional supplement of 2-4L/min of oxygen to maintain normoxia. This was immediately followed with a 60-90s breath-hold (HVBH). Images were acquired continuously during breath-holds.
- LBH: long breath-hold. A breath-hold of 60s was performed from the baseline level and imaged continuously.

- Adenosine: A measurement was obtained before and after 3 minutes of adenosine infusion (140µg/kg/min). These images served as reference for maximal pharmacological vasodilatation.

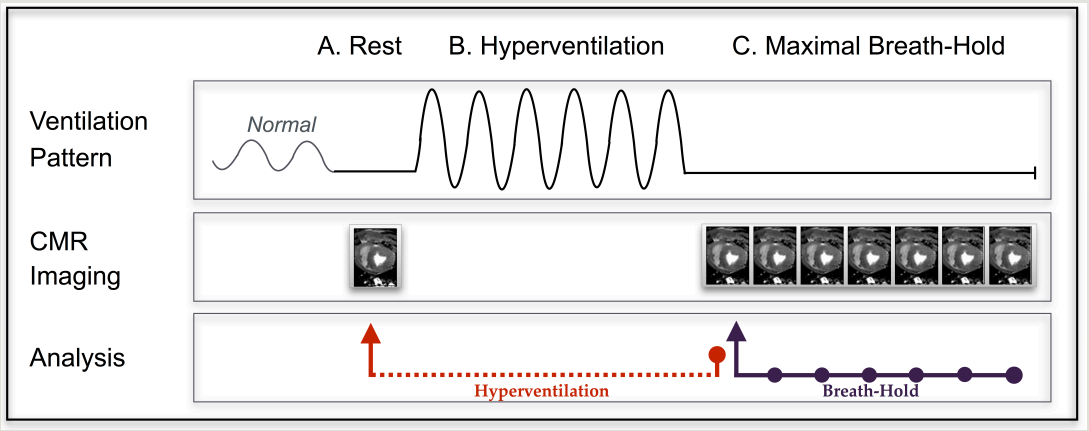

Figure 12: Chapter 1 breathing maneuver protocol and invasive measurements
For the combined hyperventilation breath-hold (HVBH) maneuver, a single rest image was obtained in a short breath-hold (A). The animal was then manually hyperventilated for 60s (B) followed immediately by a long breath-hold (C) that was imaged throughout, with a repeating OS sequence. Hyperventilation analysis was always compared between rest and the start of the breath-hold (red), while the breath-hold could be analyzed at multiple time points with comparison to data obtained at the beginning of the breath-hold (purple). The long breath-hold (LBH) followed step C, starting after a normal ventilation pattern.

At the beginning and end of each maneuver, the following invasive measurements were recorded: coronary blood flow, arterial blood gases, coronary sinus blood gases, heart-rate, invasive blood pressure and SpO_2. The myocardial oxygen extraction ratio (O_2er) was calculated from the oxygen content of the arterial (CaO_2) and coronary sinus blood ($CcsO_2$), [$O_2er=(CaO_2-CcsO_2) / CaO_2$].

Image Analysis

All CMR images were de-identified prior to analysis. For the OS-CMR images, the myocardial oxygenation response from the end-systolic images was expressed as the %-change in signal intensity (ΔSI[%]) from the maneuver to baseline (cvi[42], Circle Cardiovascular Imaging, Calgary, AB, Canada). For each group, ΔSI[%] of the LAD territory,

defined as the anteroseptal and anterior segments in mid-ventricular and mid-apical slices was averaged, and the remote region was obtained from the inferior and inferolateral wall (Figure 11). The segments from the inferoseptal and the anterolateral wall were not included in the direct comparisons due to a known possible mixed perfusion pattern[8]. Segments were entirely excluded if more than 33% of the segment area was removed during analysis due to artifact.

Statistical Analysis

Data is expressed as mean±SD. Continuous variables were assessed for normal distribution with the D'Agostino-Pearson test. Paired t-tests were used to compare the changes in variables from baseline within an animal, while independent t-tests compared data between groups. If both analyses were needed, a two-way mixed ANOVA with multiple comparisons analysis was performed. Specifically, for the OS-CMR data, the ΔSI[%] response of the LAD region in stenotic animals was compared to the remote tissue to determine a regional abnormality, and to the control animals at the same time point using a mixed two-way model. Associations between ΔSI[%] of the LAD region of all animals and FFR, O_2er, SaO_2, and coronary flow were assessed with Pearson's correlation. The breath-holds were further visualized by plotting the ΔSI[%] over time, fitted by a least-squares non-linear regression. For assessing inter-observer reliability, 54 randomly selected OS-images from 10 animals were read by an independent second reader and assessed with a two-way mixed intraclass-correlation test. Tests were performed with GraphPad Prism version 6.0 for mac (GraphPad Software, La Jolla California USA) and SPSS version 21 (SPSS IBM, New York, USA). Results were considered statistically significant with a two-tailed $P<0.05$.

1.5 Results

Eight control animals successfully completed all maneuvers; one death occurred during surgery. In the stenosis group, one death occurred during the creation of the stenosis, and a second prior to the adenosine infusion. Thus this group had 10 animals for the breathing maneuvers, and 9 for the adenosine analysis. Anaesthetics were adjusted per animal to

provide sufficient anaesthesia depth. After surgery, a higher average dose and range of remifentanil was required for control animals than the stenosed animals (0.26±0.42 (0 to 1.28) vs. 0.07±0.17 (0 to 0.55) µg/kg/min, *P*=0.009), with an equal dose of propofol (19.4±4.7 (15.5 to 33.0) vs. 16.5±4.3 (9.5 to 22.0) mg/kg/hr, *P*=0.198).

Parameter	Control (n=8)	Stenosed (n=10)	P
O_2er (%)	47±8	67±13	0.001
EF (%)	54±11	48±10	0.262
CO (L/min)	2.8±0.8	2.1±0.5	0.041
HR (beats/min)	93±14	84±18	0.282
Coronary artery stenosis			
QCA, %-Diameter	7±7	63±11	<0.001
QCA, %-Surface Area	11±8	85±6	<0.001
FFR	N/A	0.63±0.05	

Table 5: Baseline function and angiography

Mean±SD values of the baseline myocardial oxygen extraction ratio (O_2er), ejection fraction (EF), cardiac output (CO), heart rate (HR) as well as the %-decrease in diameter and surface area of the LAD obtained from quantitative coronary angiography (QCA), and the fractional flow reserve value (FFR=Distal Pressure / Proximal Pressure to the stenosis).

Fractional Flow Reserve, Quantitative Angiography and Coronary Flow

All induced coronary artery stenoses were severe, based on QCA measurements (Table 5) and haemodynamically significant, with a mean FFR of 0.63±0.05 (range 0.54-0.74). The control animals had insignificant LAD diameter reductions (7±7%).

In control animals, all breathing maneuvers had a statistically significant impact on coronary blood flow (Figure 13). While hyperventilation decreased coronary blood flow by 34±23% (*P*<0.001), the other maneuvers had vasodilating properties. Interestingly, breath-holds had a significantly stronger effect with LBH having a more than 6-fold increase (97±88%, *P*=0.005 vs baseline), and the HVBH having a 23-fold stronger response than adenosine (346±327%, *P*=0.001 vs baseline). For the stenosis group, the two breathing maneuvers of HV (-12±6%, *P*=0.032 vs baseline) and HVBH (+82±110%, *P*=0.278 vs baseline) were the only methods to show an attenuated flow response on comparison to the control (Table 7). For the LBH the change in flow for stenosed arteries (40±60%) was not

different from that in control animals. Adenosine did not yield any significant changes for control or stenotic animals (15±16%, 13±27%, P=0.204).

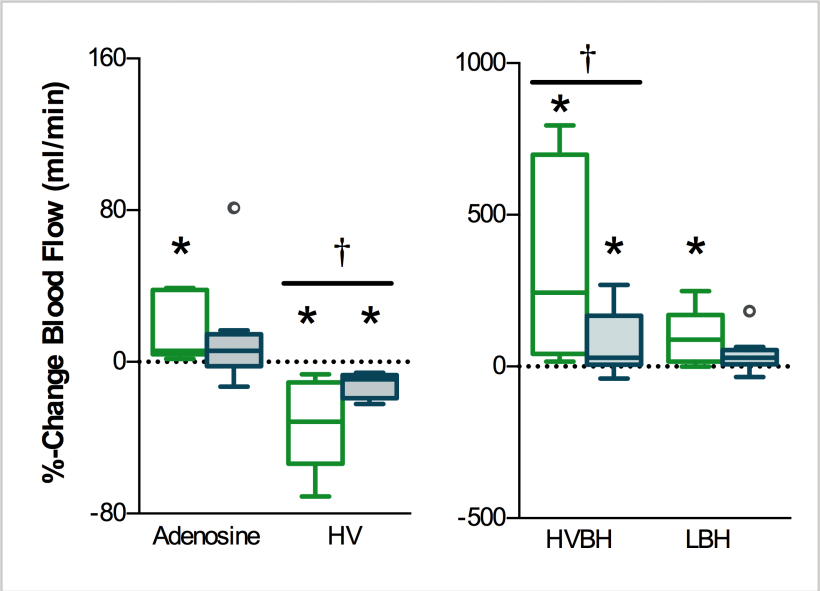

Figure 13: Changes of coronary blood flow during breathing maneuvers. Mean (min to max) %-change of coronary blood flow (ml/min) induced by adenosine and breathing maneuvers in control (green) and stenosis (blue) animals. All maneuvers significantly changed flow from baseline (*P<0.05, Table 7) for control animals. Both HV and HVBH demonstrated a significant decreased flow response in the stenosed animals (†P<0.05, circles are outliers).

Ventricular Function

The stenosis group had a lower cardiac output, while there was no significant difference of the left ejection fraction, (Table 5). Baseline heart rate was not significantly different between the groups.

Blood Gases and Oxygen Extraction Ratio

Breathing maneuvers significantly affected arterial and coronary sinus blood gas values (Table 7). While hyperventilation decreased pCO_2 and increased pO_2, an opposite effect was induced by the breath-holds, HVBH and LBH. Most changes did not statistically differ between groups. In animals with coronary artery stenosis however, there was a 22±11%

greater drop in SaO_2 than control (P=0.014) during HVBH and a 25±11% greater drop during the LBH (P=0.005). Adenosine infusion in the stenosed group was the only maneuver that induced a change in O_2er (-5±4%, P =0.014, Table 7). Furthermore, while baseline O_2er was significantly higher in the stenosed than in control animals (47±8% vs. 67±13%, P <0.001) changes in O_2er during each maneuver from these baselines did not significantly differ between groups.

OS-CMR Image Quality

Image quality was good and only 4.2% of segments had to be excluded from the analysis (2.7% and 5.7% of mid and mid-apical slice of segments, respectively). Agreement between the readers was acceptable (ICC: 0.80, 95%CI: 0.66-0.89).

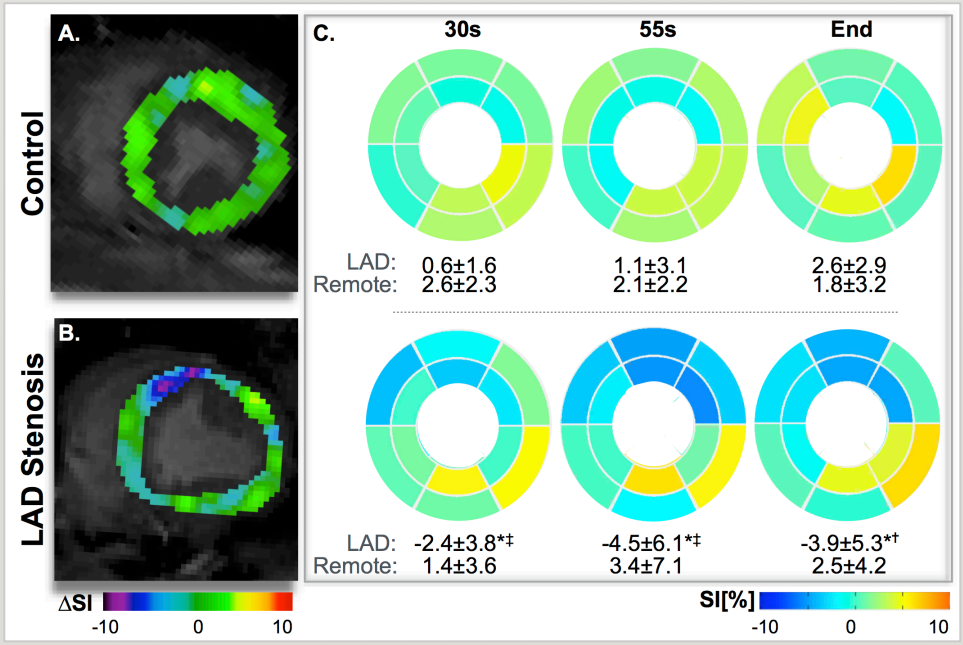

Figure 14: Segmental changes of myocardial oxygenation during the HVBH.
Subtraction images (smoothed using a 6mm Gaussian filter) demonstrate that at the 30s time-point, myocardial SI increased homogenously in the control animal (A) from the beginning of the breath-hold, while a decrease was observed in the territory of the LAD stenosis (B). Mean myocardial response (ΔSI[%]) for each segment from all animals similarly shows that in control animals (top row, n=8), ΔSI[%] increases consistently for all segments, whereas for the LAD stenosis animals (bottom row, n=10) in the LAD regions a significant decrease is already observed at 30s, and this continues throughout the breath-hold. (*P<0.05 between LAD and remote territory within the group, †P<0.05, <0.05‡P<0.01 for the difference in LAD response between groups).

Myocardial Oxygenation

Adenosine infusion had a negligible effect on myocardial oxygenation, which did not achieve statistical significance for either the control (LAD: 0.8±3.2%, remote: 0.4±2.0%) or stenosed groups (LAD: 0.3±3.5%, remote: 0.5±4.1%). On the other hand, a consistent significant reduction was observed in the LAD region with the HVBH in stenosed animals (Figure 14). _Hyperventilation alone did not induce any significant changes in the ΔSI[%], (control LAD: -0.2±2.6%, remote; -2.3±4.4%, and stenosed LAD: -0.7±2.6%, remote; -2.8±6.1%). The following breath-hold (HVBH) showed that by 30s into the breath-hold after hyperventilation the SI of the LAD region had already dropped by 2.4±3.8% in the presence of a stenosis (Figure 15). The response in this region was significantly lower (P=0.001) than in remote myocardium, and showed a trend towards a lower values than control animals (P=0.090). In remote myocardium, SI increased by 1.4±3.6%, consistent with observations in both regions of control animals (LAD: +0.6±1.6%, remote: +2.6±2.3%). The LAD signal of the stenosed animals continued to decrease throughout the breath-hold ending at -3.9±5.3 below baseline, while all other regions remained above baseline (P=0.001).

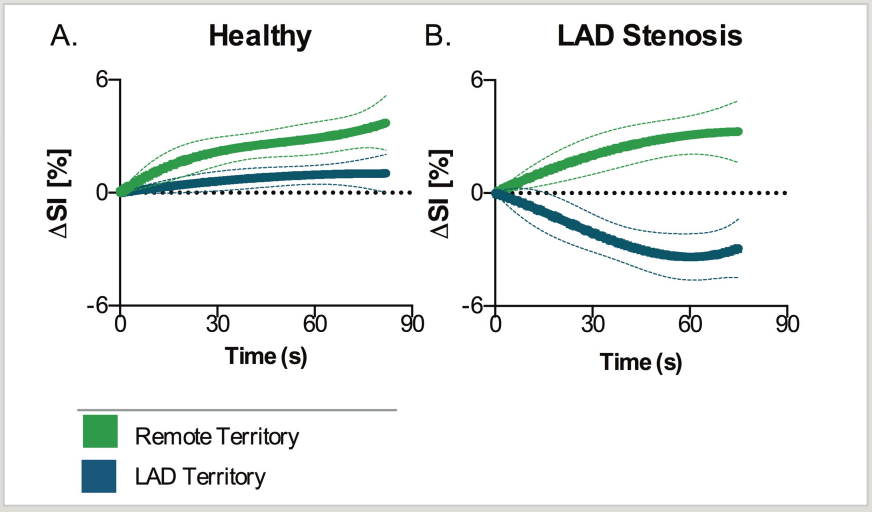

Figure 15: Mean myocardial oxygenation response curve during the HVBH. Signal intensity increases globally during the HVBH in control animals (A), yet the animals with a stenosis (B) show a significant decrease in the LAD territory (blue), while the remote region (green) remains above baseline with a similar characteristic of the control animals.

For the other breath-hold, the LBH, at 30s the LAD segments of the stenosed animals (-1.9±1.0%) were non-significantly lower than the control LAD region (0.5±2.1%, P=0.100), but this difference disappeared was not observed by the end of the maneuver (-2.9±2.9% vs -0.7±6.0%). Furthermore in this maneuver, regional abnormalities were not observed, although the LBH caused SI in the remote territories to drop below baseline for both the stenosed (30s: -1.0±3.1%, end: -1.0±3.6) and control groups (30s: -0.3±3.2%, end: -2.8±3.2%), resulting in an overall decrease.

Dependent Variable ΔSI-LAD		Independent Variables	Correlation Coefficient	P Value
Adenosine		FFR	0.173	0.508
		Flow	0.163	0.545
		O_2er	-0.170	0.529
HV		FFR	0.056	0.826
		Flow	-0.153	0.543
		O_2er	-0.107	0.120
HVBH				
	30s	FFR	0.461	0.040
	55s	FFR	0.478	0.043
	End	FFR	0.604	0.009
		Flow	0.465	0.040
		O_2er	0.237	0.360
		SaO_2	0.388	0.171
LBH				
	30s	FFR	0.655	0.003
	End	FFR	0.145	0.288
		Flow	0.045	0.864
		O_2er	-0.012	0.964
		SaO_2	0.127	0.616

Table 6: Correlation of the regional oxygenation response with measurements
Pearson's correlation (n=18) was performed for all breathing maneuvers with the oxygenation response (ΔSI%) of the LAD perfused territory as the dependent variable. All time points were compared to FFR, and to changes in LAD flow, oxygen extraction ratio (O_2er), arterial saturation (SaO_2).

Relation to Other Measurements

The ΔSI[%] in the LAD region of the HVBH was well correlated with the FFR at all time-points in the breath-hold (Table 6). Furthermore, HVBH was the only maneuver that was closely related to the change in coronary blood flow. During the LBH, only the SI response at the early time point, 30s, was correlated to FFR. No significant relationships were observed with oxygenation responses from adenosine or hyperventilation.

1.6 Discussion

Our results indicate that the oxygenation response to a combined breathing maneuver of hyperventilation followed by apnea is significantly altered in the presence of an acute yet severe coronary artery stenosis. This breathing maneuver may therefore have potential for diagnostic purposes as an alternative to pharmacological vasodilators.

Currently, the administration of pharmacologic agents such as adenosine is considered the standard procedure for assessing vascular function by inducing vasodilatation. We could recently show that in healthy humans, the HVBH maneuver may yield greater changes in myocardial oxygenation than standard peripheral iv infusion of adenosine[47], which is expected to induce near-maximal coronary vasodilatation[139]. In this experimental animal study, we found that the combination of OS-CMR with a combined breathing maneuver (HVBH) consistently revealed regional myocardial oxygenation abnormalities caused by significant coronary artery stenosis.

The data are consistent with and extend the current understanding of coronary vascular physiology. An altered change of regional myocardial oxygenation due to a blunted coronary vascular response to pharmacological vasodilation has been reported[67]. Breathing maneuvers appear suitable to assess vascular reactivity because of their impact on blood gas levels: Apnea leads to hypercapnia and hypoxia, which triggers vasodilation, while hyperventilation with associated hypocapnia and hyperoxia induce vasoconstriction[101,110]. By using a combined breathing maneuver, mild hypocapnia can be induced by hyperventilation, allowing for a greater range of CO_2 changes to be tolerated during a subsequent breath-hold[85,86]. Thus greater changes in coronary blood flow and subsequently oxygenation are expected to occur. The specific value of observing the vasoconstrictive response in combination with a subsequent vasodilatation in patients needs to be further assessed; yet it may increase the diagnostic yield.

Impact on Coronary Blood Flow and Myocardial Oxygenation

During adenosine infusion, blood gases and oxygen saturation did not change between baseline and vasodilatation; thus, changes in OS-CMR during adenosine infusion may be more

likely due to pure pharmacological vasodilation and the resulting increase in coronary blood flow, without a confounding effect of blood gases. However, the response to adenosine was weaker than expected, suggesting that our anaesthetic model may attenuate adenosine effects. In the LAD territory, breathing maneuvers induced a much stronger response of coronary blood flow. In addition, a clear distinction in the coronary flow response between control and stenosed animals was observed with the breathing maneuvers. This was paralleled by marked regional differences of myocardial oxygenation during the HVBH maneuver between hypoperfused and remote myocardium.

Comparison Between Breathing Maneuvers and Adenosine

Standard adenosine protocols provide binary snapshots during baseline with vasodilatation. Breathing maneuvers on the other hand also allows for data acquisition over time and thus may provide additional information with respect to the duration, slope and overall dynamic of the vascular response. As a potential disadvantage, changes of the saturation of incoming blood and of the cardiac workload during the maneuvers could be confounders. Of note, breathing patterns may also affect other current myocardial perfusion techniques, for example with varying durations of breath-holds during CMR or CT scans or hyperventilation in anxious patients during nuclear cardiology tests.

Different from previous human studies[47,83], hyperventilation did not induce a significant change in myocardial oxygenation, yet there was a significant decrease in coronary blood flow, and increase in blood oxygen content in both groups. Probably related to the preceding hyperventilation with vasoconstriction, there was a more pronounced response during a subsequent breath-hold (HVBH) when compared with a long breath-hold (LBH) alone. Consequently, HVBH data were also more consistent than LBH results with respect to identifying regional abnormalities caused by coronary artery stenosis, revealing a regionally blunted absolute blood flow and oxygenation response at most time points. The marked decrease in SI in the territory subtended by the stenotic coronary artery could be explained by a delayed recovery from the vasoconstrictive stimulus of hyperventilation, in combination with a coronary steal phenomenon caused by the competing vasodilation in remote

myocardium [34,140], and post-stenotic capillary recruitment[31]. Thus the HVBH maneuver may exploit two mechanisms associated with an abnormal vascular response in a hypoperfused coronary territory. In a previous human study of healthy participants, the HVBH had a much stronger effect on the oxygenation response than the LBH as well[47].

Breathing maneuvers also have a significant impact on blood oxygenation, which is a key determinant in the OS-CMR signal. It is likely that during the HVBH maneuver, blood oxygenation is higher during the subsequent breath-hold because of the preceding hyperventilation, which would explain the early SI increase in the breath-hold observed in healthy animals. Only with continued apnea, net blood oxygenation and subsequently tissue oxygenation drops[84]. In the presence of coronary artery stenosis however, the combination of hypoxemia and hypercapnia may actually induce or worsen myocardial ischemia in the jeopardized territory. In fact, we observed that in the presence of severe coronary artery stenosis, the lack of a proper compensatory increase in myocardial blood flow allows an immediate decrease in tissue oxygenation in the tissue subtended to the stenosis, in contrast to a SI increase in both, remote tissue and in control animals (Figure 15). This pattern was correlated with both, the functional severity of the stenosis (FFR) and with the observed change in coronary blood flow.

For control animals, the relatively small and insignificant difference between the LAD and remote territories may also reflect physiologic variations between coronary territories. Other studies have demonstrated that in healthy subjects, the anterior wall often had a more pronounced perfusion or oxygenation response than other territories[8,39,141].

Limitations and Future Directions

In the present animal study we observed a weaker response to adenosine and hyperventilation, including a smaller change of SI and heart rate in comparison with previous reports in humans. This may be caused by the anaesthesia, with its known cardiodepressant effects and suppression of vegetative reflexes. Recently, it has been suggested that remifentanil can crosstalk with adenosine receptors[142]. This interference could theoretically attenuate the vascular response to adenosine.

In this study, the breath-holds were maintained while more extreme blood gases levels materialized, exceeding levels tolerated by conscious human subjects[143]. Healthy human participants were able to comfortably undergo similar length of breathing maneuvers yet, without the extreme blood gas changes observed in our animal study[83]. Cardiac patients may not tolerate long breath-hold times, yet with both volunteers and the current animal model, significant results were observed within the first 30s of the breathing maneuvers, allowing for clinically feasible protocols[47]. In fact, we have already successfully applied the HVBH maneuver in a pilot study in patients with sleep apnea, who all tolerated the procedure well, with the majority maintaining a breath-hold after hyperventilation of more than 30s[88]. Our animals did not have chronic coronary atherosclerosis, but an experimentally induced acute regional stenosis with otherwise healthy microvasculature. Differences in compensatory mechanisms may alter the vascular response and it remains to be studied whether the exact values we obtained can be directly translated to humans. Additionally, coronary flow measurements do not precisely measure coronary flow reserves as tissue perfusion is regulated primarily by microvascular resistance, and not by the large conduit vessels[102].

Future studies will also help establish normal values for the myocardial response to standardized breathing maneuvers. This would also allow for detecting an abnormal response in patients with multi-vessel disease and "balanced" ischemia as well as assessing the global coronary vascular response, equivalent to the coronary flow reserve, which is an important prognostic marker[144].

1.7 Conclusion

Breathing maneuvers have a profound effect on coronary blood flow and myocardial oxygenation. Specifically, hyperventilation with subsequent breath-holding leads to a significant vasoactive response, which is markedly compromised in myocardium subtended by a significantly stenotic coronary artery. The proposed combination of oxygenation-sensitive CMR with breathing maneuvers appears to be useful for diagnostic testing in patients with suspected coronary artery stenosis, especially when contrast agents or stress protocols are not suitable. Further studies are now warranted to investigate its clinical utility in patients with suspected myocardial ischemia.

1.8 Supplemental Tables

Parameter		Control	Stenosed	P
%-change Flow				
	HV	-34 ± 23*	-12 ± 6*	<0.001
	HVBH	346 ± 327*	82 ±110	0.004
	LBH	97 ± 88*	40 ± 60	0.066
	Adenosine	15 ± 16*	13 ± 27	0.950
$\Delta paCO_2$ (mmHg)				
	HV	-15 ± 5*	-15 ± 3*	0.887
	HVBH	27± 9*	20 ± 8*	0.046
	LBH	15 ± 5*	12 ± 5*	0.250
	Adenosine	1 ± 3	1 ± 1	0.893
$\Delta pcsCO_2$ (mmHg)				
	HV	-3 ± 2*	-8 ± 5*	<0.001
	HVBH	6 ± 6*	10 ± 3*	0.094
	LBH	10 ± 7*	9 ± 5*	0.842
	Adenosine	1 ± 5	3 ± 5	0.478
ΔpaO_2 (mmHg)				
	HV	73 ± 71*	70 ± 30*	0.975
	HVBH	-117 ± 48*	-135 ± 30*	0.315
	LBH	-73 ± 9*	-80 ± 12*	0.104
	Adenosine	-1 ± 25	-1± 7	0.999
$\Delta pcsO_2$ (mmHg)				
	HV	-7 ± 17	1 ± 2	0.072
	HVBH	-12 ± 7*	-13 ± 7*	0.961
	LBH	-13 ± 7*	-15 ± 7*	0.802
	Adenosine	2 ± 2	2 ± 3	0.999
ΔSaO_2 (%)				
	HV	0 ± 0	0 ± 0	-
	HVBH	-30 ± 23*	-52 ± 24*	0.014
	LBH	-36 ± 30*	-61 ± 15*	0.005
	Adenosine	0 ± 1	0 ± 0	0.406
ΔO_2er (%)†				
	HV	-2 ± 6	-4 ± 7	0.639
	HVBH	20 ± 20*	2 ± 28	0.091
	LBH	16 ± 24	10 ± 16	0.678
	Adenosine	-5± 5*	-1 ± 8	0.138
ΔHR (bpm)				
	HV	3 ± 11	0 ± 8	0.798
	HVBH	3 ± 14	2± 12	0.996
	LBH	8 ± 20	-1 ± 14	0.208
	Adenosine	-4 ± 4*	-4 ± 5*	0.990
ΔRPP (mmHg*bpm)				
	HV	-2311±2141*	-712±2006	0.055
	HVBH	-560±1285	-1459±5580	0.106
	LBH	-4617±3292*	-2961±2835*	0.216
	Adenosine	-281±762	-233±1193	0.997

Table 7: Invasive Measurements

Mean±SD change in values during the breathing maneuvers and adenosine (* denotes significance ($p<0.05$) from baseline value). † O_2er baseline values were systematically higher in the stenosed animals. Arterial partial pressure of carbon dioxide ($paCO_2$); coronary sinus partial pressure of carbon dioxide ($pcsCO_2$); arterial partial pressure of oxygen (paO_2); coronary sinus partial pressure of oxygen ($pcsO_2$); arterial saturation (SaO_2); oxygen extraction ratio (O_2er); heart rate (HR); and rate pressure product (RPP).

1.9 Chapter References

1. Antony R, Daghem M, McCann GP, Daghem S, Moon J, Pennell DJ, Neubauer S, Dargie HJ, Berry C, Payne J, Petrie MC, Hawkins NM. Cardiovascular magnetic resonance activity in the United Kingdom: a survey on behalf of the british society of cardiovascular magnetic resonance. *J Cardiovasc Magn Reson.* 2011;13:57.

2. Iglehart JK. Health Insurers and Medical-Imaging Policy — A Work in Progress. *N Engl J Med.* 2009;360:1030–1037.

8. Donato P, Coelho P, Santos C, Bernardes A, Caseiro-Alves F. Correspondence between left ventricular 17 myocardial segments and coronary anatomy obtained by multi-detector computed tomography: an ex vivo contribution. *Surg Radiol Anat.* 2012;34:805–810.

23. Ogawa S, Lee TM, Kay AR, Tank DW. Brain magnetic resonance imaging with contrast dependent on blood oxygenation. *Proc Natl Acad Sci U S A.* 1990;87:9868 –9872.

31. Wacker CM, Hartlep AW, Pfleger S, Schad LR, Ertl G, Bauer WR. Susceptibility-sensitive magnetic resonance imaging detects human myocardium supplied by a stenotic coronary artery without a contrast agent. *J Am Coll Cardiol.* 2003;41:834–840.

34. Friedrich MG, Niendorf T, Schulz-Menger J, Gross CM, Dietz R. Blood oxygen level-dependent magnetic resonance imaging in patients with stress-induced angina. *Circulation*. 2003;108:2219–2223.

39. Arnold JR, Karamitsos TD, Bhamra-Ariza P, Francis JM, Searle N, Robson MD, Howells RK, Choudhury RP, Rimoldi OE, Camici PG, Banning AP, Neubauer S, Jerosch-Herold M, Selvanayagam JB. Myocardial Oxygenation in Coronary Artery Disease: Insights From Blood Oxygen Level–Dependent Magnetic Resonance Imaging at 3 Tesla. *Am J Cardiol*. 2012;59:1954–1964.

44. Roubille F, Fischer K, Guensch DP, Tardif J-C, Friedrich MG. Impact of Hyperventilation and Apnea on Myocardial Oxygenation in Patients With Obstructive Sleep Apnea – an Oxygenation-Sensitive CMR Study. *J Cardiol*. 2016;

47. Fischer K, Guensch DP, Friedrich MG. Response of myocardial oxygenation to breathing manoeuvres and adenosine infusion. *Eur Heart J Cardiovasc Imaging.* 2015;395–401.

71. Kastrup A, Li T-Q, Takahashi A, Glover GH, Moseley ME. Functional Magnetic Resonance Imaging of Regional Cerebral Blood Oxygenation Changes During Breath Holding. *Stroke.* 1998;29:2641–2645.

82. Guensch DP, Fischer K, Flewitt JA, Friedrich MG. Impact of Intermittent Apnea on Myocardial Tissue Oxygenation—A Study Using Oxygenation-Sensitive Cardiovascular Magnetic Resonance. *PLoS ONE.* 2013;8:e53282.

83. Guensch DP, Fischer K, Flewitt JA, Yu J, Lukic R, Friedrich JA, Friedrich MG. Breathing manoeuvre-dependent changes in myocardial oxygenation in healthy humans. *Eur Heart J Cardiovasc Imaging.* 2014;15:409–414.

84. Sasse SA, Berry RB, Nguyen TK, Light RW, Mahutte CK. Arterial blood gas changes during breath-holding from functional residual capacity. *Chest*. 1996;110:958–964.

85. Klocke FJ, Rahn H. Breath holding after breathing of oxygen. *J Appl Physiol.* 1959;14:689–693.

86. Parkes MJ. Breath-holding and its breakpoint. *Exp Physiol.* 2006;91:1–15.

101. Broten TP, Romson JL, Fullerton DA, Van Winkle DM, Feigl EO. Synergistic action of myocardial oxygen and carbon dioxide in controlling coronary blood flow. *Circ Res.* 1991;68:531–542.

102. Camici PG, Crea F. Coronary microvascular dysfunction. *N Engl J Med*. 2007;356:830–840.

110. Neill W, Hattenhauer M. Impairment of myocardial O2 supply due to hyperventilation. *Circulation.* 1975;52:854 –858.

111. Stalder AF, Schmidt M, Greiser A, Speier P, Guehring J, Friedrich MG, Mueller E. Robust cardiac BOLD MRI using an fMRI-like approach with repeated stress paradigms. *Magn Reson Med.* 2015;73:577–85.

112. Guensch DP, Fischer K, Flewitt JA, Friedrich MG. Myocardial oxygenation is maintained during hypoxia when combined with apnea – a cardiovascular MR study. *Physiol Rep.* 2013;1:e00098.

134. Gerber BL, Raman SV, Nayak K, Epstein FH, Ferreira P, Axel L, Kraitchman DL. Myocardial first-pass perfusion cardiovascular magnetic resonance: history, theory, and current state of the art. *J Cardiovasc Magn Reson.* 2008;10:18.

135. Guensch DP, Friedrich MG. Novel Approaches to Myocardial Perfusion: 3D First-Pass CMR Perfusion Imaging and Oxygenation-Sensitive CMR. *Curr Cardiovasc Imaging Rep.* 2014;7:1–6.

136. Guensch DP, Fischer K, Shie N, Lebel J, Friedrich MG. Hyperoxia Exacerbates Myocardial Ischemia in the Presence of Acute Coronary Artery Stenosis in Swine. *Circ Cardiovasc Interv.* 2015;8:e002928.

137. Kahn CM, Line S, Allen DG. The Merck veterinary manual. Merck Whitehouse Station, NJ; 2010.

138. Tanguay J-F, Hammoud T, Geoffroy P, Merhi Y. Chronic Platelet and Neutrophil Adhesion: A Causal Role for Neointimal Hyperplasia in In-Stent Restenosis. *J Endovasc Ther.* 2003;10:968–977.

139. Wilson R, Wyche K, Christensen B, Zimmer S, Laxson D. Effects of adenosine on human coronary arterial circulation. *Circulation.* 1990;82:1595 –1606.

140. Seiler C, Fleisch M, Meier B. Direct Intracoronary Evidence of Collateral Steal in Humans. *Circulation.* 1997;96:4261–4267.

141. Chareonthaitawee P, Kaufmann PA, Rimoldi O, Camici PG. Heterogeneity of resting and hyperemic myocardial blood flow in healthy humans. *Cardiovasc Res.* 2001;50:151–161.

142. Ha J-Y, Lee Y-C, Park S-J, Jang Y-H, Kim J-H. Remifentanil postconditioning has cross talk with adenosine receptors in the ischemic-reperfused rat heart. *J Surg Res.* 2015;195:37–43.

143. Breskovic T, Lojpur M, Maslov PZ, Cross TJ, Kraljevic J, Ljubkovic M, Marinovic J, Ivancev V, Johnson BD, Dujic Z. The influence of varying inspired fractions of O2 and CO2 on the development of involuntary breathing movements during maximal apnoea. *Respir Physiol Neurobiol*. 2012;181:228–233.

144. Taqueti VR, Hachamovitch R, Murthy VL, Naya M, Foster CR, Hainer J, Dorbala S, Blankstein R, Di Carli MF. Global coronary flow reserve is associated with adverse cardiovascular events independently of luminal angiographic severity and modifies the effect of early revascularization. *Circulation*. 2015;131:19–27.

2 Chapter 2 – The Coronary Blood Flow Response to Breath-Holds is Blunted by Hyperoxia

Foreword

The majority of our studies focus on maximal breath-holds. Yet, for a patient population who are unlikely to make long breath-holds, it was important to assess the impact of short feasible breath-holds.

In this chapter, the response of coronary artery blood flow to shorter breath-hold stimuli are assessed in anaesthetized swine. In particular, this study focuses on short breath-holds of less than 30s, which may not have a very strong impact on CO_2 and O_2. Furthermore, the stimuli are assessed at different arterial oxygen and carbon dioxide baselines. Proof that even short breath-holds have a significantly impact coronary flow, supports the proposal to use breathing maneuvers in clinical practice. This study does not involve MRI, but rather aims to assess how short breath-holds can affect the coronary artery blood flow response, which is often a target of cardiovascular imaging exams. Further, the altered responsiveness during certain baseline blood gas levels can be of particular importance as a fair portion of patients undergoing exams can have chronic hypoxemia, or be given supplemental oxygen resulting in blood hyperoxia.

Data from this study was presented at the 2015 Canadian Cardiovascular Congress in Toronto, Canada.

The Coronary Blood Flow Response to Breath-Holds is Blunted by Hyperoxia

Kady Fischer, BHSc;[a,b] Dominik P Guensch, MD;[a,b] Nancy Shie, BSc;[a] Julie Lebel, RLAT;[a, c] Matthias G Friedrich, MD[a,d,e,f,g]

[a]Philippa & Marvin Carsley CMR Centre at the Montreal Heart Institute, Université de Montréal, Montreal, Canada,

[b]Bern University Hospital, Department Anaesthesiology and Pain Therapy, Bern, Switzerland,

[c]McGill University Health Centre Research Institute, Montreal, Canada;

[d]Departments of Radiology, Université de Montréal, Montreal, Canada;

[e]Departments of Medicine and Diagnostic Radiology, McGill University, Montreal, Canada

[f]Department of Cardiology, Heidelberg University Hospital, Heidelberg, Germany

[g]Departments of Cardiac Sciences and Radiology, University of Calgary, Calgary, Canada

All co-authors wrote and approved the manuscript. This version, dated from February 2016 is currently in the process of being submitted to peer-reviewed journals.

2.1 Abstract

Background: Pharmacologic vasodilators and more recently vasoactive breathing maneuvers are utilized in diagnostic testing to assess coronary vascular reactivity. Carbon dioxide and oxygen however, are strong modulators of coronary blood flow and could confound the vascular response, and results of such tests may be misleading. Thus the impact of these arterial blood gases on the coronary flow response was assessed in an invasive animal model.

Methods: In 17 anaesthetized and intubated swine, 11 animals had the left descending coronary artery (LAD) partially occluded, while 6 animals serves as control. Apnea times of 3 to 30s were induced, and coronary blood flow was measured with an invasive ultrasound probe surgically placed on the LAD. These breath-hold stimuli were induced at 9 different arterial blood gas baselines, with a combination of mild hypoxemia (70mmHg), normoxemia (100mmHg), and hyperoxia (300mmHg) with hypocapnia (30mmHg), normocapnia (40mmHg), and hypercapnia (50 mmHg).

Results: Breath-holds consistently induced an increase of coronary blood flow at normal blood gases, which was linearly correlated to the duration of the breath-hold for both control and, in an overall reduced manner, stenosed animals. Whereas mild hypoxemia augmented the blood flow response, a minimal response only was observed during hyperoxia in all animals. A reduced vasodilatory capacity caused by coronary artery stenosis could be differentiated from normal blood flow only at normal blood gas levels and hypoxemic hypocapnia, but not during hyperoxia.

Conclusion: Arterial hyperoxia blunts coronary vascular reactivity and may reduce the sensitivity of tests involving vasodilatory stimuli, specifically a breath-hold stimulus.

Key Words: Experimental Model ▪ Coronary Flow Response ▪ Breath-hold ▪ Hyperoxia ▪ Hypoxemia

2.2 Introduction

In developed countries, testing for coronary artery disease is one of the most frequently performed diagnostic procedures. A large portion of such testing involves pharmacologic vasodilation using substrates such as intravenous adenosine, dipyridamole, regadenoson, and, more recently, by non-pharmacological means of hypercapnic gas mixtures and breath-holds[38,47,92,100]. The vasodilatory capacity is considered a key measure for the detection of significant coronary stenosis, overall microvascular function, or for endothelial dysfunction when using specific agents such as acetylcholine[145,146]. However, these tests assume that the stimulus produces a maximal hyperaemic response, with no attenuating factors other than the vessel dysfunction. It is however well known that arterial blood gas levels have a profound effect on coronary blood flow. Hypercapnia and hypoxia increase myocardial blood flow, while hypocapnia and hyperoxia decrease it[91,94,101,107,109,147]. Hypoxemia can be present in cardiac diseases, while other patients may have arterial hyperoxia because of the common use of supplemental oxygen in various clinical scenarios. Interestingly however, data are scarce on how arterial blood gas levels may confound the coronary vascular response to vasoactive stimuli[92]. Specifically this study investigates the use of short breath-holds as non-pharmacological stimuli. Published reports indicate that in neuro and cardiac imaging, breath-holds as short as 10s lead to a detectible hyperemic response[47,71,74,82].

In this experimental study, we assessed the impact of blood gas levels on the vasodilatory response induced by breath-holds.

2.3 Methods

Animal Preparation

Seventeen healthy swine (32±2kg, Yorkshire-Landrace) were included in the study. The surgical protocol and other data from these animals were published elsewhere[136]. All animals were intubated after pre-medication with Telazol (200mg tiletamine, 200mg zolazepam. i.m.) and atropine (0.8mg). Propofol was used for induction (2-4mg/kg, i.v.) and maintenance (4-36 mg/kg/hr, i.v.) of anaesthesia, while analgesia was provided by

remifentanil (0-3.5µg/kg/min, i.v.). For preventing arrhythmia, 75mg of amiodarone i.v. was administered and if necessary serum magnesium and potassium levels were corrected[137]. Access for arterial blood gas sampling was placed in the femoral artery. For analysis of coronary blood flow, an ultrasound flow probe was surgically implanted on the proximal left anterior descending (LAD) coronary artery (Transonic Systems, Ithica, NY, USA), requiring a left-sided thoracotomy (Figure 16).

Six animals served as controls, while in eleven animals, a hemodynamically relevant stenosis was induced using a perivascular hydraulic occluder (In Vivo Metric, CA, USA). The severity of the stenosis was visually verified with coronary angiography but also by an FFR catheter in place (St. Jude Medical, MN, USA) during inflation of the occluder. An FFR of less than 0.75 was considered reflective of clinically significant coronary artery stenosis.

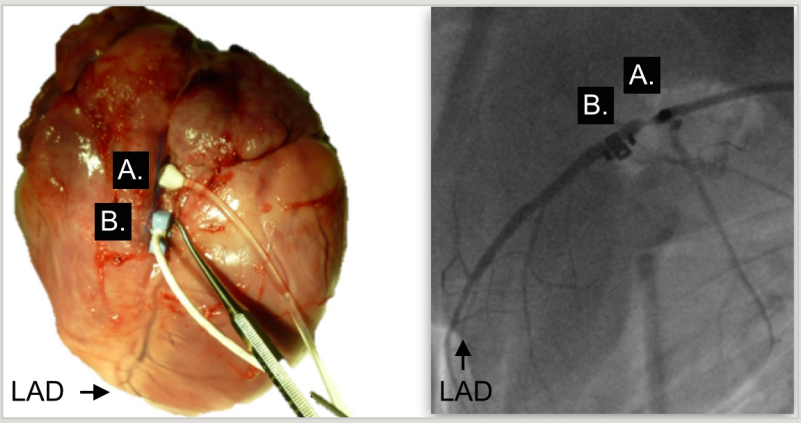

Figure 16: Surgical methods
An explanted pig heart shows the surgical placement of the perivascular occluder (A.) and the blood flow probe (B) on the left anterior descending coronary artery (LAD), as verified with fluoroscopy imaging.

Experimental Protocol

Arterial blood gas levels were targeted to nine levels for the combination of paO_2 and $paCO_2$: paO_2 of 70, 100 or >300mmHg (hypoxemia, normoxemia, hyperoxia) and a $paCO_2$ of 30, 40 or 50 mmHg (hypocapnia, normocapnia, hypercapnia). The control level of normoxemic normocapnia (paO_2=100, $paCO_2$=40mmHg) was targeted twice, once at the beginning and with the second performed in random order with the other levels to assess if

normal vasomotion changed during the duration of the protocol. After the arterial blood gas levels were stabilized, up to 6 breath-hold stimuli were induced at each baseline using an end-expiration pause in ventilation. The breath-holds ranged from 3-30s in duration. Coronary flow was measured in ml/min, both before and after each stimulus and expressed as a percent-change (Δ-%). This blood flow response was assessed for its correlation with the breath-hold duration, for differences between gas levels and for the impact of the presence of coronary artery stenosis.

Statistical Analysis

Data are expressed as mean±SD. Univariate analysis was done to investigate the linear response the change in coronary flow, in response to duration of the breath-hold. A within subjects Pearson's correlation was performed comparing the flow response (%) to the breath-hold durations, accounting for both repeated measurements within each animal, and different animal intercepts to assess if the coronary flow response changed with the breath-hold duration (Table 8). To examine the differences between groups and blood gas levels, a two-way mixed effect model was performed with an unstructured covariance and restricted maximum likelihood estimation. The model used the duration of the breath-hold as the covariate, and allowed for random intercepts of each animal. The magnitude of the flow response that occurred at the mean breath-hold time was assessed at each blood gas level between the control and stenosed groups. This was also done to compare each blood gas level to the baseline (100/40), using the Bonferroni method accounting for multiple comparisons. Because a range of breath-hold durations were used, an adjusted mean is reported for what the flow response would be at 13s for each level, which was the mean breath-hold time (Table 9).

Tests were performed with GraphPad Prism version 6.0 for mac (GraphPad Software, La Jolla California USA) and SPSS version 23 (SPSS IBM, New York, USA). Results were considered statistically significant with a two-tailed $P<0.05$.

This study was conducted in accordance with the Guide to the Care and Use of Experimental Animals by the Canadian Council on Animal Care and approved by the local Animal Care and Use Board.

2.4 Results

In six control animals, 279 breath-holds were recorded, as one control animal died during the experiment. In the stenosed group, one animal died during the coronary intervention, resulting in ten stenosed animals and 432 breath-holds. Mean FFR was 0.63±0.05 (range 0.54-0.74). Quantitative coronary angiography showed a mean diameter reduction of 63±11% in these animals.

Breath-hold Stimulus at Normoxemia Blood Gases

The normal gas level (100/40), was targeted twice during the experiment to check for consistency, and there was no difference in the coronary flow response recordings between the two sets of measurements (p=0.614), thus these were combined for further analysis. As shown in Figure 17, shorter breath-holds were able to significantly and transiently increase the coronary blood flow. In both groups, controls (r=0.533, p=0.006) and stenosed animals (r=0.566, p<0.001), the flow response was correlated with the breath-hold duration. The mixed model showed that, accounting for the breath-hold duration, the flow response was significantly lower in the stenosed group (p=0.002). Similar to the normal blood gas level, all the other normoxic levels with different $paCO_2$ responded linearly to the stimuli as well (Table 8, Figure 17). In both groups hypocapnia augmented the flow response, while hypercapnia had an attenuating effect in control animals only.

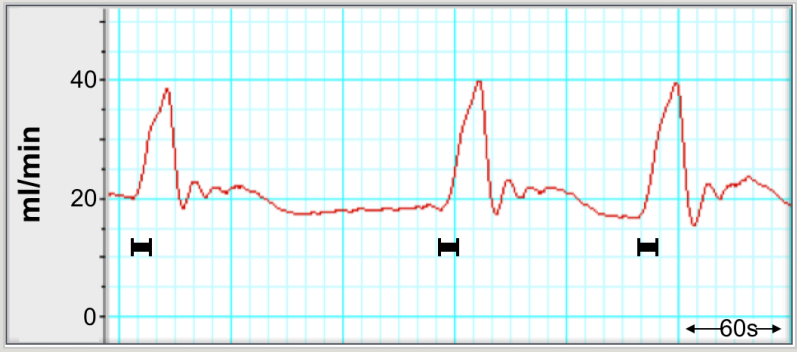

Figure 17: Coronary blood flow read-out
The coronary flow read-out shows that in a healthy test animal at normal blood gases (paO_2=100mmHg, $paCO_2$=40mmHg), end-expiratory breath-holds of 8-10s (black markers) nearly doubled the coronary blood flow before returning back to baseline (1 measurement/s, small grid; 10s, large grid; 60s).

Effect of Hypoxemia

During mild hypoxemia (paO_2=70mmHg), in both groups all levels augmented the flow response from the normal gas level ($p<0.05$), with the exception of hypoxemic hypercapnia (70/50) in control animals. Interestingly, only stenosed animals showed a dependence on breath-hold time. In control animals there was still a significant flow increase, but this data was more scattered and not linearly related to the breath-hold duration.

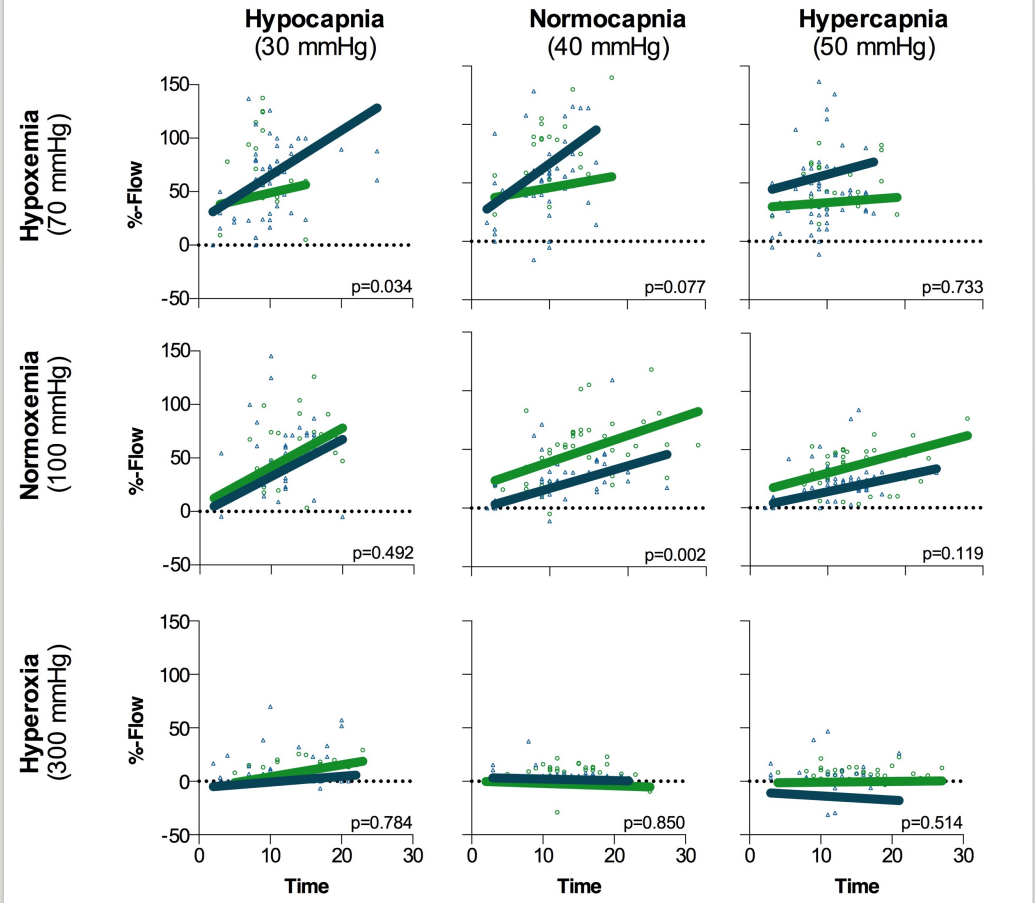

Figure 18: Coronary blood flow response to breath-hold stimuli

A Pearson's within subject correlation was performed, accounting for multiple measurements obtained per animal (table 1), and results reported on the graph (p-value) from a mixed model, showed that only at 100/40 and 70/30, could a significant difference ($p<0.05$) be observed between the groups, control animals (green) and stenosed animals (blue).

Effect of Hyperoxia

Hyperoxia blunted any response to the breath-hold duration by at least 20%, independent of the $paCO_2$ level (Table 9). No relationship was observed for any of the hyperoxic levels and no difference of coronary blood flow between healthy and stenosed animals.

	Healthy			Stenosed		
FLOW-%	n	r	p	n	r	p
100/30	29	0.533	**0.006**	42	0.631	**<0.001**
100/40	52	0.522	**<0.001**	59	0.566	**<0.001**
100/50	37	0.656	**<0.001**	52	0.616	**<0.001**
70/30	22	0.432	0.073	53	0.721	**<0.001**
70/40	20	0.164	0.529	51	0.692	**<0.001**
70/50	26	0.117	0.604	57	0.358	**0.013**
300/30	19	0.706	0.003	45	0.230	0.171
300/40	37	0.168	0.358	39	0.239	0.198
300/50	35	0.094	0.620	34	0.017	0.938

Table 8: Coronary flow response (%) to breath-hold duration

Pearson's within subject correlation was performed at each level (mmHg, $paO_2/paCO_2$) accounting for multiple measurements obtained per animal. For both groups, at normoxemia the coronary flow increases with the breath-hold duration, whereas there is no response during hyperoxia. Only the stenosed animals have a linear relationship at hypoxemia.

	Healthy			Stenosed		
FLOW-%	n	Adjusted difference	p	n	Adjusted difference	p
100/30	29	14±4	**0.009**	42	22±4	**<0.001**
100/50	37	-11.6±4	**0.003**	52	-6±4	1.000
70/30	22	20±7	**0.019**	53	35±4	**<0.001**
70/40	20	38±5	**<0.001**	51	36±4	**<0.001**
70/50	26	6±5	1.000	57	18±4	**<0.001**
300/30	19	-33±5	**<0.001**	45	-20±4	**<0.001**
300/40	37	-38±4	**<0.001**	39	-25±4	**<0.001**
300/50	35	-39 ±4	**<0.001**	34	-24±4	**<0.001**

Table 9: Within group comparison of arterial blood gas levels

A mixed effects model was used at each level (mmHg, $paO_2/paCO_2$) to determine if the magnitude in the coronary flow response (%) was significantly different from the normal blood gas value within the control or stenosis group. The adjusted difference is reported as the change from the baseline gas level, using the flow response that occurred at a time of 13s (the mean breath-hold duration).

Comparison between Control and Stenosis

While the above comparisons showed that within the group, arterial blood gases could significantly affect the coronary response from the normal gas level, it was also assessed

whether the coronary flow response could still be used to distinguish a healthy versus a significantly stenosed coronary artery in an environment of altered arterial blood gas levels. Only at normal blood gases (100/40), and hypoxemic hypocapnia (70/30), could an attenuated flow response be observed for the stenosed animals in comparison to controls, while there was a non-significant trend for hypoxic normocapnia (70/40, p=0.077). In all other comparisons, the arterial blood gas levels impacted the coronary flow response so the stenosed animals could not be distinguished from the control.

2.5 Discussion

The results demonstrate that in normal arterial blood gas conditions, a breath-hold stimulus is effective in transiently increasing coronary blood flow, and the magnitude of the response is proportionate to the duration of the breath-hold. In other arterial oxygen states however, this response is altered. Arterial hypoxemia augments the coronary flow response, even in the presence of a significant coronary stenosis, while hyperoxia attenuates the coronary vascular response, independent of the presence or absence of severe coronary artery stenosis.

The attenuation during hyperoxia to stimuli could also have implications for coronary stress testing in which supplemental oxygen is administered. For example in clinical FFR exams, especially in the setting of an acute myocardial infarction, the use of supplemental oxygen may impair the response to the pharmacological stimulus and lead to underestimation of the FFR. This can be in addition to any alterations that hyperoxia may have on the baseline image[136]. However, stimuli induced by other procedures or pharmacological agents may affect the coronary flow response differently than the breath-hold stimulus used in this study, thus our results may not be valid for these techniques. Other publications have also observed confounding effects of hyperoxia on other stimuli. A Doppler assessment of coronary flow in 5 CAD patients, showed that hyperoxia (paO_2>250mmHg) did not affect the coronary response to adenosine, yet the dilator response of acetylcholine was blunted [94]. Additionally, because hyperoxia itself already reduces coronary blood flow[94,136,148], blocking the

vasodilatory ability can further compromise the tissue oxygenation if a higher oxygen demand is required.

Opposite to the effects of hyperoxia, we observed that a strong response to coronary stimuli occurs when arterial blood gases are at a mild stage of hypoxemia (paO_2=70mmHg), in both control animals and those with a significant stenosis. This can represent the response mechanisms of the heart to ensure an adequate oxygen supply, by further increasing blood flow during lower oxygen saturation. In a high-altitude-simulation PET study, Wyss et al found that when healthy participants breathed in hypoxic gas mixtures, hypoxemia increased the myocardial blood response to exercise-induced stimulation by 38%. While in CAD patients, hypoxemia increased baseline coronary flow, but was associated with a reduced blood supply during exercise, likely due to an exhausted vasodilatory reserve or possibly a coronary steal phenomenon. In both groups hypoxemia did not significantly affect the response to adenosine[92]. Yet, in a different study looking at vascular systems of sheep foetuses, hypoxemia augmented the adenosine response when compared to normoxaemia[149]. Under these conditions, a stenotic vessel could give a flow response that would be quantitatively considered healthy under normal situations, possibly masking the vessel dysfunction. It should also be noted, that our current study focused on mild arterial hypoxemia, and not tissue hypoxia, which could have a different impact on the coronary flow response.

While the arterial oxygenation status had a significant impact on the coronary flow response, minimal effects were observed with the difference in $paCO_2$ levels. Changing CO_2 is known to have a strong impact to change the coronary blood flow itself[101], but in this study, stable states of hypocapnia and hypercapnia did not confound the response to the breath-hold stimuli as strongly as the oxygen levels. At hypercapnia in healthy animals, there is still a linear relationship to the breath-hold stimulus, yet the coronary flow did not increase to the same extent as normocapnia and hypocapnia. This may suggest that at this point, there vasodilatory capacity may have been reached due to the baseline vasodilating effects of hypercapnic itself, whereas the lower baseline allows for a larger apparent vasodilatory capacity during hypocapnia.

Our study also sheds light on the use of short breath-holds and their interaction with blood gases and the coronary vascular response. The vasodilatory effects of the breath-hold are believed to be mediated by multiple mechanisms, which focus on a combined function of the respiratory, cardiac parasympathetic and vasomotor centre[150–152]. While longer breath-holds have the potential to alter the partial pressure of O_2 and CO_2 in the blood, we applied short breath-holds, which typically are not long enough to significantly alter blood gas composition. Sasse et al demonstrated in conscious humans, blood gases, O_2 and CO_2, would not change for about 10s after an end-expiration breath-hold[84]. Yet we observed that at normal blood gases, a breath-hold shorter than 10s can still increase the coronary blood flow by more than 30%. Similarly, a brain functional magnetic resonance study observed hyperemic effects with a short 10s breath-hold as well[74]. While the observed effect may in part be related to the fact that we used end-expiratory breath-holds, which appear to cause a more rapid change in pCO_2-mediated cerebral hyperemia than an inspiratory breath-hold[71], it seems more likely that early in a breath-hold, activation of other responses that manipulate the coronary flow, occur before arterial blood gases change. Suggested mechanisms have been the activation of pulmonary stretch receptors and redirection of blood flow to the heart by sympathetically activated peripheral vasoconstriction[123–125].

Rationale for Selected Arterial Blood Gas Levels

Arterial blood oxygenation was targeted based on oxygen tension (paO_2) and not hemoglobin saturation (SaO_2), and all three levels of blood oxygen were chosen based on what could realistically be seen in a clinical setting. While a paO_2 of 70mmHg was considered mildly hypoxemic, this value is quite common in both cardiovascular and elderly populations. Additionally, this oxygen tension often results in an arterial saturation greater than 90%. In fact for relatively healthy persons over the age of 70 years without any pulmonary or respiratory diseases, the mean paO_2 for men was reported as 77mmHg, and 73mmHg for females, with the lower acceptable limits as low as 60mmHg[153]. This can be explained by the impact of age on oxygen uptake into the pulmonary capillaries from the alveoli[154]. While age does not have a significant impact on alveolar pO_2 (pAO_2), it does strongly affect the ventilation-perfusion mismatch and thus has an impact on the fraction of oxygen that will be

taken up from ventilated and perfused alveoli. This can be shown by the calculations for the approximate pAO_2 (equation 1) in which age is not a factor and the expected alveolo-arterial O_2 (A-a) gradient (equation 2), which demonstrates that elderly persons will have a bigger gradient.

$$(1) \quad Alveolar\ pO_2 = FiO_2 \times (P - P_{H2O}) - \frac{PaCO_2}{Rq}$$

$$(2)\ A\text{-}a\ gradient\ = \frac{Age}{4} + 4$$

Where FiO_2 is the inspired oxygen concentration (21%), P the atmospheric pressure (760mmHg), P_{H2O} the pressure of water vapour (47mmHg), $paCO_2$ the arterial partial pressure of CO_2 (~40mmHg) and Rq the respiratory quotient (0.8) depending on physical activity and nourishment[154].

The expected paO_2 using the formula to calculate the A-a-gradient from a pAO_2 of 100mg would be 88.5mmHg in a 30 year-old, whereas the paO_2 is expected to be approximately 76mmHg for an 80 year-old. In both settings, the saturation will be higher than 90%. Thus, we label a paO_2 of 70mmHg as mildly hypoxemic. This mean decreases further with smoking or cardiovascular disease or any condition that will alter the ventilation/perfusion ratio. Similarly, hyperoxia can be achieved quite easily and just 7 minutes of breathing oxygen through a facemask with a reservoir bag could increase paO_2>400mmHg in healthy participants and CAD patients[155]. This can be further aggravated with a positive pressure ventilation and/or the addition of a positive end-expiratory pressure. Furthermore, Kilgannon et al. found that in more than 6000 patients arriving at the ICU after cardiac arrest, 18% had hyperoxic blood (paO_2>300 mmHg)[95].

Similar to the oxygen choices, the targeted CO_2 levels are considered abnormal, but are present in clinical situations, while a normal $paCO_2$ would be about 38-40mmHg[153]. For example, a recent study found that in acute heart failure patients 34% were hypercapnic ($paCO_2$>45mmHg), while another 33% ($paCO_2$<35mmHg) were hypocapnic at the time of admission[156]. Additionally, as described in the intro, CO_2 can reach these levels also by alterations in breathing patterns[84,157]. In summary, all targeted levels in this chapter do have clinical relevance and patients with these abnormal blood gases could be referred for a cardiovascular exam.

Limitations and Future Directions

As we only assess stimuli induced by breath-holds, our results may not address any confounding effects associated with pharmaceutical stimuli. Additionally, an anesthetised animal model is not fully translational to what may be seen in a clinical setting. Anesthetics can be a cardio-depressant and attenuate the coronary vascular response. The model is limited in that we assess an essentially healthy coronary artery with a single, acute blockage, not accounting for the many mechanisms occurring with the development of coronary artery disease, including dysfunctions of the endothelial and smooth muscle cells. Additionally, longer breath-holds were not obtained at hypoxemic levels, yet we observed a strong response still with the breath-holds of under 20s. Our sample size and endpoints did not allow for assessing further associations of the coronary vascular response with the coronary artery stenosis, so observed trends such as encountered for example at hypoxic normocapnia (70/40) and normoxemic hypercapnia (100/50), may reflect true correlations. The breath-holds assessed in this chapter are more similar to the long breath-hold (LBH) maneuver assessed in chapters 1 and 4 and not the HVBH, as breath-holds were not performed after hyperventilation. Although ventilation rate would have been reduced to reach hypercapnic levels, and increased to target hypocapnia, these breathing rates were not the same as what is required for an efficient hyperventilation. Thus, following the trends of chapter 1, short breath-holds after hyperventilation may have a different response than seen in these results.

2.6 Conclusion

Short breath-holds at physiologic blood gas conditions induce an observable coronary flow response that can differentiate a healthy coronary territory from one with significant coronary stenosis. However, baseline arterial blood gas levels have a significant effect on this response. Arterial hypoxemia augments the response, while hyperoxia attenuates it, both effects reducing the ability to detect a compromised response associated with coronary stenosis. This study highlights that arterial oxygen content may be a significant confounder cardiac exams which rely on assessing the coronary perfusion reserve as a measure of vascular function, which could lead to incorrect assessments and misdiagnosis.

2.7 Chapter References

38. Luu JM, Friedrich MG, Harker J, Dwyer N, Guensch D, Mikami Y, Faris P, Hare JL. Relationship of vasodilator-induced changes in myocardial oxygenation with the severity of coronary artery stenosis: a study using oxygenation-sensitive cardiovascular magnetic resonance. *Eur Heart J Cardiovasc Imaging*. 2014;15:1358–1367.

47. Fischer K, Guensch DP, Friedrich MG. Response of myocardial oxygenation to breathing manoeuvres and adenosine infusion. *Eur Heart J Cardiovasc Imaging*. 2015;395–401.

61. Kilgannon J, Jones AE, Shapiro NI, et al. Association between arterial hyperoxia following resuscitation from cardiac arrest and in-hospital mortality. \iJAMA. 2010;303:2165–2171.

71. Kastrup A, Li T-Q, Takahashi A, Glover GH, Moseley ME. Functional Magnetic Resonance Imaging of Regional Cerebral Blood Oxygenation Changes During Breath Holding. *Stroke.* 1998;29:2641–2645.

74. Liu H.-L, Huang J.-C, Wu C-T., Hsu Y-Y. Detectability of blood oxygenation level-dependent signal changes during short breath hold duration. *Magn Reson Imaging.* 2002;20:643–648.

82. Guensch DP, Fischer K, Flewitt JA, Friedrich MG. Impact of Intermittent Apnea on Myocardial Tissue Oxygenation—A Study Using Oxygenation-Sensitive Cardiovascular Magnetic Resonance. *PLoS ONE*. 2013;8:e53282.

84. Sasse SA, Berry RB, Nguyen TK, Light RW, Mahutte CK. Arterial blood gas changes during breath-holding from functional residual capacity. *Chest.* 1996;110:958–964.

91. Hellems HK, Ord JW, Talmers FN, Christensen RC. Effects of hypoxia on coronary blood flow and myocardial metabolism in normal human subjects. *Circulation*. 1957;16:893–893.

92. Wyss CA, Koepfli P, Fretz G, Seebauer M, Schirlo C, Kaufmann PA. Influence of Altitude Exposure on Coronary Flow Reserve. *Circulation.* 2003;108:1202–1207.

94. McNulty PH, King N, Scott S, Hartman G, McCann J, Kozak M, Chambers CE, Demers LM, Sinoway LI. Effects of supplemental oxygen administration on coronary blood flow in patients undergoing cardiac catheterization. *Am J Physiol Heart Circ Physiol.* 2005;288:H1057–H1062.

100. Yang H-J, Yumul R, Tang R, Cokic I, Klein M, Kali A, Sobczyk O, Sharif B, Tang J, Bi X, Tsaftaris SA, Li D, Conte AH, Fisher JA, Dharmakumar R. Assessment of Myocardial Reactivity to Controlled Hypercapnia with Free-breathing T2-prepared Cardiac Blood Oxygen Level–Dependent MR Imaging. *Radiology*. 2014;272:397–406.

101. Broten TP, Romson JL, Fullerton DA, Van Winkle DM, Feigl EO. Synergistic action of myocardial oxygen and carbon dioxide in controlling coronary blood flow. *Circ Res.* 1991;68:531–542.

104. Powers ER, Bannerman KS, Fitz-James I, Cannon PJ. Effect of elevations of coronary artery partial pressure of carbon dioxide (Pco2) on coronary blood flow. *J Am Coll Cardiol*. 1986;8:1175–1181.

107. Case RB, Greenberg H. The response of canine coronary vascular resistance to local alterations in coronary arterial P CO2. *Circ Res*. 1976;39:558–566.

108. Atkins JL, Johnson KB, Pearce FJ. Cardiovascular responses to oxygen inhalation after hemorrhage in anesthetized rats: hyperoxic vasoconstriction. *Am J Physiol Heart Circ Physiol*. 2007;292:H776–H785.

123. Shepherd JT. The lungs as receptor sites for cardiovascular regulation. *Circulation.* 1981;63:1–10.

124. Heusser K, Dzamonja G, Tank J, Palada I, Valic Z, Bakovic D, Obad A, Ivancev V, Breskovic T, Diedrich A, Joyner MJ, Luft FC, Jordan J, Dujic Z. Cardiovascular Regulation During Apnea in Elite Divers. *Hypertension.* 2009;53:719–724.

125. Fagius J, Sundlöf G. The diving response in man: effects on sympathetic activity in muscle and skin nerve fascicles. *J Physiol.* 1986;377:429–443.

136. Guensch DP, Fischer K, Shie N, Lebel J, Friedrich MG. Hyperoxia Exacerbates Myocardial Ischemia in the Presence of Acute Coronary Artery Stenosis in Swine. Circ *Cardiovasc Interv.* 2015;8:e002928.

137. Kahn CM, Line S, Allen DG. The Merck veterinary manual. Merck Whitehouse Station, NJ; 2010.

145. Tousoulis D, Antoniades C, Stefanadis C. Evaluating endothelial function in humans: a guide to invasive and non-invasive techniques. *Heart.* 2005;91:553–558.

146. Pries AR, Habazettl H, Ambrosio G, Hansen PR, Kaski JC, Schächinger V, Tillmanns H, Vassalli G, Tritto I, Weis M, Wit C de, Bugiardini R. A review of methods for assessment of coronary microvascular disease in both clinical and experimental settings. *Cardiovasc Res.* 2008;80:165–174.

148. Farquhar H, Weatherall M, Wijesinghe M, Perrin K, Ranchord A, Simmonds M, Beasley R. Systematic review of studies of the effect of hyperoxia on coronary blood flow. *Am Heart J.* 2009;158:371–377.

149. Reller MD, Morton MJ, Giraud GD, Wu DE, Thornburg KL. Maximal myocardial blood flow is enhanced by chronic hypoxemia in late gestation fetal sheep. *Am. J. Physiol. Heart Circ. Physiol.* 1992;263:H1327–H1329.

150. Foster GE, Sheel AW. The human diving response, its function, and its control. *Scand J Med Sci Spor*. 2005;15:3–12.

151. Crystal GJ. Carbon Dioxide and the Heart: Physiology and Clinical Implications. *Anesth. Analg.* 2015;121:610–623.

152. Broten TP, Feigl EO. Role of myocardial oxygen and carbon dioxide in coronary autoregulation. *Am J Physiol Heart Circ Physiol.* 1992;262:H1231–H1237.

153. Hardie JA, Vollmer WM, Buist AS, Ellingsen I, Mørkve O. Reference values for arterial blood gases in the elderly. *Chest*. 2004;125:2053–2060.

155. Ganz W, Donoso R, Marcus H, Swan HJC. Coronary Hemodynamics and Myocardial Oxygen Metabolism during Oxygen Breathing in Patients with and without Coronary Artery Disease. *Circulation*. 1972;45:763–768.

154. Coleman MD. Chapter 2 - Respiratory and Pulmonary Physiology A2 - Duke, James. In: Anesthesia Secrets (Fourth Edition). Philadelphia: Mosby; 2011. p. 17–23.

156. Konishi M, Akiyama E, Iwahashi N, Ebina T, Kimura K. Hypercapnia in Acute Heart Failure Patients with or Without Pulmonary Edema. *Journal of Cardiac Failure*. 2014;20:S168.

157. Kety SS, Schmidt CF. The effects of active and passive hyperventilation on cerebral blood flow, cerebral oxygen consumption, cardiac output, and blood pressure of normal young men. *J Clin Invest*. 1946;25:107–119.

3 Chapter 3 – Hyperoxia exacerbates Myocardial ischemia in the Presence of acute Coronary Artery Stenosis in Swine

Foreword

In this chapter, we apply OS- CMR to measure the change in myocardial oxygenation when swine in an acute coronary artery stenosis model are ventilated with 100% oxygen. While many studies recently are reporting poorer morbidity and mortality with the administration of oxygen to human coronary heart disease patients[96], this is one of the first studies to assess the impact on myocardial oxygenation and cardiac function. This manuscript is also the first one published from this animal study.

My role in the study

This article is a parallel project of my animal study, of which I am a second author of the manuscript. My role included organizing the project, conducting data and statistical analysis and helping with the preparation of the manuscript. I also personally presented this data at the congress for the European Association of Cardiothoracic Anaesthesiologists (EACTA, 2014, Florence Italy).

Furthermore, data from this chapter was also presented at the European Society of Cardiology (ESC 2014, Barcelona, Spain) and at the Swiss Society of Anaesthesiology and Resuscitation (SGAR 2015, Schweizerische Gesellschaft für Anästhesiologie und Reanimation, St. Gallen, Switzerland) by Dr. Guensch.

Hyperoxia exacerbates Myocardial ischemia in the Presence of acute Coronary Artery Stenosis in Swine

Dominik P. Guensch[1,2], MD, **Kady Fischer[1,2],** BHSc., Nancy Shie, BSc.[1], Julie Lebel[1], RLAT
Matthias. G. Friedrich, MD, FESC, FACC[1,3]

[1]Philippa & Marvin Carsley CMR Centre at the Montreal Heart Institute, Montreal, QC, Canada,
[2]Bern University Hospital, Department Anaesthesiology and Pain Therapy, Inselspital, Bern, Switzerland,
[3]Departments of Cardiology and Radiology, Université de Montréal, Montreal, QC, Canada

All co-authors wrote and approved the manuscript. Published by *Circulation: Cardiovascular Interventions.*

(Guensch DP, Fischer K, Shie N, Lebel J, Friedrich MG. Hyperoxia Exacerbates Myocardial Ischemia in the Presence of Acute Coronary Artery Stenosis in Swine. *Circ Cardiovasc Interv*. 2015;8:e002928.)

3.1 Abstract

Background: Current guidelines limit the use of high oxygen tension after return of spontaneous circulation following cardiac arrest, focusing on neurological outcome and mortality. Little is known about the impact of hyperoxia on the ischemic heart. Oxygen is frequently administered and is generally expected to be beneficial. This study seeks to assess the effects of hyperoxia on myocardia oxygenation in the presence of severe coronary artery stenosis in swine.

Methods and Results: In 22 healthy pigs, we surgically attached an MRI compatible flow probe to the left descending coronary artery (LAD). In 11 pigs a hydraulic occluder was inflated distal to the flow probe. After increasing paO_2 to more than 300mmHg, LAD flow decreased in all animals. In 8 stenosed animals with a mean fractional flow reserve of 0.64±0.02, hyperoxia resulted in a significant decrease of myocardial signal intensity (SI) in oxygenation-sensitive CMR images of the mid-apical segments of the LAD territory. This was not seen in remote myocardium or in the other 8 healthy animals. The decreased SI was accompanied by a decrease in circumferential strain in the same segments. Further, ejection fraction, cardiac output, and oxygen extraction ratio declined in these animals. Changing $paCO_2$ levels did not have a significant effect on any of the parameters, however hypercapnia seemed to non-significantly attenuate the hyperoxia induced changes.

Conclusion: Ventilation-induced hyperoxia may decrease myocardial oxygenation and lead to ischemia in myocardium subject to severe coronary artery stenosis.

Keywords: Oxygen ▪ Ischemia ▪ Imaging

3.2 Introduction

Exogenous oxygen administration, resulting in high arterial oxygen tension, is frequently applied in medical care[158]. Importantly, oxygen and carbon dioxide both have vasoactive properties. While increased CO_2 levels have vasodilative properties in cerebral and coronary arteries[82,93], high oxygen tension may have vasoconstricting effects on coronary arteries[94]. If such vasoconstriction would result in a net reduction of blood flow in the territory of a severely stenotic coronary artery, tissue oxygenation may drop. Little however is known on whether hyperoxia can exacerbate or induce myocardial ischemia in myocardium exposed to severe coronary artery stenosis. The current ACC/AHA resuscitation guidelines limit the use of excessively high inspiratory oxygen concentrations in post-cardiac arrest care (Class I, Level of Effort (LOE) C) after return of spontaneous circulation (ROSC)[159]. Yet, these recommendations are mainly based on animal studies focusing on neurologic pathophysiology and outcome[160,161]. Similar studies have not been published related to myocardial ischemia; yet large retrospective multicenter trials have suggested that hyperoxia may increase patient mortality after cardiac arrest with ROSC[95].

Oxygenation-sensitive cardiovascular magnetic resonance (OS-CMR) imaging detects myocardial oxygenation changes by exploiting the paramagnetic properties of deoxyhaemoglobin. Reduced haemoglobin saturation, reduced myocardial blood flow, and increased oxygen extraction of the myocardium, result in a higher deoxyhaemoglobin fraction in the tissue, which will reduce signal intensity in oxygenation-sensitive sequences[162]. Thus, OS-CMR is a method that can detect myocardial ischemia on a tissue level in-vivo. It has been shown that it can detect changes in myocardial oxygenation triggered by systemic changes of blood gases i.e. oxygen and carbon dioxide[83,112].

The purpose of this study was to investigate the effect of hyperoxia on myocardial oxygenation and myocardial function parameters in animals with a significant stenosis of the left descending coronary artery (LAD) in comparison to control animals. We additionally investigated the effects of $paCO_2$ changes on myocardial oxygenation during hyperoxia in this model.

Study Implications

What is Known:

- Patients with hyperoxia after ROSC have a higher mortality.
- Current resuscitation recommendations after ROSC focus on mortality and neurologic outcome.
- Hyperoxia leads to coronary vasoconstriction.

What the Study Adds:

- Hyperoxia does not compensate for coronary vasoconstriction in swine with acute significant coronary artery stenosis.
- Hyperoxia results in a decrease in myocardial oxygenation and regional function in acute stenosis in swine.

3.3 Methods

Animal Preparation

Twenty-two healthy swine pigs (33±1 kg, Yorkshire-Landrace) were used in this study. All animals received 82.5mg Aspirin PO the evening prior to the experiments. The pigs were anesthetized with 2-4mg/kg Propofol IV after premedication with 4ml Telazol IM (200mg Tiletamine, 200mg Zolazepam). Anesthesia was maintained with Propofol (4-36 mg/kg/h IV) and Remifentanil (0-3.5µg/kg/min IV) as required for sufficient anesthesia depth. Percutaneous cannulations of the femoral artery and vein were performed for drug and fluid administration, as well for obtaining blood gases and invasive blood pressure measurements. To prevent arrhythmia, serum levels of potassium (4.4-6.5 mM) and magnesium (0.9-1.4 mM) were corrected to normal values for swine if required, and 75mg of amiodarone were administered over 30min. An 11F sheath was placed in the right jugular vein with an indwelling catheter, which was inserted into the coronary sinus under x-ray guidance for blood gas analysis. A left-sided thoracotomy was performed and after pericardiotomy a perivascular MR-compatible flow probe (Transonic Systems, Ithica, NY, USA) was placed around the proximal left anterior descending artery (LAD).

FFR-guided Stenosis of the LAD

All animals received a bolus of 5,000 U heparin IV. Eleven animals served as controls, while in 11 animals a perivascular hydraulic occluder (In Vivo Metric, CA, USA) was mounted around the LAD distal to the flow probe. Hyperemia was induced with 140µg/kg/min adenosine IV and Fractional Flow Reserve (FFR) was measured with a pressure guide wire (St. Jude Medical, MN, USA). The occluder was then inflated to yield an FFR value <0.75 during maximal hyperemia. An FFR of 1.0 was assigned to the control animals. In all animals a quantitative coronary angiography (QCA) was performed after the preparation in a single plane view to confirm normal coronaries in the control animals and the degree of stenosis in the stenosis group.

CMR Protocol

The animals were transferred to the MRI suite and placed in recumbent position. After baseline scans the FiO_2 was set to 1.0 and ventilation rate was adjusted to target $paCO_2$ levels of 30, 40 and 50mmHg, respectively. At each level, arterial and coronary sinus blood gases, heart rate, arterial blood pressure, SpO_2, changes in LAD blood flow, left ventricular function parameters and oxygenation-sensitive (OS)-CMR images were recorded. The myocardial oxygen extraction ratio (O_2er) was calculated from the oxygen content of the arterial (CaO_2) and coronary sinus ($CcsO_2$) blood: $O_2er = [CaO_2-CcsO_2] / CaO_2$. All parameters were compared to the baseline of paO_2=100mmHg and $paCO_2$=40mmHg. Blood gas levels were set in random order.

Images were acquired with a clinical 3T MRI system (MAGNETOM Skyra 3T; Siemens Healthcare, Erlangen, Germany) using an 18-channel cardiac phased array coil. LV function was imaged using an ECG-gated balanced steady-state free precession (SSFP) sequence (echo time (TE) 1.43ms, repetition time (TR) 3.3ms, flip angle 65°; voxel dimensions 1.6x1.6x6.0mm; bandwidth 962Hz), covering the entire left ventricle with a short axis stack. OS-CMR images were acquired in two short axis slices (mid ventricular, mid-apical) using an ECG triggered SSFP sequence (TE/TR 1.70ms/3.4ms; flip angle 35°; voxel dimensions 2.0x2.0x10.0mm; bandwidth 1302Hz).

Image Analysis

All images were anonymized before analysis with clinically validated software (cvi[42], Circle Cardiovascular Imaging, Calgary, AB, Canada). Analysis of left ventricular function parameters and peak circumferential strain was performed automatically after tracing endo- and epicardial contours in the short axis stack. Myocardial oxygenation was assessed by tracing myocardial borders in end-systolic frames. Changes in myocardial oxygenation for each level were expressed as %change in SI (%SI) from the baseline level for the LAD region (AHA segments 1, 2) and the remote myocardium (Segments 4, 5). Further, the %change in SI was compared between the LAD territory and the remote myocardium for the control and the stenosis group. Segments with possible mixed perfusion beds (AHA 3 and 6) were excluded from analysis.

Statistical Analysis

Data is expressed as mean ± SEM. Continuous variables were assessed for normal distribution with the D'Agostino-Pearson test. Paired t-tests or repeated measures ANOVA were used to compare data from baseline, and independent t-tests compared data between groups. In the case of multiple analyses, repeated measures ANOVA's or two-way mixed effects models were used to compare results both within and between groups, with following post-hoc tests. If the data was not normally distributed a Mann Whitney or a Wilcoxon matched-pairs signed rank test was performed. Associations between ΔSI, FFR, O_2er, and coronary flow were assessed with Pearson's correlation. Tests were performed with GraphPad Prism version 6.0 for Mac (GraphPad Software, La Jolla California USA) and SPSS version 21 (SPSS IBM, New York, USA). Results were considered statistically significant if the p-value <0.05.

This study was conducted in accordance with the ''Guide to the Care and Use of Experimental Animals'' by the Canadian Council on Animal Care and approved by the local Animal Care and Use Board.

3.4 Results

In the group of healthy pigs three animals had to be excluded: One died after surgical complications, while two animals died later during the MRI scans due to refractory cardiovascular instability. Three animals died by stenosis-induced ischemia, resulting in eight animals in both groups.

Severity of Stenosis

The inflation of the perivascular occluder around the LAD resulted in a mean FFR of 0.64±0.02 during maximal hyperemia and a reduction in vessel diameter of 62.9±4.9% versus 7.1±2.7% ($p<0.001$) in the control animals.

Myocardial Blood Flow

There was no significant difference in baseline LAD flow between the stenosis and control animals. Induced hyperoxia however resulted in a significant decrease in LAD blood flow in the stenosis animals by -24.0±4.5%, -14.8±2.0% and -13.1±5.1% for hypo-, normo- and hypercapnic hyperoxia, respectively ($p<0.05$). In control animals, hyperoxia only decreased flow under hypocapnia (-13.3±5.0%, $p<0.05$) and normocapnia (-12.7±2.3%, $p<0.01$), while hypercapnia neutralized this effect (+2.20±5.5%, n.s.). Although increasing $paCO_2$ levels seemed to attenuate the hyperoxia-mediated decrease in blood flow, there was no significant difference in the LAD flow changes between the different $paCO_2$ levels.

Myocardial Oxygen Extraction Ratio

Prior to the experimental procedure in the MRI, baseline myocardial oxygen extraction ratio was higher in the ischemic animals (59±4%) vs. healthy animals(47±3%, $p<0.05$) at physiologic blood gas levels (paO_2=100mmHg, $paCO_2$=40mmHg). In the stenosis group, myocardial oxygen extraction ratio was decreased during normocapnic hyperoxia (-6.7±1.1%,

p<0.05) and hypercapnic hyperoxia (-10.6±2.3%, p<0.01) compared to baseline, while there was no change in the control animals.

OS-CMR

9.7% of all myocardial segments had to be excluded due to predefined exclusion criteria, mostly due to susceptibility artefacts in the inferolateral wall (5.5% segments of healthy and 14.0% of stenosis animals). Inducing blood gas changes yielded no global signal intensity differences in myocardial oxygenation in either slice.

Changes in the LAD perfusion territory in the mid-apical SAX slice are shown in Table 10. Figure 21 shows the change in SI after induction of hyperoxia from baseline in a healthy and a stenosed animal, accompanied with the changes in myocardial strain. While increased supra-normal oxygen tension resulted in increased SI in healthy animals, hyperoxia resulted in a SI decrease during hypocapnia and normocapnia (Table 10, Figure 19). The SI increases were attenuated in stenosis animals compared to the control group during hypercapnic hyperoxia. There was no difference in myocardial SI in the LAD territories in the mid-ventricular slice.

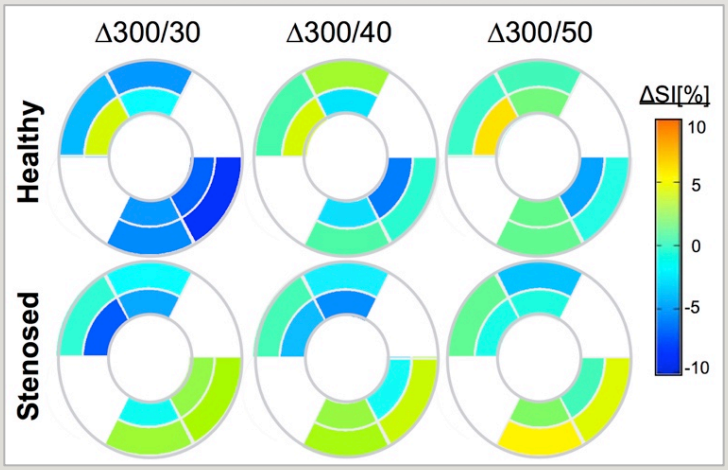

Figure 19: Mean changes in myocardial oxygenation in all hyperoxic blood gas levels. Difference in myocardial signal intensity (SI) in the mid-ventricular and mid-apical slice during hypocapnic (300/30), normocapnic (300/40) and hypercapnic (300/50) hyperoxia. Changes in myocardial SI were only different in the more distal slice to the occluder. While hypo- and normocapnic hyperoxia decreased myocardial oxygenation (p<0.05, Table 1), hypercapnia still

showed an attenuated decrease compared to the normal controls ($p<0.05$). Levels expressed as paO_2[mmHg]/$paCO_2$[mmHg].

Mid-ventricular slice			
Level	**Control**	**Stenosis**	**p**
300/30	-2.0±2.0	0.1±1.1	0.31
300/40	2.2±2.0	-0.3±1.4	0.35
300/50	0.7±1.3	0.1±1.6	0.76
Mid-apical slice			
Level	**Control**	**Stenosis**	**p**
300/30	1.9±1.7%	-2.8±0.9%	<0.05*
300/40	2.6±1.3%	-2.0±1.0%	<0.05*
300/50	4.0±1.2%	+0.2±0.7%	<0.05*

Table 10: Changes in myocardial signal intensity from baseline
Changes in myocardial signal intensity [%]from baseline (paO_2=100mmHg, $paCO_2$=40mmHg) in the mid- ventricular and mid-apical slice in the LAD-territory. Changes in signal intensity between control and stenosis animal for all hyperoxic levels are different ($p<0.05$), while none of the changes are different in the mid-ventricular slice. Levels depicted as paO_2[mmHg]/$paCO_2$[mmHg], Mean±SEM

Ejection Fraction			
Level	**Control**	**Stenosis**	**P-value**
100/40	54±4%	48±3%	0.26
300/30	56±4%	41±5%	**<0.05***
300/40	56±3%	42±4%	**<0.05***
300/50	49±7%	41±6%	0.43
Cardiac Output			
Level	**Control**	**Stenosis**	**P-value**
100/40	2813±294	2073±171	**<0.05***
300/30	3246±303	2175±180	**<0.05***
300/40	3217±308	2275±147	**<0.05***
300/50	3111±406	2125±287	0.06

Table 11: Function Parameters
Differences between control and stenosis animals in ejection fraction (EF) and cardiac output (CO). We find differences in EF and CO between control and stenosis animals during hyperoxia.
Mean±SEM, $p<0.05$ is significant. Levels reported as paO_2[mmHg]/$paCO_2$[mmHg].

Function Parameters

In stenosis animals, left ventricular ejection fraction (EF) did not differ at baseline, but was significantly reduced after induction of hypo- and normocapnic hyperoxia (Table 11, $p<0.05$) when compared to healthy animals. Cardiac output in ischemic animals was initially lower at baseline, and decreased further during hyperoxic hypo- and normocapnia ($p<0.05$).

Circumferential strain was significantly attenuated from baseline values in the LAD territory of the ischemic animals (Figure 20) at a paO_2 of 300mmHg for 30mmHg $paCO_2$ (-21.35±10.52, $p<0.05$) and 40mmHg $paCO_2$ (-18.24±9.72, $p<0.05$), while a $paCO_2$ of 50mmHg

further enforced a trend for a reduction in strain (-18.43±9.66, p=0.055). Furthermore, global strain was -16.60±7.70% reduced during hypocapnic hyperoxia. No change in myocardial strain was seen for the remote myocardium or the LAD perfusion territory in healthy animals during any hyperoxic level.

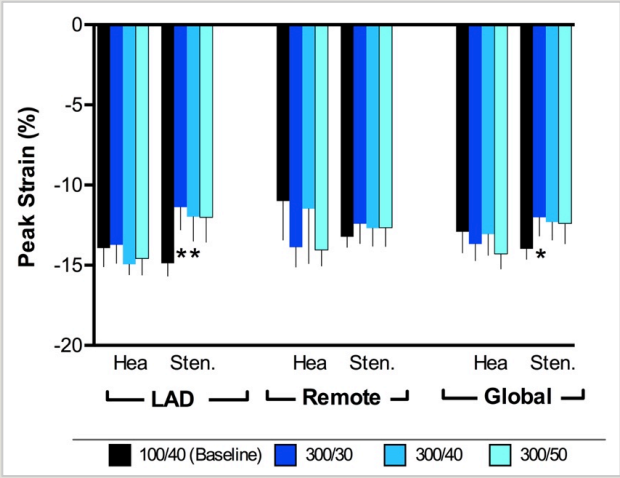

Figure 20: Peak circumferential strain during hyperoxia
Peak myocardial strain during hypo- (300/30), normo- (300/40) and hypercapnic hyperoxia (300/50) in healthy (Hea.) and animals with a significant LAD stenosis (Sten.). In the animals with a significant coronary artery stenosis, peak myocardial strain was found to be reduced in the LAD region compared to baseline strain ($p<0.05$) There was no change in strain in the LAD territory of healthy animals or remote myocardium. However, hypocapnic hyperoxia resulted in a drop on global circumferential strain in the healthy animals. Levels expressed as paO_2[mmHg]/$paCO_2$[mmHg], Mean±96% confidence intervals, *$p<0.05$.

Relationship to Oxygenation Changes

The changes in myocardial SI in the LAD territory of the mid-apical slice showed a strong association with the measured FFR of the coronary artery stenosis for all blood gas levels (hypocapnic hyperoxia: R=0.53; normocapnic hyperoxia: R=0.58; hypercapnic hyperoxia: R=0.60, $p<0.05$). Additionally, changes in flow at hypercapnic hyperoxia were also correlated with changes in OS-SI in the LAD territory (R=0.5, $p<0.05$). Otherwise, no significant correlations were observed with O_2er or flow to other levels.

These correlations were not seen in the mid-ventricular slice, more proximal to the stenosis.

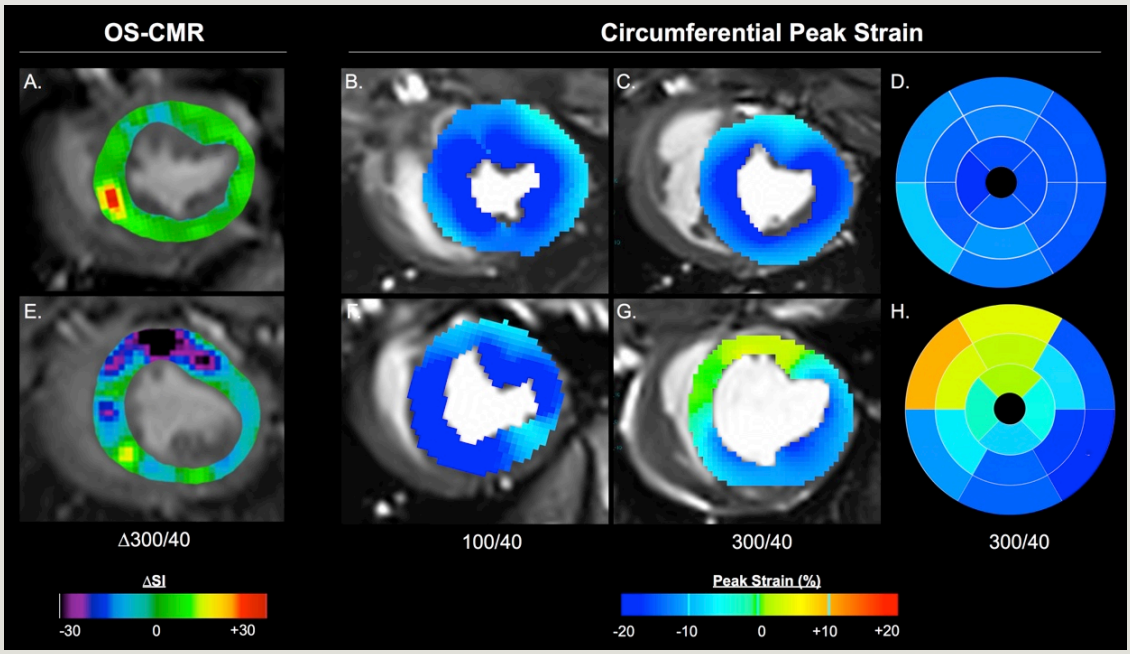

Figure 21: Changes in myocardial oxygenation and strain in a healthy and an ischemic animal during hyperoxia.

Changes in myocardial oxygenation after induction of normocapnic hyperoxia from baseline in a healthy (A) and a stenosed animal (E). A decrease in the segments perfused by the left anterior descending coronary artery (LAD) is visible in the stenosed animal. Baseline myocardial strain was similar in healthy (B) and the stenosed (F) pigs. However, when paO_2 was increased to 300mmHg the stenosed animals showed a decrease in peak circumferential strain in the LAD territory (G: mid-ventricular slice, H: AHA segmentation), which was not seen in the healthy animals (C, D). The area of reduced strain matched the region with decreased oxygenation. Levels expressed as paO_2[mmHg]/$paCO_2$[mmHg].

3.5 Discussion

Our study provides evidence that hyperoxia may worsen myocardial ischemia in severe coronary artery stenosis, accompanied by ventricular dysfunction.

Before the 2010 revision of the ACC/AHA guidelines supplementation of oxygen for patients with acute coronary syndrome was considered beneficial, based on previous findings that supplemental oxygen may decrease myocardial injury[163,164]. The studies, dating from the 1970's however were not standardized, randomized or controlled. In 1976, Rawles and Kenmure performed a randomized double-blinded controlled study and showed that oxygen therapy was associated with higher Aspartate Aminotransferase levels post infarct, indicating

more severe myocardial injury, and found no benefit with respect to mortality[165]. Although not significant, the data even suggested that mortality may be higher in the oxygen than in the control group (13.3% vs. 3.9%). In 1971, Loeb and colleagues observed in a clinical study in 31 patients with acute non-complicated myocardial infarction, that treatment with 6L/min oxygen was associated with a higher mean arterial pressure, a lower cardiac index and, in 7 patients, an increase in LV end diastolic pressure. [166] Nevertheless, the authors suggested, that oxygen should be administered in these patients due to a high incidence of concurrent hypoxemia.

Literature shows that oxygen is still administered in 80% of cases with acute myocardial infarction and more than 50% of health professionals consider it to reduce mortality[167,168167,168]. McNulty et al. showed that breathing supplemental oxygen for 15 min with a mask increases coronary vascular resistance by 40% and decreases Doppler flow velocity by 20% and coronary blood flow by 30% in patients undergoing cardiac catheterization[94].

Potential mechanisms that lead to hyperoxic coronary vasoconstriction have been outlined by Moradkhan and Sinoway[158]. Nitric Oxide (NO), which relaxes smooth muscle cells in the arterioles act as a scavenger for reactive oxygen species during hyperoxia. This results in a reduced bioavailability of NO and to vasoconstriction[169,170]. An animal study also suggested the presence L-type Calcium channels on vascular smooth muscle cells, which contribute to blood flow control in an oxygen-sensitive manner[171]. Metabolic demands are also controlled by adenosine triphosphate (ATP)-gated potassium channels. Hypoxia leads to a drop in ATP levels in the cells. These potassium channels open if the ATP concentration falls, resulting in increased tissue perfusion[172]. Hyperoxia however was found to reverse that effect, down-regulating flow in the coronary arteries[115]. Further, isolated cardiomyocytes were found to convert angiotensin I to angiotensin II during a hyperoxic stimulus, which could potentially release the vasoconstrictor endothelin-1 levels.

The mounting evidence of reduction of coronary blood flow during hyperoxia led to concern about the safety of oxygen[173]. A meta-analysis of 6 studies in 665 patients by Caldeira et al. showed that oxygen therapy for acute myocardial infarction may increase the risk of death by 16%[174]. Moradkhan and Sinoway stated that hyperoxia is not perceived to be

detrimental by medical staff, due to conflicting data and a lack of randomized, blinded and controlled studies[158]. The current AHA resuscitation 2010 guidelines do not limit the use of oxygen during cardiac arrest but in patients with ROSC (Class I, LOE C)[159]. These recommendations are based on neurologic studies where hyperoxia as a part of the ischemia/reperfusion injury exacerbated neurologic outcome,[175,176] while normoxic ventilation seems to attenuate that effect[160,161].

A retrospective multicenter cohort study in the United States included 6,326 ICU patients with ROSC in 3 groups: hypoxia (<60mmHg paO_2), normoxia (60-300mmHg) and hyperoxia (>300mmHg)[95]. The group found that hyperoxia (63% mortality, vs. 45% in normoxia and 57% in the hypoxia group) was independently associated with increased in-hospital mortality, with an odds-ratio for hyperoxia of 1.8. In a subgroup with paO_2 >400mmHg, mortality was even higher (69%). In addition, they found that hyperoxia was associated with a lower likelihood of independent functional status at hospital discharge than with normoxia. Other studies confirm these findings[177,178]

A study by Meyhoff and colleagues even reported a long-term mortality in patients receiving abdominal surgery[179]. 23% of the patients died in the group ventilated with a FiO_2 of 0.8 versus 18.3% in the group with a FiO_2 of only 0.3 in this randomized trial follow-up.

Most of the referenced studies assessed changes in neurologic outcome after ROSC or death. However, it is not clear how many of these deaths were due to a hyperoxia-induced aggravation of myocardial ischemia. There is also invasive data on changes of coronary resistance and myocardial blood flow[94], however these studies cannot assess the impact on the myocardium on a tissue level as the increase in arterial oxygen content (CaO_2) can counterbalance the reduction in myocardial blood flow.

OS-CMR can detect the changes in myocardial oxygenation in-vivo using the paramagnetic properties of deoxygenated haemoglobin as an inherent contrast[162]. Changes in delivery or myocardial oxygen demand such as myocardial blood flow, haemoglobin saturation, myocardial workload and oxygen extraction all factor in into changes in OS-SI. Myocardial oxygenation depends on the balance of oxygen delivery and demand. Delivery is determined by vascular density, blood flow, haemoglobin concentration, and haemoglobin

oxygenation, while demand is reflected by the myocardial workload. If oxygen delivery does not meet the metabolic requirements, the relative concentration of deoxygenated haemoglobin in post-capillary venules increases, while that of oxyhaemoglobin decreases. The increase in deoxyhaemoglobin leads to a decrease of SI in oxygenation-sensitive MR images. Thus, the drop in SI we observed in myocardium exposed to a stenotic coronary artery reflects a decline in myocardial oxygenation due to vasoconstriction caused by hyperoxia. Several recent studies have used OS-CMR to monitor changes of myocardial oxygenation after changing blood gas levels, especially O_2 and CO_2[47,82,83,112]. Those studies showed that OS-CMR is a reliable tool to assess the impact of hyperoxia on myocardial oxygenation [135].

Coronary artery stenosis in our animals was verified by an FFR of <0.75[180]. Consistent with other studies, we used a paO_2 of >300mmHg for hyperoxia[95,177,178] compared to a physiologic level of 100mmHg. Our model allowed for a tightly controlled setting, which is difficult to achieve in patient studies. Confirming the observations of McNulty et al., we found a substantial decrease in blood flow in the LAD during hyperoxia[94]. Adding further vasodilating (hypercapnia) and vasoconstricting (hypocapnia) stimuli we also wanted to investigate if the hyperoxic vasoconstriction could be further aggravated or attenuated. Although not significant, we found a relationship between the $paCO_2$ levels and the decrease in LAD blood flow in both groups.

The decrease in myocardial oxygen extraction during hyperoxia somewhat contradicts the underlying pathophysiology: with reduced oxygen delivery due to coronary vasoconstriction a higher oxygen extraction is to be expected, especially in the already ischemic animals. However, this decrease in myocardial oxygen consumption is well in-line with literature[181–183]. High oxygen tensions seem to decrease capillary density with a consecutive reduction of oxygen diffusion and thus extraction. Increasing CO_2 levels seem to attenuate this effect.

Interestingly, looking at peak circumferential myocardial strain after inducing hyperoxia we saw a reduction in myocardial strain in the LAD perfusion territory that was absent in the remote myocardium and in the LAD territory of the healthy animals, supporting the concept that the myocardial hyperoxia-aggravated ischemia was severe enough to result in a local myocardial dysfunction. The reduction in global myocardial strain during hyperoxic

hypocapnia can be explained by the combination of two vasoconstrictive stimuli. The fact that only the mid-apical slice showed significant differences in myocardial SI in OS-CMR images can be explained by the fact that the mid-ventricular slice may have been placed too close to the occluder. The proximal slice may be perfused mainly by vessel proximal to the stenosis, while in the lower slice the stenosis has a full effect.

Our data are in line with findings of previous studies and extend the concept further by directly demonstrating an exacerbation of myocardial ischemia by hyperoxia. The results of this pilot study now warrants for larger clinical studies with follow up to investigate the role of hyperoxia in myocardial ischemia and also the cause of in-hospital deaths after ROSC. We also expect our findings to provide further evidence supporting caution in the use of oxygen in anesthesia, especially in known coronary artery disease. If confirmed, current guidelines on the use of oxygen in cardiac patients may have to be revised.

Limitations:

This study is limited by the small sample size. Also anesthesia itself is a confounding factor altering vital parameters, potentially inducing ischemia and also reducing tissue oxygen demand. In our study the animals also had an acute stenosis, with a pathophysiology different from chronic coronary artery disease. In this study only female pigs have been used. This may be a confounder as hyperoxia and its subsequent mechanisms could vary as a function of sex. While no animal model can perfectly resemble human physiology, coronary anatomy and collateral blood flow in swine is considered very similar to humans[184].

3.6 Conclusion:

In the presence of severe coronary artery stenosis, hyperoxia induced by oxygen administration not only reduces coronary blood flow, but also leads to a regional decrease in myocardial oxygenation and myocardial function. Thus, the administration of excess oxygen in patients with severe coronary artery stenosis may exacerbate ischemia. Further research is required and current clinical practice may have to be revisited.

3.7 Chapter References

47. Fischer K, Guensch DP, Friedrich MG. Response of myocardial oxygenation to breathing manoeuvres and adenosine infusion. *Eur Heart J Cardiovasc Imaging*. 2015;16:395–401.

82. Guensch DP, Fischer K, Flewitt JA, Friedrich MG. Impact of Intermittent Apnea on Myocardial Tissue Oxygenation—A Study Using Oxygenation-Sensitive Cardiovascular Magnetic Resonance. PLoS ONE. 2013;8:e53282

83. Guensch DP, Fischer K, Flewitt JA, Yu J, Lukic R, Friedrich JA, Flewitt JA, Friedrich MG. Breathing manoeuvre-dependent changes in myocardial oxygenation in healthy humans. *Eur Heart J Cardiovasc Imaging*. 2014;15:409–14.

95. Kilgannon J, Jones AE, Shapiro NI, et al. ASsociation between arterial hyperoxia following resuscitation from cardiac arrest and in-hospital mortality. *J Am Med Assoc*. 2010;303:2165–2171.

97. Beaudin AE, Brugniaux JV, Vohringer M, Flewitt J, Green JD, Friedrich MG, Poulin MJ. Cerebral and myocardial blood flow responses to hypercapnia and hypoxia in humans. *Am J Physiol Heart Circ Physiol*. 2011;301:H1678-86.

112. Guensch DP, Fischer K, Flewitt JA, Friedrich MG. Myocardial oxygenation is maintained during hypoxia when combined with apnea - a cardiovascular MR study. *Physiol. Rep*. 2013;1:e00098.

115. Mouren S, Souktani R, Beaussier M, Abdenour L, Arthaud M, Duvelleroy M, Vicaut E. Mechanisms of coronary vasoconstriction induced by high arterial oxygen tension. *Am J Physiol*. 1997;272:H67–75.

119. McNulty PH, King N, Scott S, Hartman G, McCann J, Kozak M, Chambers CE, Demers LM, Sinoway LI. Effects of supplemental oxygen administration on coronary blood flow in patients undergoing cardiac catheterization. *Am J Physiol Heart Circ Physiol*. 2005;288:H1057–1062.

135. Guensch DP, Friedrich MG. Novel Approaches to Myocardial Perfusion: 3D First-Pass CMR Perfusion Imaging and Oxygenation-Sensitive CMR. *Curr Cardiovasc Imaging Rep*. 2014;7:1–6.

148. Farquhar H, Weatherall M, Wijesinghe M, Perrin K, Ranchord A, Simmonds M, Beasley R. Systematic review of studies of the effect of hyperoxia on coronary blood flow. *Am Heart J*. 2009;158:371–377.

158. Moradkhan R, Sinoway LI. Revisiting the Role of Oxygen Therapy in Cardiac Patients. *J Am Coll Cardiol*. 2010;56:1013–1016.

159. Peberdy MA, Callaway CW, Neumar RW, Geocadin RG, Zimmerman JL, Donnino M, Gabrielli A, Silvers SM, Zaritsky AL, Merchant R, Hoek TLV, Kronick SL. Part 9: Post–Cardiac Arrest Care 2010 American Heart Association Guidelines for Cardiopulmonary Resuscitation and Emergency Cardiovascular Care. *Circulation*. 2010;122:S768–S786.

160. Liu Y, Rosenthal RE, Haywood Y, Miljkovic-Lolic M, Vanderhoek JY, Fiskum G. Normoxic Ventilation After Cardiac Arrest Reduces Oxidation of Brain Lipids and Improves Neurological Outcome. *Stroke*. 1998;29:1679–1686.

161. Vereczki V, Martin E, Rosenthal RE, Hof PR, Hoffman GE, Fiskum G. Normoxic resuscitation after cardiac arrest protects against hippocampal oxidative stress, metabolic dysfunction, and neuronal death. *J Cereb Blood Flow Metab*. 2005;26:821–835.

162. Friedrich MG, Karamitsos TD. Oxygenation-sensitive cardiovascular magnetic resonance. *J Cardiovasc Magn Reson*. 2013;15:43.

163. Maroko PR, Radvany P, Braunwald E, Hale SL. Reduction of infarct size by oxygen inhalation following acute coronary occlusion. *Circulation*. 1975;52:360–368.

164. Madias JE, Hood WB. Reduction of precordial ST-segment elevation in patients with anterior myocardial infarction by oxygen breathing. *Circulation*. 1976;53:I198–200.

165. Rawles JM, Kenmure AC. Controlled trial of oxygen in uncomplicated myocardial infarction. *Br Med J*. 1976;1:1121–1123.

166. Loeb HS, Chuquimia R, Sinno MZ, Rahimtoola SH, Rosen KM, Gunnar RM. Effects of low-flow oxygen on the hemodynamics and left ventricular function in patients with uncomplicated acute myocardial infarction. *Chest*. 1971;60:352–355.

167. Burls A, Cabello JB, Emparanza JI, Bayliss S, Quinn T. Oxygen therapy for acute myocardial infarction: a systematic review and meta-analysis. *Emerg Med J*. 2011;28:917–923.

168. Cabello JB, Burls A, Emparanza JI, Bayliss S, Quinn T. Oxygen therapy for acute myocardial infarction. *Cochrane Database Syst Rev*. 2013;8:CD007160.

169. Mak S, Egri Z, Tanna G, Colman R, Newton GE. Vitamin C prevents hyperoxia-mediated vasoconstriction and impairment of endothelium-dependent vasodilation. *Am J Physiol Heart Circ Physiol*. 2002;282:H2414–2421.

170. Nanobashvili J, Neumayer C, Fuegl A, Punz A, Blumer R, Mittlböck M, Prager M, Polterauer P, Dobrucki LW, Huk I, Malinski T. Combined L-arginine and antioxidative vitamin treatment mollifies ischemia-reperfusion injury of skeletal muscle. *J Vasc Surg*. 2004;39:868–877.

171. Welsh DG, Jackson WF, Segal SS. Oxygen induces electromechanical coupling in arteriolar smooth muscle cells: a role for L-type Ca2+ channels. *Am J Physiol*. 1998;274:H2018–2024.

172. Tune JD, Richmond KN, Gorman MW, Feigl EO. Control of coronary blood flow during exercise. *Exp Biol Med (Maywood)*. 2002;227:238–250.

174. Caldeira D, Vaz-Carneiro A, Costa J. Cochrane Corner: What is the clinical impact of oxygen therapy for acute myocardial infarction? Evaluation of a Cochrane systematic review. *Rev Port Cardiol*. 2014;33:641–643.

175. Zwemer CF, Whitesall SE, D'Alecy LG. Cardiopulmonary-cerebral resuscitation with 100% oxygen exacerbates neurological dysfunction following nine minutes of normothermic cardiac arrest in dogs. *Resuscitation*. 1994;27:159–170.

176. Richards EM, Fiskum G, Rosenthal RE, Hopkins I, McKenna MC. Hyperoxic Reperfusion After Global Ischemia Decreases Hippocampal Energy Metabolism. *Stroke*. 2007;38:1578–1584.

177. Bellomo R, Bailey M, Eastwood GM, Nichol A, Pilcher D, Hart GK, Reade MC, Egi M, Cooper DJ, Study of Oxygen in Critical Care (SOCC) Group. Arterial hyperoxia and in-hospital mortality after resuscitation from cardiac arrest. *Crit Care*. 2011;15:R90.

178. Wang C-H, Chang W-T, Huang C-H, Tsai M-S, Yu P-H, Wang A-Y, Chen N-C, Chen W-J. The effect of hyperoxia on survival following adult cardiac arrest: a systematic review and meta-analysis of observational studies. *Resuscitation*. 2014;85:1142–1148.

179. Meyhoff CS, Jorgensen LN, Wetterslev J, Christensen KB, Rasmussen LS, PROXI Trial Group. Increased long-term mortality after a high perioperative inspiratory oxygen fraction during abdominal surgery: follow-up of a randomized clinical trial. *Anesth Analg*. 2012;115:849–854.

180. Tonino PAL, De Bruyne B, Pijls NHJ, Siebert U, Ikeno F, van `t Veer M, Klauss V, Manoharan G, Engstrøm T, Oldroyd KG, Ver Lee PN, MacCarthy PA, Fearon WF. Fractional Flow Reserve versus Angiography for Guiding Percutaneous Coronary Intervention. *N Engl J Med*. 2009;360:213–224.

181. Lindbom L, Tuma RF, Arfors KE. Influence of oxygen on perfused capillary density and capillary red cell velocity in rabbit skeletal muscle. *Microvasc Res*. 1980;19:197–208.

182. Lindbom L, Arfors KE. Mechanisms and site of control for variation in the number of perfused capillaries in skeletal muscle. *Int J Microcirc Clin Exp*. 1985;4:19–30.

183. Reinhart K, Bloos F, König F, Bredle D, Hannemann L. Reversible decrease of oxygen consumption by hyperoxia. *Chest*. 1991;99:690–694.

184. Weaver ME, Pantely GA, Bristow JD, Ladley HD. A quantitative study of the anatomy and distribution of coronary arteries in swine in comparison with other animals and man. *Cardiovasc Res*. 1986;20:907–917.

3.8 Applicability of Animal to Human Studies

Part 1 of this project used a large animal model for the foundation of the techniques that was applied to humans in part 2 & 3. An advantage of animal studies is the ability to perform invasive measurements and procedures not suitable or feasible for human studies. With respect to OS-CMR, the animal studies are the key for understanding the impact of coronary flow and blood gases on myocardial oxygenation signal, especially during breathing maneuvers. While animal studies can provide vital information for research topics, the results cannot be directly applied to clinical studies without considering confounding effects.

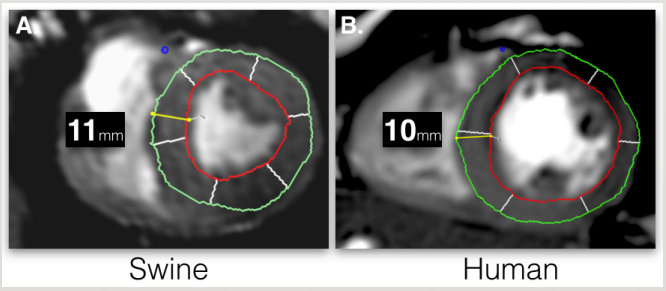

Figure 22: Comparison of the short-axis between swine and human. Short-axis view of the myocardium in the mid-ventricle between a juvenile swine (4-6 months, 30kg) used in chapters 1-3 and a healthy human volunteer from chapter 4 (Female, 20 years, 65kg). The myocardium of the left ventricles have similar areas, and thus the same approximate number of voxels are analyzed.

Application of Sequence Parameters

An advantage of using large animals is that imaging can be performed in the same clinical MRI system, using the same magnetic field strength and imaging sequences that are applied to humans. Swine have been specifically chosen for the experimental model in the project due to significant similarity of the cardiac and coronary anatomy to humans[185], including myocardial thickness. As shown in Figure 9, the myocardium has the same muscle diameter at end-systole as a healthy human. Thus allowing us to maintain the same parameters that are vital to the OS signal such as voxel size, field of view, and spatial resolution. Another major factor is the heart rate. Landrace-yorkshire swine of about 4-6 months old (20-40kg) will have heart rates ranging from about 70-120 beats/min. This is higher than in a typical

patient, and as the R-R interval decreases, temporal resolution of the sequence will change for single shot and retrospectively gated sequences. However, the majority of our imaging, specifically the OS-CMR sequence, is a prospectively gated sequence, and thus the temporal resolution does not change, rather less phases are obtained in the cardiac cycle, reducing the impact of the high heart rate.

Factors Affecting the Applicability of the Animal Model to Human Studies

The animal model in chapters 1-3, simulates an acute coronary stenosis, and is otherwise a healthy animal with fully patent microvasculature (Figure 10, situation C). The model is not necessarily representative of the many pathomechanisms occurring with the development of coronary disease, including dysfunctions of the endothelial and smooth muscle cells, stenosis and thickening of epicardial and microvascular arteries, ventricular remodelling, fibrosis and more. Specifically, the occluder only creates an intermediate stenosis in a small portion of the LAD. This would likely leave the area more prone to coronary steal as the other coronary arteries are fully functioning and because of their larger vasodilatory reserve they can have a lower vascular resistance and end up redirecting flow. However as described later in the section "*Translation of invasive measurements to human participants*", the blood flow in the other coronary arteries could not be directly measured in this study to support this theory.

Furthermore, the animal model is just an acute stenosis, in which there was no build-up up cardiovascular risk factors or mechanism leading to coronary disease such as inflammation. This model is unlike the pathophysiology of acute coronary syndromes in humans, which are commonly caused by an acute intraluminal coronary thrombus formation, often from the disruption of atherosclerotic plaques[186]. Rather the animal model is just a manual blocking of the exterior of the vessel, and the inner lining of the vessel remains intact. Additionally, tas he animals are juvenile, there should not be any vessel disease or atherosclerotic build-ups. This can be an advantage of the model, as it is assumed that the subjects have not had any previous cardiac events, such as an infarct that would cause any pre-existing injury or any ischemic preconditioning.

A stepwise intermediate occlusion was created. The animals never underwent a full coronary occlusion, nor was there reperfusion, which can cause its own myocardial injury. The occlusion was made to partially block the vessel, and it was maintained until euthanasia. Twelve hours after acute ischemia, necrosis factors can start to appear[187], but this is not relevant in this study, as all procedures were performed in this time frame. The mean time between the closing up the chest wall for transfer to the MRI (shortly after the occlusion for the stenosed animal) to the HVBH maneuver did not differ between the two groups. However, the experiment could be affected by acute injuries and some LV dysfunction was observed in the stenosed animals.

The coronary anatomy of swine has been proven to be suitably similar to humans[185], a key difference being that swine have a lack of collateral perfusion, which is a fundamental feature in compensation for coronary disease in humans. Consequently, coronary artery stenosis in swine could create a more defined regional oxygen deficit, while in human cardiac disease this deficit may be more diffuse because of partial compensation by the perfusion beds from the other coronary arteries, as well as the possibility of more widespread vascular dysfunction.

Impact of Surgical Procedures

All animal subjects in Part 1 had undergone major cardiac surgery the day of the CMR exam. The chest was opened with a thoracotomy for the placement of a flow-measuring device on the coronary artery, and for the placement of the occluder in animals allocated to undergo a coronary blockage. The thoracotomy was necessary for all subjects because of the perivascular flow probe. This type of probe was the only commercially available and MRI-compatible device for measuring coronary flow. This probe could only be used for acute purposes, thus a significant surgery had to be performed on the day of the experiment. However, all animals underwent this operation, so there should be minimal difference between the groups. Only minor additional procedures were required for the placement of the occluder, as the LAD was already prepared for the flow probe. In the future, MRI compatible flow wires that are placed percutaneously, similar to FFR measurements, could enhance these measurements and thus

painful surgical procedures and heavy analgesic doses would not be required. However, these are still in development, and were not readily available at the time of the study[188].

Possible Confounding Effects of Anaesthesia on OS-CMR Results

In order to perform the required procedures, and to follow the animal care guidelines, the animal studies required the use of anaesthetics the entire duration of the experiment. However, this does pose a major confounder to any results from the animal model, especially those data points relying on vascular reactivity. Anaesthetics may act as cardiac depressants, and reduce inotropy, but also myocardial oxygen consumption[189]. The two primary drugs used in this study were propofol, and the opioid remifentanil for analgesic effects. These common intravenous agents can reduce the coronary response, perfusion pressure and cardiac output, and adjust baseline myocardial blood flow[190].

Intravenous agents were used instead of inhalation anaesthesia. One significant reason was because of the limitations posed by the magnetic field of the MRI. All ferromagnetic materials like the ventilator, remained outside of the MRI suite with long tubing (>10m) run through specific wave guides to the animal. Because of the significant length and dead space created in the tubing, it would have been more difficult to control the concentration of anaesthetic gases reaching the animal. Especially, the minimum alveolar concentration of anaesthetics in the lungs can be affected when the ventilation pace and volume is altered for the breathing maneuvers (chapter 1) or to reach altered arterial blood gas levels (chapter 2 & 3). Additionally, swine can be susceptible to malignant hyperthermia with volatile anaesthetics, so intravenous anaesthesia was chosen as the preferred method. An MRI compatible infusion pump was available for the intravenous drugs, and these doses would not be affected by the breathing maneuvers and ventilation rate. Furthermore, since a thoracotomy is a significant surgical procedure, a potent analgesic (remifentanil) was required along with the propofol used to maintain anaesthesia, thus creating a balanced anaesthesia that does not rely on the mechanisms of a single drug. Remifentanil is an extremely short acting opioid with the shortest half-live of the opioid family before it is metabolized, and it does not accumulate during prolonged infusion[191]. Similarly, propofol also has a fast onset, allowing

for quick control of anaesthesia. Yet, propofol can accumulate especially in the adipose tissue after longer periods of infusion though, and could create a reservoir for propofol if the infusion was lowered[192]. Many anaesthetics are known to have a pre-conditional affect and can help reduce ischemic areas at risk by increasing basal blood flow or reducing myocardial workload, and this has been shown for both remifentanil and propofol[193]. Any adjustments to the basal flow would affect the perfusion and oxygenation reserve observed during the vasoactive methods. Remifentanil has been shown to reduce the hypoxic and hypercapnic respiratory drive. Although that publication did not assess the coronary response, this may explain why especially in healthy control animals the myocardial oxygenation response is diminished during the breath-holds in comparison to the human chapters. Nevertheless, anaesthesia levels are adjusted to the needs of each individual subject, and this will cause further variability within a study. This study was run by a clinically trained anaesthesiologist with a high level of experience in porcine models, and the doses given were appropriate at that specific time as judged by continuous monitoring of the animal. Overall, the exact mechanisms of these drugs, like almost all anaesthetics, are not very well known, and this anaesthesia protocol was deemed to be the most suitable for the studies, although there are some limitations and likely unknown interactions.

Because OS-CMR relies on the myocardial oxygenation response to changes in myocardial oxygen consumption and coronary blood flow, any studies performed under anaesthesia will have an altered response compared to techniques performed in conscious subjects.

Translation of Invasive Measurements to Human Participants

The animal studies provide interesting information about the cardiovascular system during the techniques, as invasive measurements can be obtained during the experiment, which not would be ethical in human studies. The invasive measurements however provide information for certain regions only, and not of the entire heart. Thus the results help to predict the response, but do not give a complete picture. Part 1 uses an ultrasound-based measurement of blood flow of just the LAD coronary artery. This however, does not give a reading of how the other coronary arteries respond, especially in the case of an LAD stenosis, and there could

be possible coronary steal effects creating different blood flow changes in the other arteries. Yet, due to feasibility, only one probe was installed in the LAD, which was also the easiest to surgically access due to its anterior positioning, reducing the amount of surgical stress for the animal. As stated in section 0.6 the majority of coronary blood flow is actually controlled by the microvessels, and not the large epicardial vessels. Thus, it is recognized that the measurements assessed in part one do not provide the entire picture of the coronary blood flow response, but rather use the LAD blood flow measurements as an example.

Due to the size of the animal, each had its own baseline blood flow. Under these circumstances, we reported the %-change in coronary flow rather than raw measurements (ml/min), similar to what has been done by other studies using the same device. Similarly, the coronary sinus measurements do not solely measure the blood from the LAD territories either. Rather it collects blood from the majority of the swine's left ventricle (95%)[66], and the remote regions influence the capillary sinus values and oxygen extraction measurements as well. However the LAD contributes to the majority of the blood collection, so the coronary sinus is subsequently one of the best available measurements that can also be accessed with a larger cannula, which is needed for rapid blood acquisition.

As previously addressed in the limitations of chapter 1, the anaesthetized animals undergo a much more extreme change in blood gases during apnea then have been published for human studies[83,84]. This alone would result in different OS-CMR responses between animals and humans. For example, some animals ended up having an arterial saturation as low as 35%, and even 10% for the coronary sinus, all with breath-hold less than 90s long. As will be seen in the upcoming chapters, both healthy participants and even patients with CAD can maintain breath-holds this long. Thus these significant changes in oxygenation are not likely due to the breath-hold duration. Breath-holds were prematurely ended if blood pressure did start to drop below a mean arterial blood pressure of about 50mmHg, but this was not the case until near the end of the breath-hold, and thus perfusion pressure should not have significantly changed either. In a separate animal study from Bern, Switzerland currently being prepared for publication, coronary blood flow and myocardial oxygenation was maintained by the coronary autoregulation range until the MAP fell below this threshold[194]. One suggested mechanism for this extreme blood gas drop is that as shown in Table 7, controls animals increased myocardial

extraction during the HVBH by a difference of 20%, and non-significantly by 16% during the LBH. As described in the introduction (section 0.3), humans do not have a large oxygenation extraction reserve, and this may also account for differences between the two models. With this extreme desaturation, the incoming blood to the myocardium will already have a lower oxygen content and will not be able oxygenate the tissue as well, even if there is a greater overall blood supply, and this could explain why the overall oxygenation response is lesser in the animals. Again, this is not expected to occur in humans, as they should feel the need to breathe once the hypoxic and hypercapnic drives kick in, and this voluntary resumption of breathing was obviously not a factor in the ventilation controlled animals. Furthermore, with anaesthesia itself, the blood gases are abnormal even at baseline, specifically coronary sinus saturation (control: 41±19, stenosed: 36±14%). Although this would be high for conscious humans, these values are consistent for what has been reported for humans under anaesthesia prior to surgical procedures (40%, and 48%), because anaesthetics are cardio-depressant and oxygen extraction will decline[195,196]. To possibly correct for arterial saturation changes during breath-holds, our group is looking into using the oxygenation signal of the blood in the left ventricular blood pool[112]. Because any tissue effects do not directly affect the blood pool signal, it is representative of arterial saturation. In future studies, myocardial oxygenation changes could be corrected to the blood pool signal, similar to what is done with some contrast agent techniques that correlate the contrast concentration in the tissue to the contrast in the blood. However, this analysis is still in progress and the current results are just using the pure, unadjusted myocardial signal.

Finally, as seen in most large animal studies, only small samples were assessed due to feasibility, and so that only the minimum amount of animals were needed, due to ethical reason. Small sample size and the factors described above do lead to a bigger standard deviation in the observed results. While the results are still significant, the variation can lead to questioning whether the technique is consistent. As described, this model has many confounding factors. The results from the animal models should be more cautiously interpreted as a demonstration of the general trends of the OS response during breathing maneuvers, but not specifically the same situation that is expected in humans. As will be seen in the forthcoming chapters, the reported values during the breathing maneuvers are greater

with conscious humans, and are similar between different studies and institutions using the same sequence and technique. The future goal is to expand the study into a much larger trial with more than 100 subjects, and this is best done with human studies, rather than surgical animal models, as this would allow for true assessment of reproducibility and accuracy.

Animal models are useful as models for human cardiac diseases while allowing for invasive procedures that may otherwise not be acquired in human studies. Further, isolated pathologies can be examined. For example, investigating the stenosis of an epicardial vessel as opposed to complex networks, such as in coronary artery disease, where vascular lesions of the conduit vessels are often accompanied by microvascular dysfunction and inflammatory processes. While animal models are necessary for the assessment of these invasive measurements however, the issues described above limit the direct translation of the results to a clinical scenario. Consequently, the next steps are translating the techniques to human studies.

Part 2: Translation into a healthy volunteer population

4 Chapter 4 - Response of myocardial oxygenation to breathing manoeuvres and adenosine infusion

Foreword

In this chapter, the first direct comparison of breathing maneuvers on myocardial oxygenation in a human population is assessed against the gold standard of pharmacologic vasodilation, intravenous adenosine. This work represents evidence that, for assessing coronary vascular function, breathing maneuvers may be a safe and efficient alternative to intravenous injections of vasodilatory agents. This refers to one of the most expensive factors in medicine, thus the clinical and societal implications may be substantial. These volunteers also serve as a control for two ongoing studies investigating the myocardial oxygenation response in participants with obstructive sleep apnea[44], and patients with cardiac transplantation. This data was presented at the Society of Cardiovascular Magnetic Resonance congress in New Orleans (SCMR 2014).

Acknowledgements

The authors wish to thank the CMR research team at the Montreal Heart Institute, especially Dr. François-Pierre Mongeon, Dr. François Marcotte for their valuable support in supervising the exams, Camilo Molina for data gathering and Tarik Hafyane for image processing. Funding was provided by the Montreal Heart Institute Foundation, the Canadian Foundation for Innovation and the *Fonds de Recherche Santé Québec.*

Response of myocardial oxygenation to breathing manoeuvres and adenosine infusion

Kady Fischer, B.H.Sc.[1]; Dominik P. Guensch, M.D.[1,2];
Matthias G. Friedrich, M.D., FESC, FACC [1,2,3]

[1] Philippa & Marvin Carsley CMR Centre at the Montreal Heart Institute, Montreal, QC, Canada
[2] Bern University Hospital, Department Anesthesiology and Pain Therapy, Bern, Switzerland
[3] Departments of Cardiology and Radiology, Université de Montréal, Montreal, QC, Canada

All co-authors wrote and approved the manuscript. Published by the *European Heart Journal Cardiovascular Imaging.*

(Fischer K, Guensch DP, Friedrich MG. Response of myocardial oxygenation to breathing manoeuvres and adenosine infusion. *Eur Heart J Cardiovasc Imaging*. 2015;16:395–401.

4.1 Abstract

Background: Testing for inducible myocardial ischemia is one of the most important diagnostic procedures and has a strong impact on clinical decision-making. Current standard protocols are typically limited by the required infusion of vasodilatory substances. Recent data indicate that changes of myocardial oxygenation induced by hyperventilation and breath-holds can be monitored by oxygenation-sensitive (OS)-CMR and may be useful for assessing coronary vascular function. As tests using breathing manoeuvres may be safer, easier and more comfortable than vasodilator stress agent infusion, we compared its impact on myocardial oxygenation to that of a standard adenosine infusion protocol.

Methods: In twenty healthy volunteers, we assessed changes of myocardial oxygenation using OS-CMR at 3T during adenosine infusion (140µg/kg/min iv) and during voluntary breathing manoeuvres: a maximal breath-hold following normal breathing, and a maximal breath-hold following 60s of hyperventilation.

Results: The study was successfully completed in 19 subjects. There was a significantly stronger myocardial response for hyperventilation (decrease of -10.6 ± 7.8%) and the following breath-hold (increase of 14.8 ± 6.6%) than adenosine (3.9±6.5%), while a simple maximal voluntary breath-hold yielded a similar signal intensity increase (3.1±3.9%). Subjective side effects occurred significantly more often with adenosine, especially in females.

Conclusions*:* Hyperventilation combined with a subsequent long breath-hold and hyperventilation alone both have a greater impact on myocardial oxygenation changes than an intravenous administration of a standard dose of adenosine, as assessed by oxygenation-sensitive CMR. Breathing manoeuvres may be more efficient, safer, and more comfortable than adenosine for the assessment of the coronary vasomotor response.

Key Words: Oxygenation-Sensitive ▪ CMR ▪ BOLD (blood oxygen level-dependent) ▪ adenosine ▪ vasodilation ▪ vasoconstriction

4.2 Introduction

Ischemic heart disease is the most frequent cause of death in developed countries and imaging for inducible myocardial perfusion defects is one of the most frequent diagnostic procedures performed. Typically, a vasodilator agent is injected to trigger a response in the coronary perfusion beds, which, when compared to a baseline scan may identify areas of impaired perfusion. Vasodilator agents commonly used in clinical settings include non-selective (adenosine and dipyridamole) and selective adenosine agonists (regadenoson and others).[197] With respect to their clinical utility for diagnostic purposes however, adenosine and its agonists have limitations: While generally considered safe, more than 90% of patients report side effects,[69] including chest pain, palpitations, dyspnea, light-headedness, flushing, sweating, nausea, headache and anxiety, and recently the US food and drug administration released a warning due to adenosine as a rare, but serious risk of heart attack and death.[70] Adenosine infusion can cause arrhythmia, especially SA- and AV block and thus the presence of a trained health professional during infusion is required. It is contraindicated in patients with second or third degree AV block and sinus node disease, and should also be avoided in patients with known bronchoconstrictive disease. Furthermore, the short half-life and variable response to adenosine may make it difficult to verify that an adequate level of adenosine is reached in the coronary vasculature, especially in patients with low cardiac output where the long transit time between the peripheral injection site and the myocardium may lead to its inactivation. Importantly, adenosine and regadenoson also add significant costs to the diagnostic procedure.

It is known that breathing manoeuvres, i.e. hyperventilation and long breath-holds elicit significant changes of cerebral and coronary perfusion,[83,110,198] largely induced by the vasodilatory effects of blood carbon dioxide, which increases with apnea and decreases with hyperventilation. While most imaging methods do not have sufficient temporal or spatial resolution to monitor these changes, oxygenation-sensitive cardiovascular magnetic resonance (OS-CMR) allows for monitoring changes of myocardial oxygenation, including those induced by adenosine infusion.[7-14] In both an animal model and healthy volunteers, it has recently been shown that OS-CMR can also track changes of myocardial oxygenation during breathing manoeuvres[82,83] which could be very well induced by long breath-holds and

hyperventilation. It is however unknown how the response to these breathing manoeuvres on myocardial perfusion/oxygenation compares to that of standard adenosine infusion. If such impact would be similar or even stronger, breathing manoeuvres may be considered an alternative to vasodilator infusion in patients with suspected inducible myocardial ischemia.

We hypothesized that breathing manoeuvres, specifically long breath-holds and hyperventilation as well as a combination thereof, lead to myocardial oxygenation changes at least as significant as those induced by intravenous adenosine.

4.3 Methods

Participants

We studied 20 healthy subjects without a history of smoking, cardiovascular or respiratory disease, and aged 18 years or older. All participants were newly recruited for this study through public advertisements. Participants were required to provide informed written consent, and were interviewed to rule out general MRI contraindications. Furthermore, they were asked to refrain from the consumption of adenosine antagonizing agents such as caffeine for at least 12h prior to the MRI exam.

Protocol

Before image acquisition, resting non-invasive blood pressure and heart rate were obtained in a supine position. An alarm ball was provided and heart rate, peripheral hemoglobin saturation (SpO_2), respiratory rate and blood pressure were monitored during the scan.

CMR

Imaging was performed in a clinical 3T scanner (MAGNETOM Skyra 3T; Siemens, Erlangen, Germany) using an 18-channel cardiac coil. Images were obtained during breath-holds at comfortable end-expiration. LV function was assessed using an ECG gated balanced

steady-state free precession (bSSFP) sequence (TE/TR 1.43ms/3.3ms, flip angle 65°, voxel size 1.6x1.6x6.0mm, matrix 192x120, bandwidth 962Hz/Px) in six long axis slices with LV-centered radial positioning and three short axis views. OS-CMR images were acquired in one mid-ventricular short axis slice using an ECG triggered bSSFP sequence (TE/TR 1.70ms/3.4ms, flip angle 35°, voxel size 2.0x2.0x10.0mm, matrix 192x120, bandwidth 1302Hz/Px, acquisition time/measurement 4 heartbeats). Shimming was always performed along with frequency scouts if required

The OS-CMR protocol (Figure 23) included:

1. Combined hyperventilation/breath-hold (HVBH): Hyperventilation for 60s aiming for a rate of 35-40 breaths per minute, followed by a maximal voluntary breath-hold with a single measurement acquired prior to hyperventilation and continuously during the entire breath-hold after hyperventilation. When participants announced their need for inspiration by using the alarm ball, scanning was stopped.

2. Maximal voluntary breath-hold (LBH) from normal respiration with continuous imaging; as for the previous maximal breath-hold, participants were asked to indicate their need for inspiration.

3. Adenosine infusion (140µg/kg/min) with single image acquisitions before and 3.5 minutes into the drug infusion.

Imaging during adenosine infusion was randomly performed either before or after imaging during breathing manoeuvres. There was a break of at least 3min between each series to allow for the patient to recover. After the MRI exam, the participants completed a questionnaire on the difficulty of each manoeuvres, using a scale of increasing difficulty of 1 to 5, and were also asked to identify the incidence of any adverse effects for each manoeuvres.

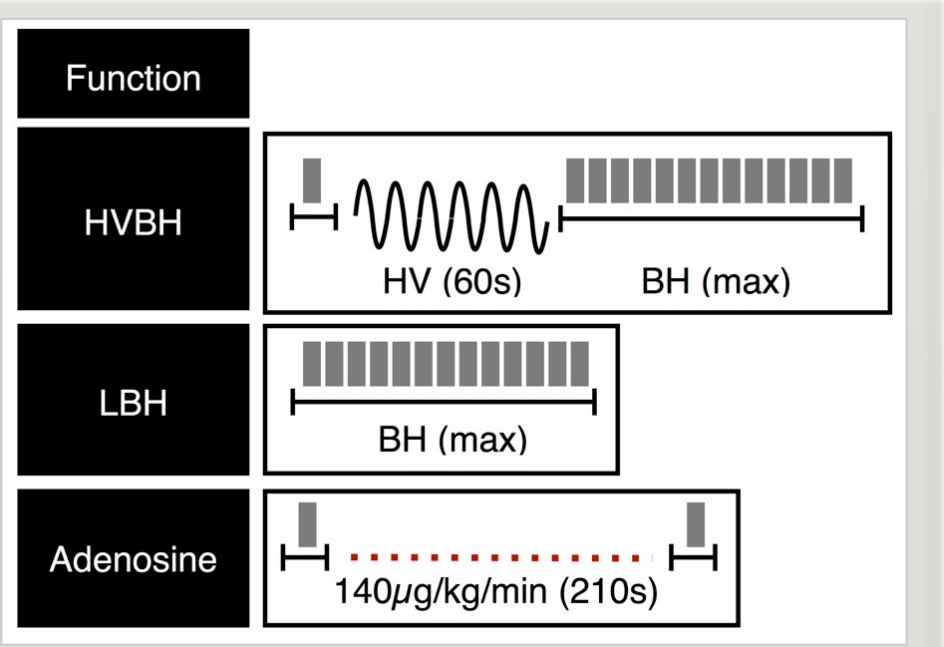

Figure 23: Representation of scanning protocol.

OS images (grey) are obtained during a breath-hold. Extended breath-holds are imaged continuously with repeating measurements, while baseline and adenosine images with a single measurement. HVBH: hyperventilation (HV) followed by a maximal breath-hold (BH), LBH: maximal breath-hold from normal respiration.

Image Analysis

Analysis of left-ventricular function was performed from epicardial and endocardial contours in diastolic and systolic images of the six long axis views using certified software (cvi[42], Circle Cardiovascular Imaging, Calgary, AB, Canada). For OS-CMR images the end-systolic image from each measurement was chosen for analysis. Images were first visually graded on image quality scale from 1 to 4 with decreasing image quality[83]. Individual segments were entirely excluded if >33% of the segment area was removed due to artefact. The mean myocardial signal intensity (SI) in the OS-CMR images was automatically calculated after manual tracing of endocardial and epicardial contours and further segmented based on current recommendations.[9] A blood pool contour was drawn in the middle of the left-ventricular cavity (SI_{BP}[%]). SI was expressed as the %-change (ΔSI[%]) between two images. Both hyperventilation and adenosine were compared to their respective baseline images obtained prior to the manoeuvres, while for the HVBH and LBH the first measurement of the breath-hold was used as the reference. SI changes were specifically assessed for: 1) SI

at 15s into the breath-hold; 2) SI at 30s into the breath-hold; 3) the maximum SI reached during the breath-hold; and 4) SI at the end of the breath-hold.

Statistical Analysis

Data is expressed as mean ± SD. Continuous variables were assessed for normal distribution with the D'Agostino-Pearson test. A paired student t-test was used to compare signal intensities within a subject, and comparisons of variation between groups were assessed with an F-test. Associations among groups were assessed with analysis of variance and multiple comparison tests. To account for excluded segments, a linear mixed effects analysis was performed to assess the within-subjects relationship between the change in signal intensity and the myocardial segment using a compound symmetry covariance structure and segment identification as a fixed factor. The breath-holds were further analyzed by plotting the SI over time fitted by non-linear regression. The questionnaire and image quality results were analyzed with the Friedman's non-parametric test. For assessing inter-observer reliability, 66 randomly selected images were read by an independent second reader and assessed with a one-way mixed intraclass-correlation test. Tests were performed with GraphPad Prism version 6.0 for mac (GraphPad Software, La Jolla California USA) and SPSS version 21 (SPSS IBM, New York, USA). Results were considered statistically significant if the p-value was less than 0.05.

The local scientific and ethics committees at the Montreal Heart Institute approved the study.

4.4 Results

Participant Characteristics

Nineteen participants completed all manoeuvres of the protocol. One participant withdrew from the study due to claustrophobia. Data from the left-ventricular function analysis is shown in Table 12.

Measurement	
Age (years)	43 ± 14
Gender	8F / 11M
BMI (kg/m^2)	24.0 ± 3.0
Resting BP (mmHg)	128±17 / 81±13
Resting HR (bpm)	62 ± 6
EF (%)	67 ± 6
CO (L/min/m^2)	3.4 ± 1.0
LV mass index (g/m^2)	69 ± 20

Table 12: Volunteer characteristics and function analysis

Mean ± SD age, gender, body mass index (BMI), resting systolic / diastolic blood pressure (BP, mmHg), Resting heart rate (HR, beats/min), ejection fraction (EF, %), Cardiac output index (CO, L/min/m^2) and myocardial mass (g/m^2) indexed to body surface area.

Image Quality

Overall image quality was good (1.8±0.6) and did not differ between the manoeuvres. No complete image set was excluded due to poor image quality. In the segment-based analysis, 38/684 (5.8%) data points were excluded, primarily in the anterior wall, based on pre-defined criteria for severe artefacts. There was an excellent inter-observer reliability between the two readers with an intraclass-correlation of 0.94 (CI: 0.90-0.96; *p<0.01).

Myocardial Signal Intensity Changes in OS-CMR Images

Compared with the baseline, all manoeuvres induced a significant SI change (Figure 24b and Table 13). Of note, this was the case even only 15 seconds into the breath-hold following hyperventilation (HVBH; SI increase 7.6±5.7%; p<0.05), which was statistically not different from the response to adenosine (3.9±6.5%; p=0.07). An even stronger effect was observed by 30s (11.7±6.4) with the maximal effect of 14.8±6.6 observed at an average time of 40s, all greater than the adenosine change (*p<0.05). On the other hand, during the maximal breath-hold from normal respiration (LBH), only the maximum peak differed significantly from baseline, while other time points did not. The maximal signal intensities in both, HVBH and LBH, were significantly greater than at the end of the breath-hold and were the values used for subsequent calculations. There was a significant change in the ΔSI_{BP}[%] at the end of the maximal breath-holds (-2.6±4.9%; p<0.05) for the HVBH as well as for the LBH (-3.2±5.4%; p<0.05) but not at the maximal myocardial ΔSI[%].

After hyperventilation participants were able to hold their breath for 28±23s longer than after regular ventilation ($p<0.05$). In addition, the maximum SI occurred 14±19s later with HVBH than with LBH ($p<0.05$). In HVBH experiments, the variation of the time to maximal SI time was significantly less than the variation of the time to the end of the breath-hold, which was not the case in LBH.

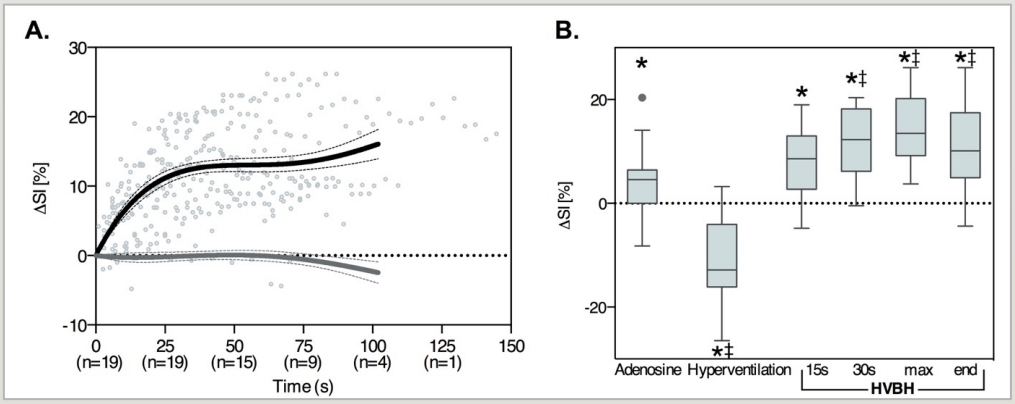

Figure 24: Oxygenation signal intensity

A) The fitted curve demonstrates the increase in myocardial (black) signal intensity (ΔSI[%]), while bloodpool ΔSI[%] simultaneously decreased (dashed grey). B) OS-SI global myocardial results. All manoeuvres (mean ± SD) significantly changed signal intensity from baseline (*$p<0.05$), including just 15s into the HVBH. Additionally, the oxygenation responses from hyperventilation and time points from 30s and later in the HVBH were significantly different than that of adenosine (‡$p<0.05$, n=19).

	n	Δ SI (%)	Time (s)	ΔHR
Adenosine	19	3.9 ± 6.5*		17.8 ± 14.4*
Hyperventilation	19	-10.6 ± 7.8*‡	60	25.2 ± 14.0*‡
HVBH				
15s	18	7.6 ± 5.7*	15.1 ± 1.2	
30s	18	11.7 ± 6.4*‡	29.7 ± 1.1	
Maximum	19	14.8 ± 6.6*‡	40.3 ± 16.1	
End	19	10.3 ± 7.7*‡	73.6 ± 28.6	-15.0 ± 18.7*‡
LBH				
15s	19	-0.6 ± 2.9‡	15.0 ± 1.0	
30s	16	-1.3 ± 4.8	30.0 ± 1.6	
Maximum	19	3.1 ± 3.9*	25.9 ± 19.5	
End	19	1.4 ± 5.5‡	45.3 ± 20.9	2.8 ± 10.4‡

Table 13: Manoeuvres and related changes of heart rate and myocardial oxygenation

Mean ± SD values from each manoeuvres including the actual time points of data acquisition (s) and change in heart rate (HR, beats/min). Both the ΔSI[%] at the maximum and the end of the breath-hold are shown for the LBH and HVBH. SI, signal intensity; HVBH, hyperventilation breath-hold; LBH, long breath-hold from normal breathing.

*: Significantly different from baseline ($p < 0.05$).

‡: Significantly different from the adenosine manoeuvres ($p < 0.05$)

Segmental Analysis

There were no differences in SI changes between segments with hyperventilation (Figure 3b). Yet, with HVBH, the anterior and anterolateral segments had significantly higher ΔSI[%] than the inferior and inferoseptal segments, while similarly with adenosine, the anterior segment also had the greatest increase of ΔSI[%], greater than the lateral segments ($p<0.05$).

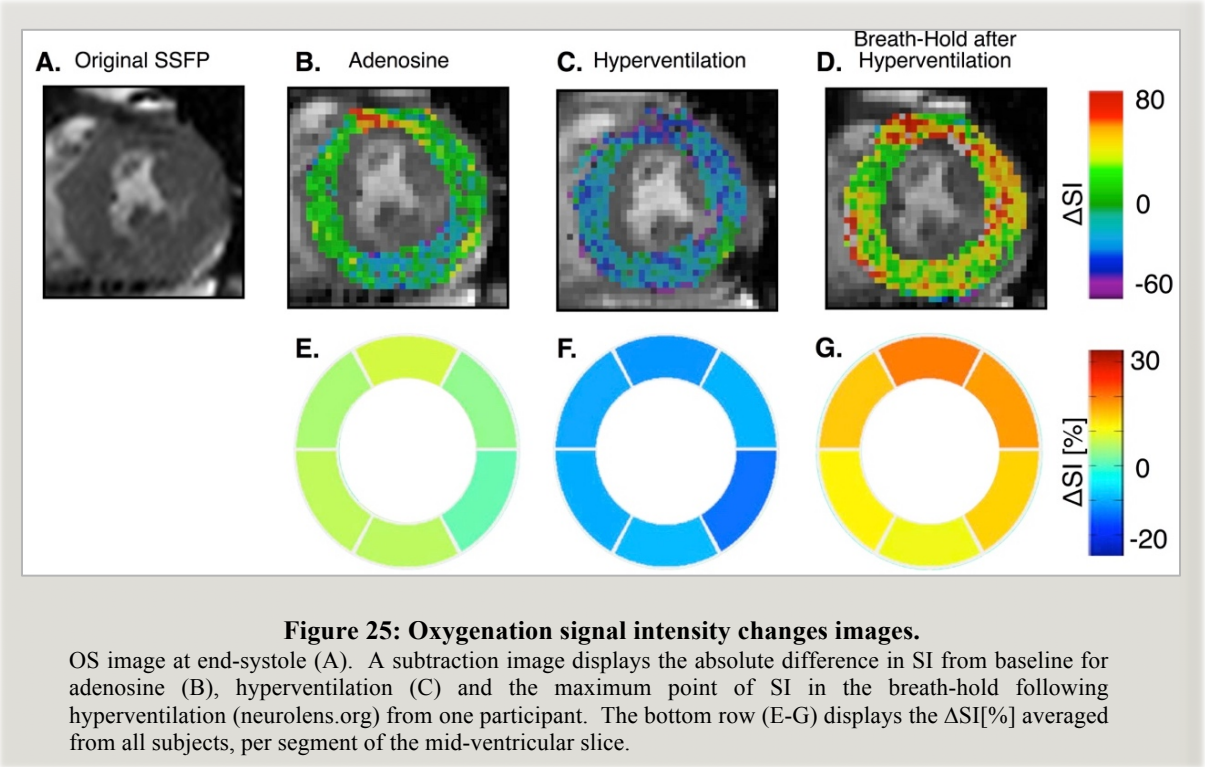

Figure 25: Oxygenation signal intensity changes images.
OS image at end-systole (A). A subtraction image displays the absolute difference in SI from baseline for adenosine (B), hyperventilation (C) and the maximum point of SI in the breath-hold following hyperventilation (neurolens.org) from one participant. The bottom row (E-G) displays the ΔSI[%] averaged from all subjects, per segment of the mid-ventricular slice.

Relationship to Gender and Heart Rate

Only gender was a factor for the adenosine protocol, in which the females had a larger ΔSI[%]. There was an increase in heart rate of 25.2±14.0 beats/min after hyperventilation (Table 13), yet the increase of heart rate was not significantly correlated with ΔSI[%] ($r=-0.41$, $p=0.10$, $n=18$). Heart rate was not a statistically relevant factor for the other manoeuvres.

Subjective Difficulty and Side Effects

The difficulty score was the same for all manoeuvres (1.8±1.0, p=n.s.). Side effects were not noted with the LBH test. The HVBH led to mild side effects in 5 (26%) of the participants, most notably tingling in the fingers during hyperventilation (n=3), dizziness (n=1) and dry mouth (n=1) which disappeared after the manoeuvres and normal breathing recommenced in all cases. With adenosine, 13 (68%) of the participants noted side effects, most commonly chest tightness (n=6), flushing (n=4), breathing difficulties (n=4), and dizziness (n=3). When asked about the duration of side effects from adenosine, two of these participants responded that they still felt the adverse effects more than 60s after the drug infusion had stopped. Of note, all females experienced side effects during adenosine.

4.5 Discussion

Our head-to-head comparison data provide evidence that in healthy participants, breathing manoeuvres, specifically hyperventilation alone and in combination with a maximal voluntary breath-hold have an impact on myocardial oxygenation at least as strong as an intravenous administration of a standard dose of adenosine. This has potentially strong clinical implications, as the combination of breathing manoeuvres with oxygen-sensitive CMR would allow for assessing coronary vascular function without the need for contrast agents or vasodilating drugs. Moreover, the test directly reflects tissue oxygenation in contrast to currently used surrogate markers such as tracer accumulation, first-pass perfusion inflow characteristics or fractional flow reserve.

The concept combines the validated technique of oxygenation-sensitive CMR with relatively simple physiologic manoeuvres. Multiple studies have used OS-CMR to assess this response in cardiac disease using adenosine or dipyridamole and validated this technique against quantitative coronary angiography[35], first pass perfusion,[40] positron emission tomography[36] and fractional flow reserve.[37] Breathing manoeuvres can significantly alter systemic O_2 and CO_2 tensions within a relatively short time.[84,85] Both, adenosine and the primary metabolites, O_2 and CO_2, have a direct impact on the arterioles,[201,202] which keep

approximately 40% of the coronary resistance at rest. When dilated, these vessels are responsible for the large decrease in vascular resistance and the strong increase in coronary blood flow.[203,204] The arteriolar response is blunted in diseases related to atherosclerosis such as hypercholesterolemia, diabetes, and hypertension, as well as in coronary artery disease.[102] In the presence of significant coronary artery stenosis, these arterioles are already dilated at rest in order to maintain adequate myocardial perfusion and thus show a blunted response to a vasodilator stimulus.

As with previous studies,[205] we found that hyperventilation is associated with minor side effects. Our data however indicate that breathing manoeuvres may be better tolerated than adenosine infusion, especially by women. The interesting observation that female participants are more prone to discomfort during adenosine infusion is in agreement with previous reports.[206] Even if side effects occurred during breathing manoeuvres, they appear to be of shorter duration. Another advantage of breathing manoeuvres is that patients have full control over their breathing and thus can resume normal breathing if they feel uncomfortable, without requiring immediate action by medical staff. This on the other hand requires compliance to yield meaningful results, similar to physical stress tests. We did not assess patients and thus cannot infer that long breath-holds with or without hyperventilation are as easily tolerated by subjects with heart disease. Thus, results may be different in patients. Yet, the fact that none of the participants reported the test to be difficult or inconvenient indicates, that also patients would likely tolerate breathing manoeuvres better than vasodilator infusions.

The duration of a voluntary breath-hold may be influenced by many factors such as initial gas content, lung volume, chemoreceptor sensitivity, secondary diseases, tolerance, and patient compliance.[86]

Interestingly, we observed that the maximal change, independent from the duration of the breath-hold was rather consistent among individuals, suggesting that this parameter may be less reliant on patient compliance than the overall change and could more accurately distinguish the vascular response with minimal influence of breath-holding ability. As we could show, preceding hyperventilation facilitates long breath-holds and participants were able to hold their breath on average for >60 seconds, while the maximum SI was reached after about 40 seconds. Yet, even as early as 15s into the breath-hold after hyperventilation, we

observed significant changes. In addition to its apparently better feasibility, the HVBH protocol demonstrated stronger and more consistent results than the breath-hold without hyperventilation (LBH). With CO_2 being the strongest breathing stimulus, previous hyperventilation extends the breath-hold duration by reducing the CO_2 content and thus shifting the starting level farther from the thresh-hold at which the breakpoint of a breath-hold occurs.[85,86] With the extended breath-hold, the participant undergoes a greater range in CO_2 and coronary vasomotion. On the other hand, hyperventilation has a vasoconstrictive effect, which may not be tolerated as well in patients, and the relationship between hyperventilation-induced vasoconstriction and the severity of coronary artery stenosis deserves more research. Furthermore, the significant increase of heart rate we have observed may increase oxygen demand and thus hyperventilation-related changes may be more pronounced in patients.

The evaluation and interpretation of oxygenation-sensitive CMR images during voluntary breathing manoeuvres in patients' needs to be further elucidated. While this study demonstrates that changes myocardial oxygenation can be induced with breathing manoeuvres, we are unable to assess the ability of the technique to detect myocardial ischemia until a patient population is investigated. While SI changes may be simple, this approach can be compared with parameters such as area under the curve, maximal slope or specific time-points. Furthermore, several potential confounders for the signal intensity in OS-CMR images have to be considered, such as the total amount of dHb as well as the ratio of dHb to free tissue water.[24,207,208]

Of note, our observation that breathing manoeuvres have a strong effect on the myocardial oxygenation also indicates that breathing patterns during standard imaging protocols with pharmacological agents may be important confounders.

Limitations

As discussed before, the utility of breathing manoeuvres may be subject to participant compliance. Hyperventilation may induce coronary vasospasms, yet such reports however related to hyperventilation periods longer than 5 minutes[110,205] and thus, the risk of a 60s period likely is smaller. We only acquired data on a single slice in order to achieve the

temporal resolution for monitoring oxygenation changes. In clinical settings, the experiment may have to be repeated for more coverage. Yet as the entire data acquisition time per slice mounts to less than 5 minutes, this may not be a truly limiting factor.

As the expected risk is very small, our sample size did not allow us to assess safety.

4.6 Conclusion

Our data provide evidence that breathing manoeuvres, specifically hyperventilation with or without a subsequent long breath-hold, may have a stronger impact on myocardial oxygenation than intravenous administration of a standard dose of adenosine. Both the vasoconstrictive and vasodilative response of the coronary vasculature can be observed by oxygenation-sensitive CMR during the same manoeuvres. Breathing manoeuvres may serve as a safer, more comfortable and more efficient alternative to intravenous vasodilators for diagnostic procedures and future development for this technique would be to assess if breathing manoeuvress can detect inducible myocardial ischemia in clinical settings.

4.7 Chapter References

9. Cerqueira MD, Weissman NJ, Dilsizian V, Jacobs AK, Kaul S, Laskey WK *et al*; American Heart Association Writing Group on Myocardial Segmentation and Registration for Cardiac Imaging. Standardized Myocardial Segmentation and Nomenclature for Tomographic Imaging of the Heart A Statement for Healthcare Professionals From the Cardiac Imaging Committee of the Council on Clinical Cardiology of the American Heart Association. *Circulation* 2002;105:539-542.

34. Friedrich MG, Niendorf T, Schulz-Menger J, Gross CM, Dietz R. Blood oxygen level-dependent magnetic resonance imaging in patients with stress-induced angina. *Circulation* 2003;108:2219-2223.

24. Ogawa S, Lee TM, Nayak AS, Glynn P. Oxygenation-sensitive contrast in magnetic resonance image of rodent brain at high magnetic fields. *Magn Reson Med* 1990;14:68-78.

35. Manka R, Paetsch I, Schnackenburg B, Gebker R, Fleck E, Jahnke C. BOLD cardiovascular magnetic resonance at 3.0 tesla in myocardial ischemia. *J Cardiovasc Magn Res* 2010;12:54.

40. Jahnke C, Gebker R, Manka R, Schnackenburg B, Fleck E, Paetsch I. Navigator-Gated 3D Blood Oxygen Level–Dependent CMR at 3.0-T for Detection of Stress-Induced Myocardial Ischemic Reactions. *J Am Coll Cardiol Img*. 2010;3:375–384.

39. Arnold JR, Karamitsos TD, Bhamra-Ariza P, Francis JM, Searle N, Robson MD *et al*. Myocardial Oxygenation in Coronary Artery Disease: Insights From Blood Oxygen Level–Dependent Magnetic Resonance Imaging at 3 Tesla. *J Am Coll Cardiol* 2012;59:1954-1964.

36. Karamitsos TD, Leccisotti L, Arnold JR, Recio-Mayoral A, Bhamra-Ariza P, Howells RK, Searle N, Robson MD, Rimoldi OE, Camici PG, Neubauer S, Selvanayagam JB. Relationship between Regional Myocardial Oxygenation and Perfusion in Patients with Coronary Artery Disease: Insights from Cardiovascular Magnetic Resonance and Positron Emission Tomography. *Circ Cardiovasc Imaging*. 2010;3:32–40.

37. Walcher T, Manzke R, Hombach V, Rottbauer W, Wöhrle J, Bernhardt P. Myocardial Perfusion Reserve Assessed by T2-Prepared Steady-State Free Precession Blood Oxygen Level–Dependent Magnetic Resonance Imaging in Comparison to Fractional Flow ReserveClinical Perspective. *Circ Cardiovasc Imaging* 2012;5:580-586.

69. Adenosine Side Effects in Detail - Drugs.com. Available at: http://www.drugs.com/sfx/adenosine-side-effects.html. Accessed November 27, 2013.

70. Commissioner O of the. Safety Alerts for Human Medical Products - Lexiscan (regadenoson) and Adenoscan (adenosine): Drug Safety Communication - Rare but Serious Risk of Heart Attack and Death. Available at: http://www.fda.gov/Safety/MedWatch/SafetyInformation/SafetyAlertsforHumanMedicalProducts/ucm375981.htm. Accessed May 20, 2014.

82. Guensch DP, Fischer K, Flewitt JA, Friedrich MG. Impact of Intermittent Apnea on Myocardial Tissue Oxygenation—A Study Using Oxygenation-Sensitive Cardiovascular Magnetic Resonance. *PLoS ONE* 2013;8:e53282.

83. Guensch DP, Fischer K, Flewitt JA, Yu J, Lukic R, Friedrich JA, Friedrich MG. Breathing manoeuvre-dependent changes in myocardial oxygenation in healthy humans. *Eur Heart J Cardiovasc Imaging*. 2014;15:409–414.

84. Sasse SA, Berry RB, Nguyen TK, Light RW, Mahutte CK. Arterial blood gas changes during breath-holding from functional residual capacity. *Chest* 1996;110:958-964.

85. Klocke FJ, Rahn H. Breath holding after breathing of oxygen. *J Appl Physiol* 1959;14:689-693.

86. Parkes MJ. Breath-holding and its breakpoint. *Exp Physiol* 2006;91:1-15. doi:10.1113/expphysiol.2005.031625.

102. Camici PG, Crea F. Coronary microvascular dysfunction. *N Engl J Med* 2007;356:830-840.

110. Neill W, Hattenhauer M. Impairment of myocardial O2 supply due to hyperventilation. *Circulation* 1975;52:854-858.

112. Guensch DP, Fischer K, Flewitt JA, Friedrich MG. Myocardial oxygenation is maintained during hypoxia when combined with apnea – a cardiovascular MR study. *Physiol Rep*. 2013;1(5):300098.

197. Zoghbi GJ, Iskandrian AE. Selective adenosine agonists and myocardial perfusion imaging. *J Nucl Cardiol* 2012;19:126-141.

198. Posse S, Olthoff U, Weckesser M, Müller-Gärtner HW, Dager SR. Regional dynamic signal changes during controlled hyperventilation assessed with blood oxygen level-dependent functional MR imaging. *AJNR Am J Neuroradiol* 1997;18:1763-1770.

199. Fieno DS, Shea SM, Li Y, Harris KR, Finn JP, Li D. Myocardial Perfusion Imaging Based on the Blood Oxygen Level–Dependent Effect Using T2-Prepared Steady-State Free-Precession Magnetic Resonance Imaging. *Circulation* 2004;110:1284-1290.

200. McCommis KS, O'Connor R, Lesniak D, Lyons M, Woodard PK, Gropler RJ, Zheng J. Quantification of global myocardial oxygenation in humans: initial experience. *J Cardiovasc Magn Res* 2010;12:34.

201. Kuo L, Davis MJ, Chilian WM. Longitudinal Gradients for Endothelium-Dependent and -Independent Vascular Responses in the Coronary Microcirculation. *Circulation* 1995;92:518-525.

202. Duling BR. Changes in Microvascular Diameter and Oxygen Tension Induced by Carbon Dioxide. *Circ Research* 1973;32:370-376.

203. Chilian WM, Eastham CL, Marcus ML. Microvascular distribution of coronary vascular resistance in beating left ventricle. *Am J Physiol* 1986;251(4 Pt 2):H779-788.

204. Chilian WM, Layne SM, Klausner EC, Eastham CL, Marcus ML. Redistribution of coronary microvascular resistance produced by dipyridamole. *Am J Physiol Heart Circ Physiol* 1989;256:H383-H390.

205. Sueda S, Saeki H, Otani T, Ochi N, Kukita H, Kawada H *et al*. Investigation of the most effective provocation test for patients with coronary spastic angina: usefulness of accelerated exercise following hyperventilation. *Jpn Circ J* 1999;63:85–90.

206. Cerqueira MD, Nguyen P, Staehr P, Underwood SR, Iskandrian AE. Effects of Age, Gender, Obesity, and Diabetes on the Efficacy and Safety of the Selective A2A Agonist Regadenoson Versus Adenosine in Myocardial Perfusion ImagingIntegrated ADVANCE-MPI Trial Results. *J Am Coll Cardiol Img* 2008;1:307-316.

207. Hess A, Stiller D, Kaulisch T, Heil P, Scheich H. New insights into the hemodynamic blood oxygenation level-dependent response through combination of functional magnetic resonance imaging and optical recording in gerbil barrel cortex. *J Neurosci* 2000;20:3328-3338.

208. Kim S-G, Ogawa S. Biophysical and physiological origins of blood oxygenation level-dependent fMRI signals. *J Cereb Blood Flow Metab* 2012;32:1188-1206.

4.8 Translation from healthy participants to patients

Limitations of a Younger Control Group

The mean ages of the healthy volunteers for both chapter 4 (43 years) and for the upcoming chapter 5 (28 years), and these are both significantly younger than typical cardiovascular patients. This can pose a limitation, as attenuated responses in the patient groups in comparison to these young controls could be due to both cardiovascular disease and increased age. If the data from the healthy volunteers of both chapters are combined, currently there is not a linear relationship to the age of the participant (Figure 26), although this analysis is just from a fairly small study population. Thus, the current data cannot answer about the impact of age on the oxygenation response to breathing maneuvers.

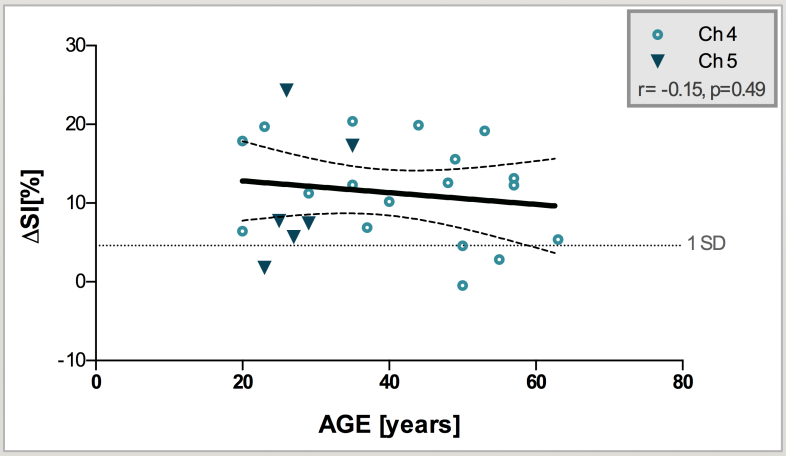

Figure 26: Effect of age on the healthy control OS-CMR response
Combined data from chapter 4 (circle) and chapter 5 (triangle) show that with the age range assessed, there is no relationship between the signal response at 30s into the HVBH and the age of the participant. Both chapters used the same sequence, MRI scanner, and breathing maneuver protocol. From the data in the graph, the lower limit of 1 standard deviation of the mean was 4.6%, which most healthy participants exceeded, the three low data points all had poor image quality (graded 3/4).

The rationale, for younger participants in chapter 5 will be discussed further in the chapter discussion, but in summary for the upcoming chapter it was decided to obtain a young healthy participant group that would have a minimal likelihood of microvascular dysfunction. While not specifically reported for OS-CMR imaging, perfusion imaging studies have shown that after the age of 70, perfusion is significantly diminished in relatively healthy but elderly

participants, while up until the age of 60 the response appears stable[209,210]. Consequently, a patient could have a diminished response due to age as well as to cardiovascular disease. Nevertheless, as the oldest age of healthy participants in this thesis was only 63, the effect of advanced age cannot really be assessed with this data. A larger scale trial currently being prepared will recruit larger samples of volunteers to better assess this factor.

Preparing the Protocol for Clinical Studies

In chapter 4, three vasomotor response tests were assessed with OS-CMR: adenosine, the combined hyperventilation breath-hold (HVBH) and a normal long breath-hold (LBH) from baseline breathing. Specifically, between the two breath-holds, chapter 1 and 4 showed that the HVBH was the more consistent maneuver and induced a greater change in SI than the LBH. Additionally, as shown in chapter 4 and described in the introduction as well, hyperventilation pre-conditions a person to make a longer breath-hold, which in healthy volunteers could be maintained for almost an additional 30s. This is due to the fact that even just 60s of hyperventilation induces hypocapnia[83,211], and a greater range of CO_2 can be assessed before the participant gets hypercapnic and needs to breathe. This is important as for the next chapter, the coverage for the OS imaging will be increased from one slice to 2 slices. This will allow for more data across the heart. However, this will also decrease the data obtained within a specific time period by half, as the MRI will now alternate the acquisition of the two slices in each measurement. Subsequently, a longer breath-hold is preferred to ensure enough data points are acquired, and commonly cardiovascular patients coming for CMR exams do not hold their breath for much longer than 15s if they do not hyperventilate first. Furthermore, a key goal in CMR exams is to make new techniques as fast and simple as possible, and refining the breathing maneuver protocol to just one method should require less than 5 minutes to set up and perform. And finally, although most vascular exams rely on the response to a vasodilating stimulus, the vasoconstrictive mechanism of hyperventilation may provide useful information as well. Consequently, the HVBH has been chosen to be the optimum breathing maneuver to progress into clinical studies.

Part 3: Assessment in a Cardiac Patient Population

5 Chapter 5 - Revealing the impact of breathing maneuvers on myocardial oxygenation in multi-vessel coronary artery disease: an interim analysis

Foreword

This chapter presents an interim analysis of a study in progress at the Bern University Hospital (Inselspital), Switzerland. All participants are recruited from Europe and thus represent a different population from the Canadian healthy controls reported in chapter 4. This interim report includes data from 6 healthy volunteers, and the first 7 CAD patients recruited into the study. Eventually the full sample size will include 10 healthy volunteers and 26 CAD patients. This study continues from chapter 4 and applies the breathing maneuvers as a technique to assess if there are myocardial oxygenation abnormalities in CAD patients that can be detected by OS-CMR. For this study, I spent one year in Switzerland helping to prepare the study, conduct some of the MRI exams, performing the primary MR image and statistical analysis, as well as composing the manuscript. Funding was provided locally by the Department of Anaesthesia and Pain Medicine at the Inselspital. This data is also used for a scientific presentation at the congress for the European Society of Cardiothoracic Anaesthesia (EACTA 2016) in Basel, Switzerland.

Acknowledgments

This study was made possible by the collaboration of the Departments of Anaesthesiology and Pain Therapy, the Institute of Diagnostic, Interventional and Pediatric Radiology and Cardiology at the Inselspital. In particular thanks to the co-authors, the imaging technicians of radiology Leonie Schuener and Verena Beutler, the physicist Bernd Jung, and the study nurses Loreen Errass and Monika Pia Stucki.

Revealing the impact of breathing maneuvers on myocardial oxygenation in multi-vessel coronary artery disease: an interim analysis

Kady Fischer, BHSc.[1,2]; Dominik P. Guensch, MD[1,3]; Kyohei Yamaji, MD[4]. Bernd Jung, PhD[2]. Johannes T. Heverhagen, MD PhD[2], Stephan Windecker, MD[4]. Matthias G. Friedrich, M.D.,[5,6,7,8], Balthasar Eberle. MD[1].

[1] Department Anaesthesiology and Pain Therapy, Inselspital, Bern University Hospital, University of Bern, Bern, Switzerland

[2] Department of Biomedical Sciences, University of Montreal, Montreal, Canada

[3] Department of Interventional and Paediatric Radiology, Inselspital, Bern University Hospital, University of Bern, Switzerland

[4] Department of Cardiology, Inselspital, Bern University Hospital, University of Bern, Switzerland

[5]Departments of Radiology, Université de Montréal, Montreal, Canada;

[6]Departments of Medicine and Diagnostic Radiology, McGill University, Montreal, Canada

[7]Department of Cardiology, Heidelberg University Hospital, Heidelberg, Germany

[8]Departments of Cardiac Sciences and Radiology, University of Calgary, Calgary, Canada

Clinical Trials Identifier: NCT02233634

All co-authors wrote and approved the manuscript. This is a manuscript currently in preparation, which will be completed upon full recruitment and analysis of the study.

5.1 Abstract

Background: The use of a breathing maneuver combining hyperventilation and a subsequent breath-hold has been successfully used as a non-pharmacological vasoactive stimulus to induce changes in myocardial oxygenation in healthy volunteers and animal models. This study was undertaken to assess if this maneuver is feasible in CAD patients with multi-vessel disease, and effective at detecting haemodynamically relevant coronary artery stenosis.

Methods & Results: An interim analysis was performed from a study that will eventually incorporate 26 patients and 10 healthy controls. Six healthy controls, and seven patients with angiographically verified coronary artery stenosis underwent a contrast-free cardiovascular magnetic resonance (CMR) exam involving function imaging, T1 mapping for edema, and oxygenation-sensitive CMR (OS-CMR) imaging. During OS-CMR, patients performed a controlled hyperventilation for 60s and immediately thereafter held their breath as long as they felt comfortable. All CAD patients were able to complete the breathing maneuvers including an extended breath-hold after hyperventilation (69±25s). While function and edema analysis did not significantly differ between groups, CAD patients had a significantly attenuated global myocardial oxygenation response in comparison to the healthy controls during both the hyperventilation (-1.8±3.8 vs -11.0±6.6%, p=0.003) and breath-hold (1.4±2.5 vs 10.7±8.4%, p=0.010) components. Furthermore, in CAD patients the regions subtended by a stenotic vessel differed in their response to the breath-hold technique from the remote territories.

Conclusion: Breathing maneuvers in combination with oxygenation-sensitive cardiovascular magnetic resonance, are clinically feasible and may detect myocardial oxygenation abnormalities related to coronary artery stenosis in patients with CAD, without the use of any pharmacological vasodilators or contrast agents. These results come from a small sample size, and analysis of the complete study will provide a greater understanding of the technique.

Keywords: Coronary Artery Disease ▪ Oxygenation-Sensitive Cardiovascular Magnetic Resonance ▪ Breathing Maneuvers ▪ Quantitative Coronary Angiography

5.2 Introduction

The current imaging recommendations for assessing the impact of coronary artery disease (CAD) on myocardial vascular function involve using a stressor or vasodilator with a functional imaging modality such as myocardial perfusion scintigraphy (MPS), cardiovascular magnetic resonance imaging (CMR) or echocardiography[212]. CMR first-pass perfusion combines the iv administration of a contrast agent with a pharmacological vasodilator. This approach however only observes the contrast agent inflow into the myocardium and not myocardial oxygenation, which would precisely reflect the balance of both perfusion-dependent oxygen delivery and myocardial oxygen demand. Furthermore, this sequence requires the injection of a contrast agent, commonly gadolinium agents, which may have short-term and long-term side effects and are also contraindicated in patients with renal failure or known gadolinium allergy. This presents a significant problem, as the prevalence of kidney failure at any stage (glomerular filtration rate, GFR<60ml/min/1.73m^2) in stable CAD has been reported to be as high as 22% in a large international trial including more than 22,000 patients[21]. Thus these patients may not undergo important imaging exams due to risks posed by the contrast agent. Furthermore, recent evidence indicates that gadolinium may accumulate in brain tissue of healthy individuals[22]. Recently, oxygenation-sensitive (OS)-CMR has been proposed for assessing myocardial oxygenation. These CMR sequences do not rely on pharmacological contrast agents, and thus can be performed when contrast agents are contraindicated. OS-CMR instead is based on the signal attenuating effects of the local deoxyhaemoglobin fraction, which were first described by blood oxygen level-dependent (BOLD) studies in brain MRI[24]. In the presence of a short-term vasoactive stimulus, the tissue oxygenation response can be derived from the signal intensity changes in OS-CMR images, due to respective changes in the local deoxyhaemoglobin fraction. In healthy vasculature, vasoactive stimuli will increase blood supply without an accompanying increase in oxygen demand, and thus an increase in myocardial oxygenation will be observed. However, in the presence of a fixed coronary stenosis or microvascular dysfunction, the blood vessels cannot respond as effectively, or the more peripheral vessels are already at a chronic maximum dilation. Consequently, myocardial oxygenation will not increase to the same extent as in healthy myocardium, or even a decrease may be recorded as signal deficit, due to effects such

as coronary steal, increased oxygen demand without a compensatory increase in blood flow, or post-stenotic capillary recruitment, i.e., when vessels down-stream of a stenosis dilate with deoxygenated blood[31]. In combination with pharmacological vasodilation, OS-CMR has been successfully used to detect myocardial oxygenation abnormalities in CAD[34,35,38]. Recently, we have investigated the use of breathing maneuvers as an endogenous non-pharmacological and less expensive vasomotor stimulus. In healthy volunteers, breathing maneuvers had a significantly stronger impact on myocardial oxygenation than the gold-standard of adenosine[47], and in an animal model, breathing maneuvers combined with OS-CMR could detect myocardial oxygenation deficits in the presence of an induced coronary stenosis (chapter 1).

In this study, we focus on hyperventilation combined with a breath-hold (HVBH). It is known that hyperventilation induces myocardial and cerebral vasoconstriction[110,157], but hyperventilation with its state of hypocapnia not only allows for a longer breath-hold immediately thereafter[86], but also for monitoring a greater range of vasoreactivity, going from vasoconstriction to vasodilation. So far, such breathing maneuvers in combination with OS-CMR have not been tested as a diagnostic technique in a human population with CAD. This study implements this technique to assess myocardial oxygenation in CAD patients, by comparing it in a known stenosis-dependent territory with remote territories of the same patient, as well as in healthy volunteers.

5.3 Methods

Interim Analysis

Sample size calculated prior to enrolment called for the inclusion of 10 healthy volunteers and 26 CAD patients. This interim analysis includes data from 6 healthy volunteers, and 7 CAD patients.

Participants

Healthy participants were recruited by public notification, and were required to be non-smokers for the last six months, free of any medication that would affect the cardiac or circulatory system, and with a medical history free of cardiac or pulmonary disorders, or disorders which are known to affect the microvasculature such as diabetes and previous chemotherapy. Eligible patients for the CAD group were identified from catheterization laboratory schedules for staged percutaneous coronary intervention (PCI) procedures, and were included if their first quantitative angiographic analysis showed at least one untreated major vessel with a diameter stenosis of >50%. All participants must have been older than 18 years, capable of providing consent and not be pregnant or have any MRI contraindications, including MRI non-compatible metallic objects such as pacemakers and defibrillator leads. Patients with acute myocardial infarction, coronary bypass grafts, or severe pulmonary diseases were also excluded.

Quantitative Coronary Angiography (QCA)

QCA of all vessels was performed for research purposes post-angiography by a trained cardiologist independent from the MR analysis (QangioXA version 7.3, Medis Medical Imaging Systems, Leiden, the Netherlands). This reader then coded each AHA segment as either 1, remote, perfused by a healthy coronary artery; or 2, affected by a significant stenosis; or 3, perfused by a stented vessel; or 4, undetermined.

CMR Protocol

The CMR exam was performed between the two angiographic visits of the staged PCI, allowing for quantification in myocardium subtended by untreated vessels in non-acute patients. Prior to the CMR exam, participants were asked to refrain from consuming caffeine or taking any medication with calcium antagonists or nitrates within 12h prior to the exam.

As shown in Figure 27, for the CMR exam, localisation, cardiac function, T1 maps and oxygenation-sensitive images were acquired. All images were obtained at an end-expiratory

breath-hold. OS-CMR was imaged during breathing maneuvers as vasoactive stimuli[47]. This breathing maneuver protocol involved a baseline image, followed by 60s of voluntary hyperventilation at a rate of 30 breaths/min paced by a metronome. Immediately after hyperventilation, the participant performed a long breath-hold during which the heart was imaged continuously with the OS-CMR sequence. The breath-hold was sustained until the participant indicated the need to breathe. Blood pressure, heart rate and SpO_2 (transcutaneous pulse-oximetric arterial oxygen saturation) were monitored continuously and were recorded prior to hyperventilation, post-hyperventilation, and at the end of the breath-hold. The patients reported any adverse effects to the study nurse immediately after the breathing maneuvers.

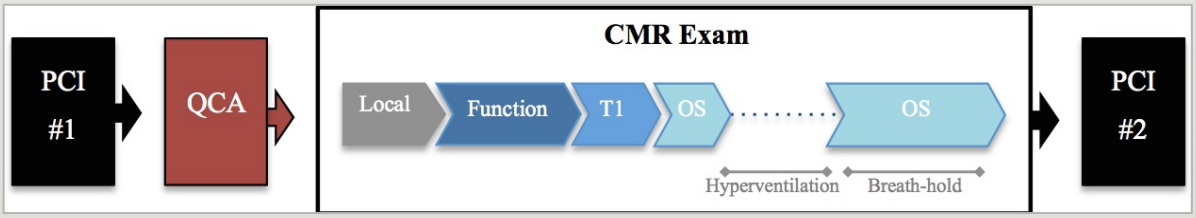

Figure 27: Schematic of protocol
The imaging exam was performed between the two visits of a staged PCI, so that the degree of a stenosis was verified by quantitative coronary analysis (QCA) prior to the CMR exam. Localizers, Function imaging, T1-mapping were acquired according to normal protocol, and OS-CMR was performed during a breathing maneuver of hyperventilation and subsequent breath-hold.

CMR Parameters

All imaging took place in a clinical 3T MRI system (MAGNETOM Skyra 3T; Siemens Healthcare, Erlangen, Germany). Function images were obtained covering the ventricles with 7 to 10 short-axis (SAX) slices using a standard ECG-gated balanced steady-state free precession (bSSFP) cine sequence (temporal resolution/echo-time (TR/TE) 1.43ms/3.3ms, flip angle 65°, voxel size 1.6x1.6x6.0mm, matrix 192x120, bandwidth 962Hz/Px). T1 maps were imaged in the basal and mid-ventricular SAX slices to assess edema with a 5(3)3-modified Look-Locker sequence (MOLLI: TR/TE 281ms/1.12ms, flip angle 35°, voxel size 1.4x1.4x8.0mm, bandwidth 1085Hz/Px). OS-CMR images were obtained in the same two slices with an ECG gated bSSFP sequence that acquired a measurement every 4 heartbeats (TR/TE 1.70ms/3.4ms, flip angle 35°, voxel size 2.0x2.0x10.0mm, matrix 192x120, bandwidth 1302Hz/Px).

CMR Image Blinding & Analysis

The MR exam of each participant was re-coded so the CMR reader was blinded to the identity of the participant, allocation to group, and any angiography results. All CMR analysis was performed using cvi[42] (Circle CVI, Calgary, Canada). Standard function parameters were calculated including ejection fraction (EF), stroke volume (SV), cardiac output (CO), and myocardial mass indexed to the body surface area (BSA). From the same function images, circumferential strain was calculated for the left ventricle from the apex to the base, excluding slices that included the outflow tract. T1 and OS-CMR images were analyzed using manually defined epicardial and endocardial contours. The analysis software further segmented the myocardium automatically following the AHA definitions, and reported an individual value for each segment in addition to a global value for the entire slice. After image analysis, the results of the group and angiography were un-blinded, and the segmental MR values were grouped based on the QCA categorization, as defined above (Figure 28).

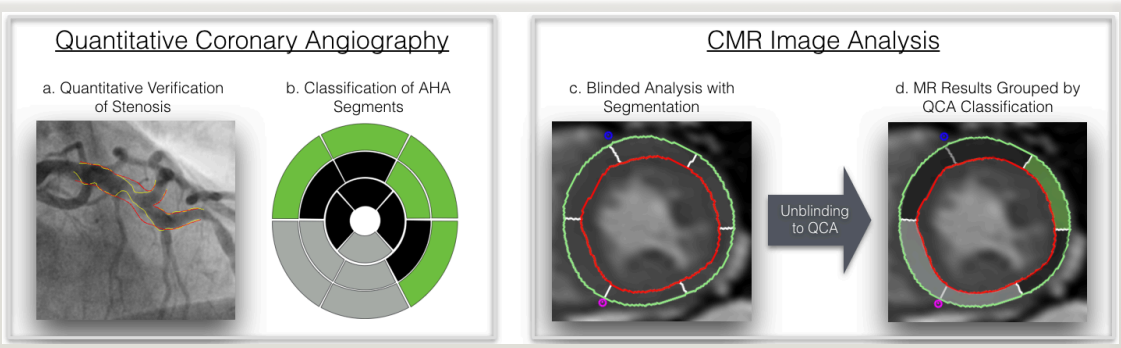

Figure 28: Analysis of Angiography and CMR Images
Quantitative coronary angiography was performed to verify the degree of the stenosis (a), and based off these results, (b) the reader classified what regions of the left ventricle would be affected by a significant lesion >50% (black), affected by a recently stented coronary artery (grey), or as unaffected remote territory (green). CMR analysis was performed blinded to the angiography results, and values were obtained per segment (c), after which the angiographic results were unblended and MR values per segment were averaged based on the QCA classification (d).

Thus, for the CAD patients, measurements were obtained for the global myocardium, as well as for the affected and remote segments. Only global values were measured for the myocardium of the healthy volunteers. Relative OS signal intensity (SI) was reported as a %-

change from the baseline image for the hyperventilation analysis, while for the breath-hold analysis a %-change was calculated for each measurement compared to the initial image of the breath-hold period: the measurement at a breath-hold duration of 30s was used for statistical analysis.

Statistical Analysis

All values are reported as mean±SD. Demographics and function analysis was compared between the two groups with independent t-tests. A univariate ANOVA with Bonferroni correction for multiple comparisons was used to compare the global and regional CMR results from CAD patients to the healthy controls; additional within-group analysis compared affected regions to remote myocardium. Paired t-tests for the breathing maneuvers assessed if the SI and haemodynamic measurements changed from baseline. Tests were performed with GraphPad Prism version 6.0 (GraphPad Software, La Jolla California USA) and SPSS version 23 (SPSS IBM, New York, USA). Results were considered statistically significant at a two-tailed $P<0.05$.

5.4 Results

Participant Characteristics

All six of the reported healthy participants were aged 35 years or younger, had a BMI below 28 kg/m^2, and did not report any cardiovascular related medical history or medication. The CAD patient group was significantly older and in its majority on chronic medication (Table 14).

	Healthy	CAD
Demographics		
n	6	7
Age (years)	28 ± 4	65 ± 15
range	(23 – 35)	(47 - 84)
BMI (kg/m^2)	24.4 ± 2.7	27.8 ± 3.7
range	(19.9 – 28.0)	(23.4 – 34.0)
sex	4M / 2F	7M / 0F
Comorbidities		
Dyslipidemia	-	5 (71)
Hypertension	-	4 (57)
Diabetes	-	2 (28)
Smoker	-	2 (28)
OSAS	-	1 (14)
Medications		
Aspirin	-	7 (100)
Anti-Platelet	-	7 (100)
Statins	-	7 (100)
Beta-Blockers	-	6 (86)
ACE-Inhibitors	-	4 (57)
AT2R-antagonist	-	2 (28)
Calcium channel blocker	-	1 (14)
Other	-	4 (57)

Table 14: Participant Characteristics
Demographics are reported as mean±SD, or as patient count and prevalence (n; %) of known diseases and medications, as reported by the volunteer or on file in patients´ hospital records. BMI: body mass index, OSAS: obstructive sleep apnea syndrome, ACE: angiotensin-converting-enzyme, AT2R: angiotensin-II receptor.

Function, Strain and T1

Between the two groups, there were only minor and statistically insignificant differences in functional parameters or abnormalities (Table 16). In CAD patients there were non-significant trends of a lower stroke volume index and cardiac index ($0.10>p>0.05$). All participants, including the CAD patients, had a normal ejection fraction above 50%. When compared to the healthy myocardium of volunteer participants, CAD segments affected by a

significant stenosis showed a non-significant trend to abnormal peak circumferential strain (CAD, -19.0±2.4%, vs. healthy volunteer, -21.6±1.1%; p=0.145). This however did not amount to a significant global strain abnormality in CAD patients (Figure 29). Myocardial T1 as a marker for edema did not differ between groups.

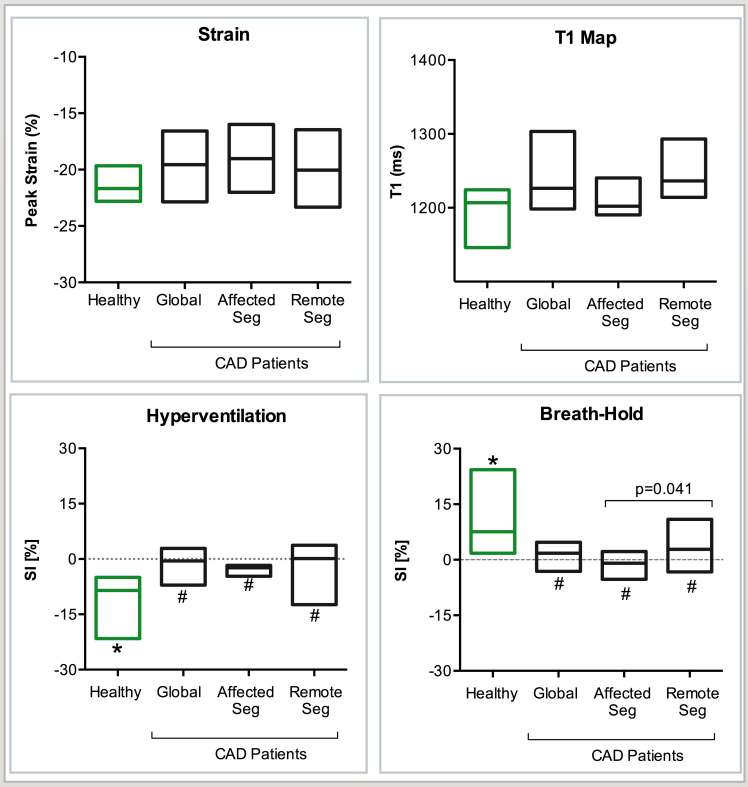

Figure 29: Global and regional CMR results

Mean (Min-Max) results of peak global circumferential strain, T1 mapping, and %-change in SI from the OS-CMR during hyperventilation and at the 30s time-point in the breath-hold. CAD patients (black) were assessed for the global myocardium, as well as for regional analysis of segments affected by a significant stenosis, and the remote territory, whereas data for the healthy volunteers is reported as a global value (green). In CAD patients, both the affected segments and global myocardium mounted only a significantly attenuated response to the breathing maneuvers, when compared to healthy controls (#p<0.05). Healthy volunteers had a significant decrease in myocardial SI after hyperventilation, and a significant increase after 30s into the breath-hold (*p<0.05 for difference to baseline).

Breathing Maneuvers

All participants completed the breathing maneuvers, with only one healthy volunteer (t=28s) and one patient (t=19s) not maintaining the breath-hold for 30s. However, the OS response of both participants fit well within the mean±1SD for their respective groups, despite the abbreviated breath-hold.

In healthy controls, hyperventilation had the strongest effect upon the rate pressure product. Here, blood pressure increased by a mean of 8 mmHg and heart rate rose by a mean of 59 bpm, which normalized during breath-hold (Table 15). The CAD patients experienced no comparable rate pressure product response, most likely since the majority (6/7) were treated with a beta-blocker. Participants only reported three types of adverse effects during the breathing maneuvers: tingling in the extremities (Healthy: n=2, CAD: n=2), temporary headache (Healthy: n=1) and dizziness (Healthy: n=1), while 3 healthy participants and 5 CAD patients reported no side effects.

	Hyperventilation		Breath-Hold	
	Healthy	**CAD**	**Healthy**	**CAD**
Δ Blood Pressure (SYS/DIA, mmHg)	8±7/8±4*	-1±6/-2±7	4±5/5±6	6±9/0±5
Δ Heart Rate (bpm)	59 ± 23*	2 ± 4	- 44 ± 24*	6 ± 11
Δ SpO_2 (%)	3 ± 2*	1 ± 2	-11 ± 8*	-7 ± 12
Duration (Range; s)	-	-	63 ± 25 (28 – 98)	69 ±37 (19 – 141)

Table 15: Measurements during breathing maneuvers
Mean±SD changes in haemodynamics and oxygenation during the hyperventilation and breath-hold maneuvers (*p<0.05 difference between end and start of maneuver). SYS, systolic; DIA, diastolic; bpm, beats per minute; SpO_2, transcutaneous pulse-oximetric arterial oxygen saturation.

OS-CMR

During hyperventilation, healthy volunteers responded with a significant reduction in SI (-11.0 ±6.6%; p<0.001 vs baseline), whereas the global myocardial response of the CAD patients was attenuated in comparison to the healthy response (-1.8±3.8%; p=0.003 vs. healthy), and did not significantly differ from baseline. No difference was observed with this maneuver between segments subtended by a significant coronary artery stenosis and remote territory (Figure 30); however, during the subsequent breath-hold the two types of segments responded differently (affected, -1.1±2.9; vs remote, 2.9±4.7, p=0.041, Figure 30). Globally, healthy volunteers were able to increase their myocardial oxygenation during this vasodilating stimulus (10.7±8.4%; p=0.026 vs baseline), whereas CAD patients (global; 1.4±2.5%, p=0.010) responded significantly less than the control (p=0.010 vs control).

5.5 Discussion

Without the use of any pharmacological vasodilators or contrast agents, the combination of oxygenation-sensitive CMR and a combined hyperventilation/breath-hold breathing maneuver appears to allow for the detection of an attenuated myocardial oxygenation response in patients with stenotic coronary artery disease. When combining a vasoconstrictive phase with a vasodilating-breathing maneuver, a wide range of vasomotion can be assessed. It should be noted that the reported results are just from an interim analysis with a small sample size. Nevertheless, these preliminary results are promising, since even in this limited dataset there are clear oxygenation abnormalities detected by the technique.

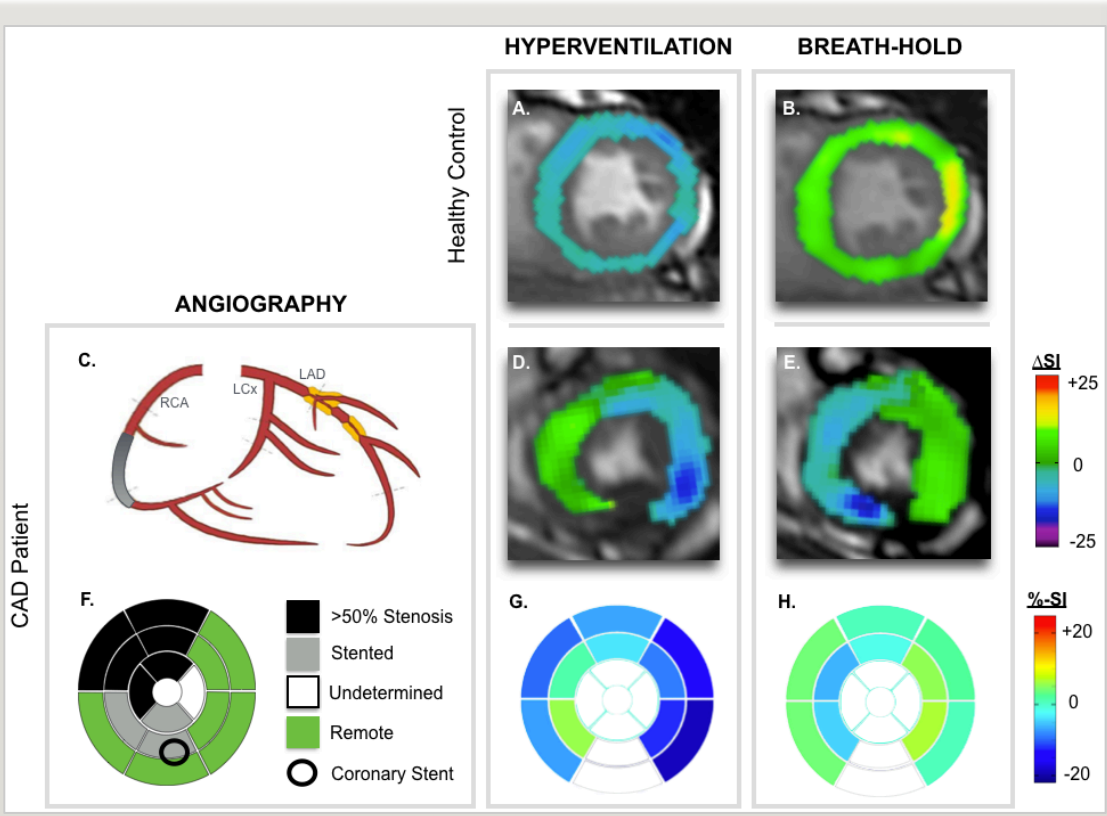

Figure 30: Myocardial oxygenation in coronary artery disease

In a healthy participant, subtraction images of the mid-ventricle slice display the difference in signal intensity (SI) per voxel between two images (neurolens.org) and demonstrate that in a healthy participant hyperventilation causes a uniform decrease in myocardial oxygenation (A), whereas an increase is observed during the breath-hold (B). For the CAD patient presented, angiography showed un-treated stenosis in the left anterior descending coronary artery (LAD), with the right coronary artery (RCA) recently stented, while the patent left circumflex artery (LCx), responsible for blood supply of the lateral wall, was relatively normal according to the QCA (C). During hyperventilation (D, G), the remote territory responded similarly to the healthy volunteer, whereas an abnormal response was seen in the affected territory with an increase in SI. Similarly during the breath-hold, the remote territory responded with a normal increase in SI, but the affected regions had an oxygenation decrease. Bulls-eye plots of the %-SI change in this patient (G, H) show that the effect is more pronounced in the mid-slice, than in the basal slice. A coronary stent in the RCA caused artifacts in the inferior wall of the MR images for the CAD patient.

CAD

The patients included in this study had multi-vessel coronary artery disease, in which vascular dysfunction has very likely developed over time, rather than as an acute vessel obstruction. The regional differences observed in our sequences varied between patients. Some patients had clear differences in MRI results between affected and remote territory, whereas other patients had a more consistent global abnormality. Furthermore, as seen in Figure 29, values obtained from the affected regions were fairly consistent, whereas remote regions showed large variation. For example, 3 of the 7 patients showed a regional difference with at least a 4% difference between the two territories, in which the remote territory showed an increase in signal (Figure 31B). On the other hand, 2 other participants showed an oxygenation abnormality in the regions subtended to a significant stenosis, and the remaining myocardium was affected as well, resulting in a global deficit (Figure 31C). This is likely due to a widely variable pattern of microvascular dysfunction in multi-vessel disease, which may also affect vasomotion of remote myocardium. Furthermore, variability in collateralization and coronary steal can also produce variable results in the remote territories[34,140].

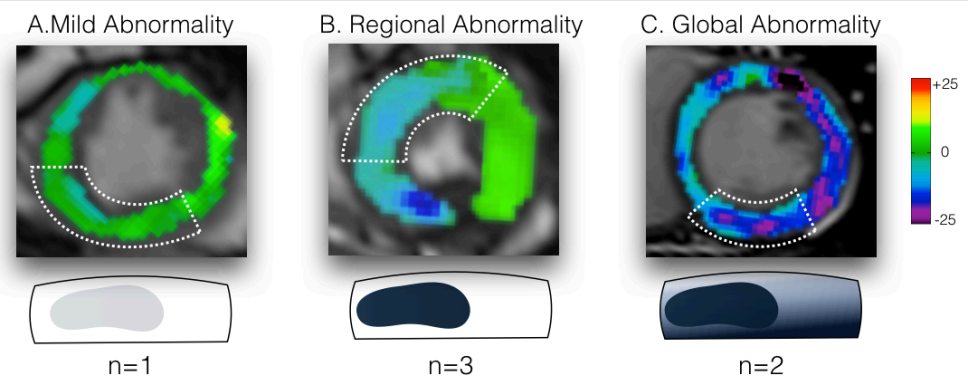

Figure 31: Patterns of oxygenation during the HVBH

As described in the introduction (section 0.7, Figure 10), there were three patterns of oxygenation observed in the CAD group. The most common pattern (n=3/7) was the regional abnormalities (b), where there was an oxygenation abnormality in the affected regions, but the remote regions had a normal or mild abnormal response. On the other hand, 2 participants, showed a global abnormality (C), in which the majority of the myocardium showed an oxygenation deficit. One participant, showed only a mild OS abnormality despite significant lesions (a), while the remaining participant had results in between B and C. The affected territory, perfused by an artery with an untreated lesion is shown in white.

For example, in the presented case study (Figure 30), during the vasodilatory breath-hold, the decreased resistance in the healthy vessels may redirect blood flow away from the affected regions, which are unable to dilate as effectively (steal effect). The opposite effect may occur during hyperventilation when healthy vasculature is able to constrict and thereby increase its coronary resistance (reverse steal or Robin Hood effect). Thus more blood flow may be redirected to affected segments with dysfunctional vasculature that may not have been able to constrict as well. In Figure 30, hyperventilation actually decreased myocardial oxygenation less in affected segments, compared to the marked OS-CMR decrements seen in healthy myocardium. Similar to the animal results in chapter 1, during the breath-hold the OS imaging can significantly detect abnormal regional myocardial oxygenation in territories subtended to a coronary lesion. This chapter however also shows that the hyperventilation maneuver has a significant effect on signal, and there is a much stronger oxygenation response is observed in humans. This leads to greater differences between abnormal and healthy myocardium (mean 11.8%) in the human analysis, which could allow for a greater confidence when determining if a patient has an oxygenation abnormality.

This interim analysis did not assess specifically myocardial regions subtended by vessels that had just been treated in the primary angiography, other than their inclusion in the global myocardial analysis. As seen in the CAD patient presented in Figure 30, such regions may still react similarly to the affected regions. This presents an interesting aspect that can be assessed when the study has recruited the full sample size.

Furthermore, we did not rule out the presence of scar tissue, which is a common finding in coronary artery disease and can affect perfusion or oxygenation results owing to the loss of vessels and viable tissue in the affected region. While native T1 values (i.e. without contrast agent) have been shown to be associated with myocardial edema[213], recent reports suggest that myocardial fibrosis can be interpreted from these values as well[214]. Mildly increased T1 values may signal fibrosis, whereas higher T1 can be a result of myocardial

edema[215]. At the current stage, however, no significant T1 findings were observed in this small sample of CAD patients.

Feasibility of the Protocol

A possible concern about the breathing maneuver protocol is its clinical feasibility; including the ability or willingness of patients to perform the breathing maneuvers and maintain a breath-hold for 30s, which is the primary analysis point. However, we now demonstrated that in our typically elderly patient group with multi-vessel CAD, the mean breath-hold time was still around a minute (69±37s) and matched the healthy volunteer group. All participants completed the breathing maneuvers, and only minor adverse effects were reported, for instance tingling in the extremities or temporary dizziness from hyperventilation.

Limitations

In the present study, severe coronary stenosis is determined by QCA measurements, rather than with fractional flow reserve (FFR), which is considered the gold standard for verifying a clinically significant coronary artery stenosis. Whereas QCA provides a visual assessment of the stenosis, FFR can determine its haemodynamic severity and clinical relevance with respect to the need for revascularization. In the case of multi-vessel disease, the FAME trial showed that only 46% of the angiographically defined multi-vessel disease cases were considered a functional multi-vessel disease when accounting for FFR measurements[216]. In our study a degree of stenosis, angiographically quantified at >50%, may not have a significant impact on the blood supply to the myocardium. Another study using OS-CMR with adenosine as the vasodilator had shown that the changes in SI were also correlated to the degree of stenosis assessed by QCA, albeit weaker than with FFR in the same study[38].

Rationale for Healthy Group

In this study, younger participants in good general health were recruited since they most likely have minimal microvascular or other cardiovascular dysfunction, which in turn

may cause an abnormal oxygenation response. Thus we clearly recognize that differences in CMR results between the CAD group and the healthy volunteers could also be caused or influenced by numerous other factors such as age, BMI, and use of medications. Yet, The oxygenation response of these volunteers was similar to the results of chapter 4, which recruited an older healthy population[47]. As discussed in section 4.8, the perfusion reserve is known to decrease with age, especially once participants are older than 70 years old. Often there is greater variation in data with increasing age, as there is a more diversity in the degree of microvascular dysfunction that could have built up in a lifetime. Yet this is information that cannot be accurately assessed in a small sample of healthy participants. The impact of age on the myocardial oxygenation reserve during breathing maneuvers will have to be assessed in a larger scale study that will recruit larger numbers of elderly yet healthy participants.

5.6 Conclusion

A combined respiratory maneuver of hyperventilation and subsequent breath-holding is a feasible and effective method for inducing a coronary vasomotor response. In combination with oxygenation-sensitive CMR, it may allow for detecting myocardial oxygenation abnormalities associated with significant coronary artery stenosis in patients with multi-vessel CAD. Completion of the study will help to further evaluate diagnostic accuracy of the technique and to define its applicability in assessing regional myocardial oxygenation abnormalities in multi-vessel coronary artery disease.

5.7 Supplemental Information

	Healthy	CAD	*P*
Ejection Fraction (%)	72 ± 3 (range: 68-76)	65 ± 10 (range: 52-77)	*0.109*
EDV/BSA (ml/m2)	91 ± 15	82 ± 10	*0.264*
ESV/BSA (ml/m2)	25 ± 5	29 ± 10	*0.378*
SV/BSA (ml/m2)	65 ± 12	53 ± 10	*0.069*
Mass/BSA (g/m2)	65 ±17	65 ± 13	*0.957*
Cardiac Index (L/min/m2)	4.5 ± 0.9	3.4 ± 1.1	*0.067*
Blood Pressure (SYS/DIA, mmHg)	122±14/60±11	135±15/78±10	

Table 16: Supplemental - cardiac function parameters

Mean±SD of the functional measurements, and resting non-invasive blood pressure obtained at the beginning of the CMR exam. EF, ejection fraction; EDV/BSA, end-diastolic volume indexed to body surface area; ESV/BSA, end systolic volume indexed to body surface area; SV/BSA, stroke volume indexed to body surface area, and mass indexed to body surface area. *p<0.05 for differences observed between groups.

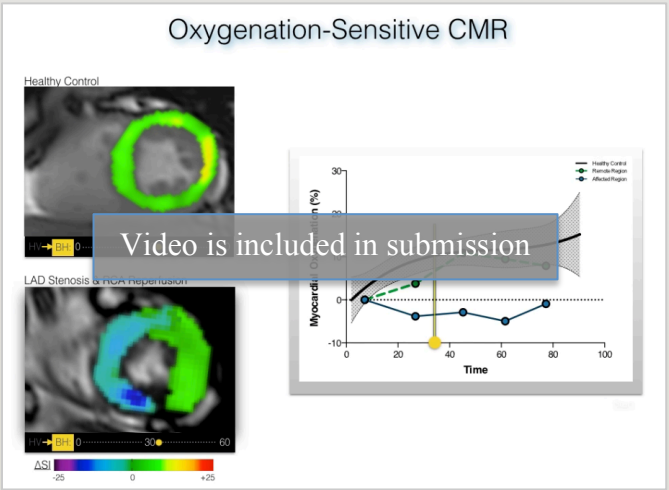

Supplemental Video 1: Dynamic oxygenation response

The dynamic response of the myocardial oxygenation response over the breath-hold following hyperventilation (HVBH) is shown for the data in figure 30. A healthy participant (top), demonstrates OS increases homogenously in the first 30s and then plateaus. For the patient with an LAD stenosis and RCA stent, the anterior and septal walls show an oxygenation deficit that decreases during the breath-hold, while the remote territory in the lateral wall shows a healthy response. The graph shows the mean response of all healthy participants, and the data of the mid-apical slice of the individual patient.

5.8 Chapter References

21. Kalra PR, García-Moll X, Zamorano J, Kalra PA, Fox KM, Ford I, Ferrari R, Tardif J-C, Tendera M, Greenlaw N, Ph. Gabriel Steg for the CLARIFY Investigators. Impact of Chronic Kidney Disease on Use of Evidence-Based Therapy in Stable Coronary Artery Disease: A Prospective Analysis of 22,272 Patients. *PLoS ONE*. 2014;9:e102335.

22. McDonald RJ, McDonald JS, Kallmes DF, Jentoft ME, Murray DL, Thielen KR, Williamson EE, Eckel LJ. Intracranial Gadolinium Deposition after Contrast-enhanced MR Imaging. *Radiology*. 2015;275:772–782.

24. Ogawa S, Lee TM, Nayak AS, Glynn P. Oxygenation-sensitive contrast in magnetic resonance image of rodent brain at high magnetic fields. *Magn Reson Med*. 1990;14:68–78.

31. Wacker CM, Hartlep AW, Pfleger S, Schad LR, Ertl G, Bauer WR. Susceptibility-sensitive magnetic resonance imaging detects human myocardium supplied by a stenotic coronary artery without a contrast agent. *J Am Coll Cardiol*. 2003;41:834–840.

34. Friedrich MG, Niendorf T, Schulz-Menger J, Gross CM, Dietz R. Blood oxygen level-dependent magnetic resonance imaging in patients with stress-induced angina. *Circulation*. 2003;108:2219–2223.

35. Manka R, Paetsch I, Schnackenburg B, Gebker R, Fleck E, Jahnke C. BOLD cardiovascular magnetic resonance at 3.0 tesla in myocardial ischemia. *J Cardiovasc Magn Reson.* 2010;12:54.

38. Luu JM, Friedrich MG, Harker J, Dwyer N, Guensch D, Mikami Y, Faris P, Hare JL. Relationship of vasodilator-induced changes in myocardial oxygenation with the severity of coronary artery stenosis: a study using oxygenation-sensitive cardiovascular magnetic resonance. *Eur Heart J Cardiovasc Imaging.* 2014;15:1358–1367.

47. Fischer K, Guensch DP, Friedrich MG. Response of myocardial oxygenation to breathing manoeuvres and adenosine infusion. *Eur Heart J Cardiovasc Imaging*. 2015;395–401.

86. Parkes MJ. Breath-holding and its breakpoint. *Exp Physiol.* 2006;91:1–15.

110. Neill W, Hattenhauer M. Impairment of myocardial O2 supply due to hyperventilation. *Circulation*. 1975;52:854 –858.

140. Seiler C, Fleisch M, Meier B. Direct Intracoronary Evidence of Collateral Steal in Humans. *Circulation*. 1997;96:4261–4267.

157. Kety SS, Schmidt CF. The effects of active and passive hyperventilation on cerebral blood flow, cerebral oxygen consumption, cardiac output, and blood pressure of normal young men. *J Clin Invest*. 1946;25:107–119.

212. Demir OM, Alfakih K, Plein S. Current international guidelines for the investigation of patients with suspected coronary artery disease. *Eur Heart J Cardiovasc Imaging*. 2014;jeu168.

213. Germain P, El Ghannudi S, Jeung M-Y, Ohlmann P, Epailly E, Roy C, Gangi A. Native T1 Mapping of the Heart – A Pictorial Review. *Clin Med Insights Cardiol*. 2014;8:1–11.

214. Malek ŁA, Werys K, Kłopotowski M, Śpiewak M, Miłosz-Wieczorek B, Mazurkiewicz Ł, Petryka-Mazurkiewicz J, Marczak M, Witkowski A. Native T1-mapping for non-contrast assessment of myocardial fibrosis in patients with hypertrophic cardiomyopathy — comparison with late enhancement quantification. *Magn Reson Imaging*. 2015;33:718–724.

216. Tonino PAL, Fearon WF, De Bruyne B, Oldroyd KG, Leesar MA, Ver Lee PN, MacCarthy PA, van't Veer M, Pijls NHJ. Angiographic Versus Functional Severity of Coronary Artery Stenoses in the FAME Study: Fractional Flow Reserve Versus Angiography in Multivessel Evaluation. *J Am Coll Cardiol*. 2010;55:2816–2821.

6 Summary and Conclusion

The work presented in this manuscript describes the development of a novel technique for assessing the capacity of the coronary vascular system to increase myocardial oxygenation in response to breathing maneuvers as a vasodilatory stimulus. Specifically, our data show, that a breathing maneuver combining hyperventilation with a breath-hold consistently induces a significant change in myocardial oxygenation, which is impaired in the presence of coronary stenosis. The oxygenation response can be reliably measured by oxygenation-sensitive cardiovascular magnetic resonance (OS-CMR).

The breathing maneuver combines the vasoconstrictive effect of hyperventilation with the strong vasodilating stimulus from the breath-hold. This allows for assessing both, constrictive and dilative function and thus a broad range of coronary vascular reactivity.

Validation in an animal model demonstrated that breath-holds (induced by a pause in ventilation) had an even stronger impact on coronary blood flow than adenosine, which is currently considered the standard agent for inducing vasodilation. Moreover, breath-holds of even very short duration had a significant impact on invasively measured coronary blood flow, while hyperventilation significantly reduced blood flow. The strong vasomotor tone induced by the breathing maneuvers also resulted in significant changes to myocardial oxygenation. While hyperventilation resulted in an OS signal decrease, there was a strong signal increase during the breath-hold. Again, this led to a stronger increase of the OS signal than observed with adenosine. The clinical feasibility of breathing maneuvers for diagnostic purposes was demonstrated in chapters 4 & 5, as human participants could always perform the maneuvers and reported minimal side-effects, even in an aging cardiac disease patient group.

Our experiments in animals with experimentally induced coronary artery stenosis and in a small patient population with multi-vessel coronary artery disease have shown that this technique appears feasible for diagnostic testing in patients with suspected myocardial ischemia. Now further studies are warranted to better understand the clinical utility and diagnostic performance of breathing maneuvers in combination with OS-CMR. This may be particularly useful when contrast agents, or pharmacological vasodilators are contraindicated

but also for avoiding associated side effects and cost. The studies may provide an important step toward a comprehensive diagnostic test, without radiation, invasive measures, physical stress, pharmaceutical agents, or complicated (re-)breathing circuits.

Furthermore, the experiments described in chapters 2 and 3 also looked at the impact of steady adjustments of arterial carbon dioxide and oxygen levels on coronary blood flow and myocardial oxygenation. In the animal model, hyperoxia, induced by supplemental oxygen, blunted the coronary response to breath-holds and CO_2 stimuli, and decreased blood supply to the myocardium, further reducing oxygen supply in the presence of a coronary stenosis. This suggests that high levels of oxygen could be detrimental in the care of patients with myocardial ischemia, and that the use of oxygen during diagnostic exams that rely on a vasodilatory response could be a significant confounder. Thus the data also demonstrates the importance of breathing patterns of patients as a result of exam-related stress, and acknowledge their strong vasoactive effects as a confounder for diagnostic tests using vasoactive stimuli.

Continuing with the Hyperventilation Breath-Hold (HVBH) Maneuver

Overall, the combined breathing maneuver of hyperventilation and breath-holding appears to be the best breathing maneuver for inducing consistent and strong myocardial oxygenation responses. Already described in more detail in section 4.8, the preceding period of hyperventilation allows a sufficient breath-hold to be more feasible (Table 2), and secondly the vasoconstrictive stimulus lowers the blood flow and oxygenation baseline, so that when a breath-hold is applied a greater range in both vasomotor response and subsequently myocardial oxygenation can be measured. As seen in chapter 5, the hyperventilation effect may also be useful in detecting oxygenation abnormalities, based on vasoconstrictive stimuli alone, yet this will need to be investigated further. This combined technique of hyperventilation and breath-holding will be the primary breathing maneuver moving forward.

Limitations of Small Samples and the Impact on Final Conclusions

The presented data demonstrate that the technique is feasible and effective for inducing a different myocardial oxygenation response between healthy controls and coronary artery

disease patients, and more specifically, for inducing a different response within the same myocardium between healthy and dysfunctional territories in the same myocardium. However, as these chapters have only assessed small populations, especially in the human studies, we can only assess the general function of the technique. These samples are not complete enough to calculate the accuracy and reliability of the data. Assessment in larger sample sizes would allow for testing to evaluate if the method is truly consistent and diagnostic by calculating reference values, and determining specificity and sensitivity of the technique. Because the thesis has demonstrated there is promise with the breathing maneuver method, a larger multi-center trial is now underway to recruit hundreds of patients and investigate these points listed above. When these results will be available, a more in depth assessment of the technique can be made. Additionally, this future study can look at the relationship of the OS-CMR to the angiographic results, fractional flow reserve, and in most cases nuclear perfusion imaging as well. Yet, as described in the introduction, myocardial oxygenation is not equal to myocardial perfusion. The OS sequences incorporate blood supply yet the final measurement is one step further, based on the oxygenation balance of the tissue, a factor that is not measured with perfusion alone. Also, the microvascular dysfunction is not solely dependent on the coronary anatomy and presence of significant lesions. However, it is still useful to compare the techniques.

The majority of myocardial vascular function imaging is performed to detect inducible ischemia, occuring when there is a net lack of oxygen in the myocardium often caused by a mismatch of blood supply to the metabolic demands. Oxygenation-sensitive imaging is a better measurement for assessing ischemia because it goes beyond the standard perfusion techniques that just focus on blood supply, and adds the secondary component of assessing the oxygenation. Therefore, OS-CMR is a more direct marker for tissue deoxygenation and thus microvascular dysfunction or ischemia, unlike other imaging modalities, which only use perfusion, pressure gradients or coronary anatomy as surrogate markers.

The work presented demonstrates that breathing maneuvers and arterial blood gases have a significant impact on the coronary vasculature, which in turn affects blood supply to the heart and ultimately myocardial oxygenation. By harnessing these mechanisms, breathing

maneuvers can be used as a technique to induce a vascular response, and thus, when combined with diagnostic imaging, can be useful for identifying inducible myocardial ischemia or assessing the oxygenation reserve without the need for pharmaceutical vasodilators, stress agents, radiation, contrast agents or physical stress.

7 Future Implications

The projects laid out in this thesis have resulted in the development of a breathing maneuver protocol that is now being tested in several clinical trials, assessing myocardial oxygenation in healthy controls and cardiovascular patient groups such as heart failure, obstructive sleep apnea, single-vessel coronary artery disease and heart transplants. The next phase in progressing this technique for clinical application would then be to assess the impact of how other confounders may affect the results and how to reduce these impacts to increase the reproducibility of the results. In particular, the most pressing confounders to investigate would include heart rate changes, patient positioning, and the impact of co-morbidities, especially other significant cardiopulmonary disorders.

Future developments would include simplification or automatization of the analysis for better integration into the diagnostic report, such as including colour maps, which allow for a quick visual analysis of myocardial oxygenation abnormalities. Because of the promising data shown in this thesis, this step is already currently underway as of 2016, in which an OS (BOLD) analysis module is being prepared by a software company (cvi[42], Circle Cardiovascular Imaging, Calgary, AB, Canada) and tested by our group. The prototype already significantly reduces post-processing time by automatically creating contours on the images, calculating the %-change across the breath-hold and visually displaying it in a bull's-eye plot. This is still under development to also automatically create visual colour maps superimposed right on the image, as demonstrated in the images throughout the thesis (for example Figure 29). Because there is a high importance to make this technique implementable into a diagnostic routine, our research group will take on the task of making information materials and guides so that the post-processing can be as simple and efficient as possible.

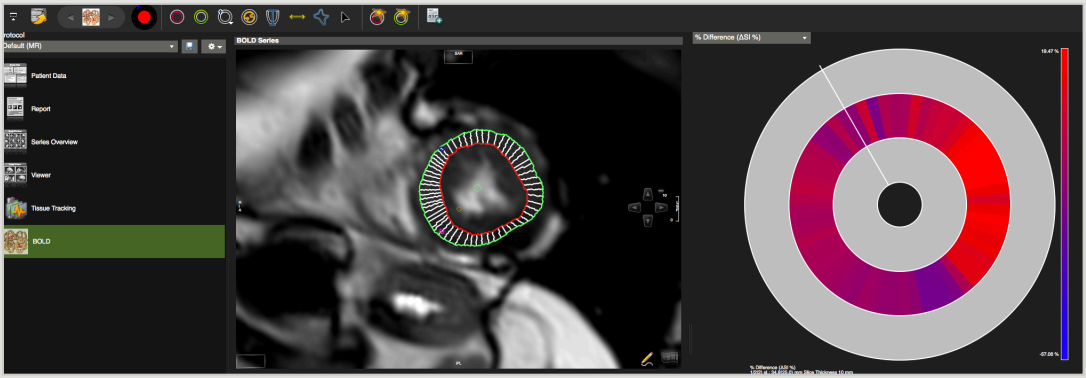

Figure 32: Example of the new analysis prototype
A screenshot of the new prototype for analysis shows that the %-change in signal is automatically calculated by the software and displayed as a bulls-eye plot. This is of the same patient who is shown in Figure 30, in which the lateral wall was healthy territory (high response in this image shown as red), where as the anterior and inferior wall were affected by a stenosis or recent stent (blue and purple).

As non-invasive imaging becomes more frequent in cardiovascular care, health-care organizations and patients prefer diagnostic techniques that are as non-invasive as possible and simple to both perform and analyze. The use of CMR with breathing maneuvers present a safe, simple, and cost-effective alternative that does not require any injections and gives control to the participant thus presenting a possible improvement to the patient experience. Future implementation of the technique will most likely depend on the ability of technologists to consistently perform the protocol and on the tools for a fast, accurate and reliable data analysis of the data.

These breathing maneuvers are also not just limited to oxygenation-sensitive CMR, but also have the potential to be used as a vasoactive stimulus for any procedure. As recently published by our group, the same combined breathing maneuver of hyperventilation and breath-holding could significantly induce a perfusion response as assessed by first pass perfusion CMR, another well-established sequence that often relies on adenosine as a vasodilator[217]. Furthermore, as shown in chapter 2, the breathing maneuvers induce significant blood flow changes in the coronary arteries, and future studies could look into investigating this technique for use in fractional flow reserve exams as well.

The approach has the potential to revolutionize the diagnostic approaches to heart disease. Further testing will be needed to verify its clinical utility.

8 Disclosures

Authors of the presented studies, Kady Fischer, Dominik P. Guensch and Matthias G. Friedrich, hold a pending patent along with Jacqueline Flewitt for inducing and measuring myocardial oxygenation changes as a marker for heart disease (patent pending, Serial No. PCT/CA2013/050608).

References

1. Antony R, Daghem M, McCann GP, Daghem S, Moon J, Pennell DJ, Neubauer S, Dargie HJ, Berry C, Payne J, Petrie MC, Hawkins NM. Cardiovascular magnetic resonance activity in the United Kingdom: a survey on behalf of the british society of cardiovascular magnetic resonance. *J Cardiovasc Magn Reson*. 2011;13:57.

2. Iglehart JK. Health Insurers and Medical-Imaging Policy — A Work in Progress. *N Engl J Med*. 2009;360:1030–1037.

3. Government of Canada PHA of C. 2009 Tracking Heart Disease and Stroke in Canada - Public Health Agency of Canada [Internet]. 2009 [cited 2015 Oct 15];Available from: http://www.phac-aspc.gc.ca/publicat/2009/cvd-avc/index-eng.php

4. Nichols M, Townsend N, Scarborough P, Rayner M. Cardiovascular disease in Europe 2014: epidemiological update. *Eur Heart J*. 2014;35:2950–2959.

5. Campbell F, Thokala P, Uttley LC, Sutton A, Sutton AJ, Al-Mohammad A, Thomas SM. Systematic review and modelling of the cost-effectiveness of cardiac magnetic resonance imaging compared with current existing testing pathways in ischaemic cardiomyopathy. *Health Technol Assess*. 2014;18:1–120.

6. Goldman MR, Pohost GM, Ingwall JS, Fossel ET. Nuclear magnetic resonance imaging: potential cardiac applications. *Am J Cardiol*. 1980;46:1278–1283.

7. McGee K, Martinez M, Williamson E. Mayo Clinic Guide to Cardiac Magnetic Resonance Imaging. Second Edition. Rochester, MN : Oxford ; New York: Oxford University Press; 2015.

8. Donato P, Coelho P, Santos C, Bernardes A, Caseiro-Alves F. Correspondence between left ventricular 17 myocardial segments and coronary anatomy obtained by multi-detector computed tomography: an ex vivo contribution. *Surg Radiol Anat*. 2012;34:805–810.

9. Cerqueira MD, Weissman NJ, Dilsizian V, Jacobs AK, Kaul S, Laskey WK, Pennell DJ, Rumberger JA, Ryan T, Verani MS. Standardized Myocardial Segmentation and Nomenclature for Tomographic Imaging of the Heart A Statement for Healthcare Professionals From the Cardiac Imaging Committee of the Council on Clinical Cardiology of the American Heart Association. *Circulation*. 2002;105:539–542.

10. Kramer CM, Barkhausen J, Flamm SD, Kim RJ, Nagel E. Standardized cardiovascular magnetic resonance (CMR) protocols 2013 update. *J Cardiovasc Magn Reson*. 2013;15:91.

11. Bistoquet A, Oshinski J, Skrinjar O. Left ventricular deformation recovery from cine MRI using an incompressible model. *IEEE Trans Med Imaging*. 2007;26:1136–1153.

12. Carbone I, Friedrich MG. Myocardial Edema Imaging by Cardiovascular Magnetic Resonance: Current Status and Future Potential. *Curr Cardiol Rep*. 2011;14:1–6.

13. Ferreira VM, Piechnik SK, Dall'Armellina E, Karamitsos TD, Francis JM, Choudhury RP, Friedrich MG, Robson MD, Neubauer S. Non-contrast T1-mapping detects acute myocardial edema with high diagnostic accuracy: a comparison to T2-weighted cardiovascular magnetic resonance. *J Cardiovasc Magn Reson*. 2012;14:42.

14. Goldman MR, Brady TJ, Pykett IL, Burt CT, Buonanno FS, Kistler JP, Newhouse JH, Hinshaw WS, Pohost GM. Quantification of experimental myocardial infarction using nuclear magnetic resonance imaging and paramagnetic ion contrast enhancement in excised canine hearts. *Circulation*. 1982;66:1012–1016.

15. Doltra A, Amundsen BH, Gebker R, Fleck E, Kelle S. Emerging Concepts for Myocardial Late Gadolinium Enhancement MRI. *Curr Cardiol Rev*. 2013;9:185–190.

16. Bellin M-F, Van Der Molen AJ. Extracellular gadolinium-based contrast media: An overview. *Eur J Radiol*. 2008;66:160–167.

17. Saraste A, Nekolla S, Schwaiger M. Contrast-enhanced magnetic resonance imaging in the assessment of myocardial infarction and viability. *J Nucl Cardiol*. 2008;15:105–117.

18. Watzinger N, Lund GK, Higgins CB, Wendland MF, Weinmann H-J, Saeed M. The potential of contrast-enhanced magnetic resonance imaging for predicting left ventricular remodeling. *J Magn Reson Imaging*. 2002;16:633–640.

19. Grobner T, Prischl FC. Gadolinium and nephrogenic systemic fibrosis. *Kidney Int*. 2007;72:260–264.

20. Arora P, Vasa P, Brenner D, Iglar K, McFarlane P, Morrison H, Badawi A. Prevalence estimates of chronic kidney disease in Canada: results of a nationally representative survey. *Can Med Assoc J*. 2013;185:E417–E423.

21. Kalra PR, García-Moll X, Zamorano J, Kalra PA, Fox KM, Ford I, Ferrari R, Tardif J-C, Tendera M, Greenlaw N, Ph. Gabriel Steg for the CLARIFY Investigators. Impact of Chronic Kidney Disease on Use of Evidence-Based Therapy in Stable Coronary Artery Disease: A Prospective Analysis of 22,272 Patients. *PLoS ONE*. 2014;9:e102335.

22. McDonald RJ, McDonald JS, Kallmes DF, Jentoft ME, Murray DL, Thielen KR, Williamson EE, Eckel LJ. Intracranial Gadolinium Deposition after Contrast-enhanced MR Imaging. *Radiology*. 2015;275:772–782.

23. Ogawa S, Lee TM, Kay AR, Tank DW. Brain magnetic resonance imaging with contrast dependent on blood oxygenation. *Proc Natl Acad Sci U S A*. 1990;87:9868 –9872.

24. Ogawa S, Lee TM, Nayak AS, Glynn P. Oxygenation-sensitive contrast in magnetic resonance image of rodent brain at high magnetic fields. *Magn Reson Med*. 1990;14:68–78.

25. Krainik A, Hund-Georgiadis M, Zysset S, von Cramon DY. Regional impairment of cerebrovascular reactivity and BOLD signal in adults after stroke. *Stroke*. 2005;36:1146–1152.

26. Mandell DM, Han JS, Poublanc J, Crawley AP, Fierstra J, Tymianski M, Fisher JA, Mikulis DJ. Quantitative Measurement of Cerebrovascular Reactivity by Blood Oxygen Level-Dependent MR Imaging in Patients with Intracranial Stenosis: Preoperative Cerebrovascular Reactivity Predicts the Effect of Extracranial-Intracranial Bypass Surgery. *AJNR Am J Neuroradiol*. 2011;32:721–727.

27. Mutch WAC, Mandell DM, Fisher JA, Mikulis DJ, Crawley AP, Pucci O, Duffin J. Approaches to Brain Stress Testing: BOLD Magnetic Resonance Imaging with Computer-Controlled Delivery of Carbon Dioxide. *PLoS ONE*. 2012;7:e47443.

28. Matthews PM, Honey GD, Bullmore ET. Applications of fMRI in translational medicine and clinical practice. *Nat Rev Neurosci*. 2006;7:732–744.

29. Li L-P, Halter S, Prasad PV. BOLD MRI of the Kidneys. *Magn Reson Imaging Clin N Am*. 2008;16:613–viii.

30. Wacker CM, Bock M, Hartlep AW, Beck G, van Kaick G, Ertl G, Bauer WR, Schad LR. Changes in myocardial oxygenation and perfusion under pharmacological stress with dipyridamole: Assessment using T*2 and T1 measurements. *Magn Reson Med*. 1999;41:686–695.

31. Wacker CM, Hartlep AW, Pfleger S, Schad LR, Ertl G, Bauer WR. Susceptibility-sensitive magnetic resonance imaging detects human myocardium supplied by a stenotic coronary artery without a contrast agent. *J Am Coll Cardiol*. 2003;41:834–840.

32. Bauer WR, Nadler W, Bock M, Schad LR, Wacker C, Hartlep A, Ertl G. The relationship between the BOLD-induced T(2) and T(2)(*): a theoretical approach for the vasculature of myocardium. *Magn Reson Med*. 1999;42:1004–1010.

33. Beache GM, Herzka DA, Boxerman JL, Post WS, Gupta SN, Faranesh AZ, Solaiyappan M, Bottomley PA, Weiss JL, Shapiro EP, Hill MN. Attenuated Myocardial Vasodilator Response in Patients With Hypertensive Hypertrophy Revealed by Oxygenation-Dependent Magnetic Resonance Imaging. *Circulation*. 2001;104:1214–1217.

34. Friedrich MG, Niendorf T, Schulz-Menger J, Gross CM, Dietz R. Blood oxygen level-dependent magnetic resonance imaging in patients with stress-induced angina. *Circulation*. 2003;108:2219–2223.

35. Manka R, Paetsch I, Schnackenburg B, Gebker R, Fleck E, Jahnke C. BOLD cardiovascular magnetic resonance at 3.0 tesla in myocardial ischemia. *J Cardiovasc Magn Reson*. 2010;12:54.

36. Karamitsos TD, Leccisotti L, Arnold JR, Recio-Mayoral A, Bhamra-Ariza P, Howells RK, Searle N, Robson MD, Rimoldi OE, Camici PG, Neubauer S, Selvanayagam JB. Relationship Between Regional Myocardial Oxygenation and Perfusion in Patients With Coronary Artery Disease. Insights From Cardiovascular Magnetic Resonance and Positron Emission Tomography. *Circ Cardiovasc Imaging*. 2010;3:32–40.

37. Walcher T, Manzke R, Hombach V, Rottbauer W, Wöhrle J, Bernhardt P. Myocardial Perfusion Reserve Assessed by T2-Prepared Steady-State Free Precession Blood Oxygen Level–Dependent Magnetic Resonance Imaging in Comparison to Fractional Flow ReserveClinical Perspective. *Circ Cardiovasc Imaging*. 2012;5:580–586.

38. Luu JM, Friedrich MG, Harker J, Dwyer N, Guensch D, Mikami Y, Faris P, Hare JL. Relationship of vasodilator-induced changes in myocardial oxygenation with the severity of coronary artery stenosis: a study using oxygenation-sensitive cardiovascular magnetic resonance. *Eur Heart J Cardiovasc Imaging*. 2014;15:1358–1367.

39. Arnold JR, Karamitsos TD, Bhamra-Ariza P, Francis JM, Searle N, Robson MD, Howells RK, Choudhury RP, Rimoldi OE, Camici PG, Banning AP, Neubauer S, Jerosch-Herold M, Selvanayagam JB. Myocardial Oxygenation in Coronary Artery Disease: Insights From Blood Oxygen Level–Dependent Magnetic Resonance Imaging at 3 Tesla. *Am J Cardiol*. 2012;59:1954–1964.

40. Jahnke C, Gebker R, Manka R, Schnackenburg B, Fleck E, Paetsch I. Navigator-Gated 3D Blood Oxygen Level–Dependent CMR at 3.0-T for Detection of Stress-Induced Myocardial Ischemic Reactions. *J Am Coll Cardiol Img*. 2010;3:375–384.

41. Bernhardt P, Walcher T, Rottbauer W, Wöhrle J. Quantification of myocardial perfusion reserve at 1.5 and 3.0 Tesla: a comparison to fractional flow reserve. *Int J Cardiovasc Imaging*. 2012;

42. Karamitsos TD, Arnold JR, Pegg TJ, Francis JM, Birks J, Jerosch-Herold M, Neubauer S, Selvanayagam JB. Patients With Syndrome X Have Normal Transmural Myocardial Perfusion and Oxygenation A 3-T Cardiovascular Magnetic Resonance Imaging Study. *Circ Cardiovasc Imaging*. 2012;5:194–200.

43. Karamitsos TD, Dass S, Suttie J, Sever E, Birks J, Holloway CJ, Robson MD, Jerosch-Herold M, Watkins H, Neubauer S. Blunted Myocardial Oxygenation Response During Vasodilator Stress in Patients With Hypertrophic Cardiomyopathy. *Journal of the American College of Cardiology*. 2013;61:1169–1176.

44. Roubille F, Fischer K, Guensch DP, Tardif J-C, Friedrich MG. Impact of Hyperventilation and Apnea on Myocardial Oxygenation in Patients With Obstructive Sleep Apnea – an Oxygenation-Sensitive CMR Study. *J Cardiol*. 2016;

45. Levelt E, Rodgers CT, Clarke WT, Mahmod M, Ariga R, Francis JM, Liu A, Wijesurendra RS, Dass S, Sabharwal N, Robson MD, Holloway CJ, Rider OJ, Clarke K, Karamitsos TD, Neubauer S. Cardiac energetics, oxygenation, and perfusion during increased workload in patients with type 2 diabetes mellitus. *European Heart Journal*. 2015;ehv442.

46. Parnham S, Gleadle JM, Bangalore S, Grover S, Perry R, Woodman RJ, Pasquale CGD, Selvanayagam JB. Impaired Myocardial Oxygenation Response to Stress in Patients With Chronic Kidney Disease. *J Am Heart Assoc*. 2015;4:e002249.

47. Fischer K, Guensch DP, Friedrich MG. Response of myocardial oxygenation to breathing manoeuvres and adenosine infusion. *Eur Heart J Cardiovasc Imaging*. 2015;395–401.

48. Karamitsos TD, Leccisotti L, Arnold JR, Recio-Mayoral A, Bhamra-Ariza P, Howells RK, Searle N, Robson MD, Rimoldi OE, Camici PG, Neubauer S, Selvanayagam JB. Relationship between Regional Myocardial Oxygenation and Perfusion in Patients with Coronary Artery Disease: Insights from Cardiovascular Magnetic Resonance and Positron Emission Tomography. *Circ Cardiovasc Imaging*. 2010;3:32–40.

49. Bauer WR, Nadler W, Bock M, Schad LR, Wacker C, Hartlep A, Ertl G. Theory of Coherent and Incoherent Nuclear Spin Dephasing in the Heart. *Phys Rev Lett*. 1999;83:4215–4218.

50. Thulborn KR, Waterton JC, Matthews PM, Radda GK. Oxygenation dependence of the transverse relaxation time of water protons in whole blood at high field. *Biochim Biophys Acta*. 1982;714:265–270.

51. Toronov V, Walker S, Gupta R, Choi JH, Gratton E, Hueber D, Webb A. The roles of changes in deoxyhemoglobin concentration and regional cerebral blood volume in the fMRI BOLD signal. *NeuroImage*. 2003;19:1521–1531.

52. Gödecke A. Myoglobin: safeguard of myocardial oxygen supply during systolic compression? *Cardiovascular Research*. 2010;87:4–5.

53. Meeson AP, Radford N, Shelton JM, Mammen PPA, DiMaio JM, Hutcheson K, Kong Y, Elterman J, Williams RS, Garry DJ. Adaptive Mechanisms That Preserve Cardiac Function in Mice Without Myoglobin. *Circ Res*. 2001;88:713–720.

54. Endeward V, Gros G, Jürgens KD. Significance of myoglobin as an oxygen store and oxygen transporter in the intermittently perfused human heart: a model study. *Cardiovasc Res*. 2010;87:22–29.

55. Lin P-C, Kreutzer U, Jue T. Myoglobin translational diffusion in rat myocardium and its implication on intracellular oxygen transport. *J Physiol (Lond)*. 2007;578:595–603.

56. Stoker ME, Gerdes AM, May JF. Regional differences in capillary density and myocyte size in the normal human heart. *Anat Rec*. 1982;202:187–191.

57. Shimoni S, Frangogiannis NG, Aggeli CJ, Shan K, Quinones MA, Espada R, Letsou GV, Lawrie GM, Winters WL, Reardon MJ, Zoghbi WA. Microvascular structural correlates of myocardial contrast echocardiography in patients with coronary artery disease and left ventricular dysfunction: implications for the assessment of myocardial hibernation. *Circulation*. 2002;106:950–956.

58. Lanza GA, Crea F. Primary Coronary Microvascular Dysfunction Clinical Presentation, Pathophysiology, and Management. *Circulation*. 2010;121:2317–2325.

59. Hoffman JI. Transmural myocardial perfusion. *Prog Cardiovasc Dis*. 1987;29:429–464.

60. Algranati D, Kassab GS, Lanir Y. Why is the subendocardium more vulnerable to ischemia? A new paradigm. *Am J Physiol Heart Circ Physiol*. 2011;300:H1090–H1100.

61. Schwartzkopff B, Mundhenke M, Strauer BE. Alterations of the Architecture of Subendocardial Arterioles in Patients With Hypertrophic Cardiomyopathy and Impaired Coronary Vasodilator Reserve: A Possible Cause for Myocardial Ischemia 1. *Journal of the American College of Cardiology*. 1998;31:1089–1096.

62. Scheeren TWL, Schober P, Schwarte LA. Monitoring tissue oxygenation by near infrared spectroscopy (NIRS): background and current applications. *J Clin Monit Comput*. 2012;26:279–287.

63. Li D, Dhawale P, Rubin PJ, Haacke EM, Gropler RJ. Myocardial signal response to dipyridamole and dobutamine: Demonstration of the BOLD effect using a double-echo gradient-echo sequence. *Magnetic Resonance in Medicine*. 1996;36:16–20.

64. Grubbström J, Berglund B, Kaijser L. Myocardial oxygen supply and lactate metabolism during marked arterial hypoxaemia. *Acta Physiologica Scandinavica*. 1993;149:303–310.

65. Colin P, Ghaleh B, Monnet X, Su J, Hittinger L, Giudicelli J-F, Berdeaux A. Contributions of heart rate and contractility to myocardial oxygen balance during exercise. *American Journal of Physiology - Heart and Circulatory Physiology*. 2003;284:H676–H682.

66. Schook LB, Tumbleson ME. Advances in Swine in Biomedical Research. Springer Science & Business Media; 1997.

67. Friedrich MG, Karamitsos TD. Oxygenation-sensitive cardiovascular magnetic resonance. *J Cardiovasc Magn Reson*. 2013;15:43.

68. Vohringer M, Flewitt J, Green J, Dharmakumar R, Wang J, Tyberg J, Friedrich M. Oxygenation-sensitive CMR for assessing vasodilator-induced changes of myocardial oxygenation. *J Cardiovasc Magn Reson*. 2010;12:20.

69. Adenosine Side Effects in Detail - Drugs.com [Internet]. [cited 2013 Nov 27];Available from: http://www.drugs.com/sfx/adenosine-side-effects.html

70. Commissioner O of the. Safety Alerts for Human Medical Products - Lexiscan (regadenoson) and Adenoscan (adenosine): Drug Safety Communication - Rare but Serious Risk of Heart Attack and Death [Internet]. [cited 2014 May 20];Available from: http://www.fda.gov/Safety/MedWatch/SafetyInformation/SafetyAlertsforHumanMedicalProducts/ucm375981.htm

71. Kastrup A, Li T-Q, Takahashi A, Glover GH, Moseley ME. Functional Magnetic Resonance Imaging of Regional Cerebral Blood Oxygenation Changes During Breath Holding. *Stroke*. 1998;29:2641–2645.

72. Handwerker DA, Gazzaley A, Inglis BA, D'Esposito M. Reducing vascular variability of fMRI data across aging populations using a breathholding task. *Hum Brain Mapp*. 2007;28:846–859.

73. Hsu Y-Y, Kuan W-C, Lim K-E, Liu H-L. Breathhold-regulated blood oxygenation level-dependent (BOLD) MRI of human brain at 3 tesla. *J Magn Reson Imaging*. 2010;31:78–84.

74. Liu H.-L, Huang J.-C, Wu C-T., Hsu Y-Y. Detectability of blood oxygenation level-dependent signal changes during short breath hold duration. *Magn Reson Imaging*. 2002;20:643–648.

75. Vazquez AL, Cohen ER, Gulani V, Hernandez-Garcia L, Zheng Y, Lee GR, Kim S-G, Grotberg JB, Noll DC. Vascular dynamics and BOLD fMRI: CBF level effects and analysis considerations. *NeuroImage*. 2006;32:1642–1655.

76. Chen JJ, Pike GB. Global cerebral oxidative metabolism during hypercapnia and hypocapnia in humans: implications for BOLD fMRI. *J Cereb Blood Flow Metab*. 2010;30:1094–1099.

77. Gauthier CJ, Madjar C, Tancredi FB, Stefanovic B, Hoge RD. Elimination of visually evoked BOLD responses during carbogen inhalation: implications for calibrated MRI. *Neuroimage*. 2011;54:1001–1011.

78. Sicard KM, Duong TQ. Effects of hypoxia, hyperoxia, and hypercapnia on baseline and stimulus-evoked BOLD, CBF, and CMRO2 in spontaneously breathing animals. *Neuroimage*. 2005;25:850–858.

79. Geranmayeh F, Wise RJS, Leech R, Murphy K. Measuring vascular reactivity with breath-holds after stroke: A method to aid interpretation of group-level BOLD signal changes in longitudinal fMRI studies. *Hum Brain Mapp*. 2015;36:1755–1771.

80. Glodzik L, Randall C, Rusinek H, de Leon MJ. Cerebrovascular reactivity to carbon dioxide in Alzheimer's disease. A review. *J Alzheimers Dis*. 2013;35:427–440.

81. Thomason ME, Burrows BE, Gabrieli JDE, Glover GH. Breath holding reveals differences in fMRI BOLD signal in children and adults. *Neuroimage*. 2005;25:824–837.

82. Guensch DP, Fischer K, Flewitt JA, Friedrich MG. Impact of Intermittent Apnea on Myocardial Tissue Oxygenation—A Study Using Oxygenation-Sensitive Cardiovascular Magnetic Resonance. *PLoS ONE*. 2013;8:e53282.

83. Guensch DP, Fischer K, Flewitt JA, Yu J, Lukic R, Friedrich JA, Friedrich MG. Breathing manoeuvre-dependent changes in myocardial oxygenation in healthy humans. *Eur Heart J Cardiovasc Imaging*. 2014;15:409–414.

84. Sasse SA, Berry RB, Nguyen TK, Light RW, Mahutte CK. Arterial blood gas changes during breath-holding from functional residual capacity. *Chest*. 1996;110:958–964.

85. Klocke FJ, Rahn H. Breath holding after breathing of oxygen. *J Appl Physiol*. 1959;14:689–693.

86. Parkes MJ. Breath-holding and its breakpoint. *Exp Physiol*. 2006;91:1–15.

87. Chiarelli PA, Bulte DP, Wise R, Gallichan D, Jezzard P. A calibration method for quantitative BOLD fMRI based on hyperoxia. *NeuroImage*. 2007;37:808–820.

88. Roubille F, Fisher K, Guensch D, Cloutier I, Tardif J, Friedrich M. Is There a Different Response to Hypoxia in Patients With Sleep Apnea Syndrome Compared to Healthy Volunteers Assessed With Oxygenation Sensitive CMR? [Abstract]. *Can J Cardiol*. 2013;29:S272–S272.

89. Nadeshalingam G, Guensch DP, Fischer K, Friedrich MG. The relationship of hemoglobin concentration and signal intensity changes in oxygenation-sensitive cardiovascular magnetic resonance imaging [Abstract]. *J Cardiovasc Magn Reson*. 2015;17:Q110.

90. Teixeira T, Nadeshalingam G, Marcotte F, Friedrich MG. Breathing maneuvers as a metabolic coronary vasodilator for first-pass perfusion MR imaging [Abstract]. *J Cardiovasc Magn Reson*. 2015;17:Q115.

91. Hellems HK, Ord JW, Talmers FN, Christensen RC. Effects of hypoxia on coronary blood flow and myocardial metabolism in normal human subjects. *Circulation*. 1957;16:893–893.

92. Wyss CA, Koepfli P, Fretz G, Seebauer M, Schirlo C, Kaufmann PA. Influence of Altitude Exposure on Coronary Flow Reserve. *Circulation*. 2003;108:1202–1207.

93. Beaudin AE, Brugniaux JV, Vöhringer M, Flewitt J, Green JD, Friedrich MG, Poulin MJ. Cerebral and myocardial blood flow responses to hypercapnia and hypoxia in humans. *Am J Physiol Heart Circ Physiol*. 2011;301:H1678–H1686.

94. McNulty PH, King N, Scott S, Hartman G, McCann J, Kozak M, Chambers CE, Demers LM, Sinoway LI. Effects of supplemental oxygen administration on coronary blood flow in patients undergoing cardiac catheterization. *Am J Physiol Heart Circ Physiol*. 2005;288:H1057–H1062.

95. Kilgannon J, Jones AE, Shapiro NI, et al. Association between arterial hyperoxia following resuscitation from cardiac arrest and in-hospital mortality. \iJAMA. 2010;303:2165–2171.

96. Stub D, Smith K, Bernard S, Nehme Z, Stephenson M, Bray JE, Cameron P, Barger B, Ellims AH, Taylor AJ, Meredith IT, Kaye DM. Air Versus Oxygen in ST-Segment Elevation Myocardial Infarction. *Circulation*. 2015;e114.014494.

97. Beaudin AE, Brugniaux JV, Vöhringer M, Flewitt J, Green JD, Friedrich MG, Poulin MJ. Cerebral and myocardial blood flow responses to hypercapnia and hypoxia in humans. *Am J Physiol Heart Circ Physiol*. 2011;301:H1678–H1686.

98. Case RB, Greenberg H. The response of canine coronary vascular resistance to local alterations in coronary arterial P CO2. *Circulation Research*. 1976;39:558–566.

99. Shoemaker JK, Vovk A, Cunningham DA. Peripheral chemoreceptor contributions to sympathetic and cardiovascular responses during hypercapnia. *Can J Physiol Pharmacol*. 2002;80:1136–1144.

100. Yang H-J, Yumul R, Tang R, Cokic I, Klein M, Kali A, Sobczyk O, Sharif B, Tang J, Bi X, Tsaftaris SA, Li D, Conte AH, Fisher JA, Dharmakumar R. Assessment of Myocardial Reactivity to Controlled Hypercapnia with Free-breathing T2-prepared Cardiac Blood Oxygen Level–Dependent MR Imaging. *Radiology*. 2014;272:397–406.

101. Broten TP, Romson JL, Fullerton DA, Van Winkle DM, Feigl EO. Synergistic action of myocardial oxygen and carbon dioxide in controlling coronary blood flow. *Circ Res*. 1991;68:531–542.

102. Camici PG, Crea F. Coronary microvascular dysfunction. *N Engl J Med*. 2007;356:830–840.

103. Maseri A, Crea F, Kaski JC, Crake T. Mechanisms of angina pectoris in syndrome X. *J Am Coll Cardiol*. 1991;17:499–506.

104. Powers ER, Bannerman KS, Fitz-James I, Cannon PJ. Effect of elevations of coronary artery partial pressure of carbon dioxide (Pco2) on coronary blood flow. *J Am Coll Cardiol*. 1986;8:1175–1181.

105. Berne RM. The role of adenosine in the regulation of coronary blood flow. *Circ Res*. 1980;47:807–813.

106. Shryock JC, Belardinelli L. Adenosine and Adenosine Receptors in the Cardiovascular System: Biochemistry, Physiology, and Pharmacology. *Am J Cardiol*. 1997;79:2–10.

107. Case RB, Greenberg H. The response of canine coronary vascular resistance to local alterations in coronary arterial P CO2. *Circ Res*. 1976;39:558–566.

108. Case RB, Greenberg H, Moskowitz R. Alterations in coronary sinus pO2 and O2 saturation resulting from pCO2 changes. *Cardiovasc Res*. 1975;9:167–177.

109. Atkins JL, Johnson KB, Pearce FJ. Cardiovascular responses to oxygen inhalation after hemorrhage in anesthetized rats: hyperoxic vasoconstriction. *Am J Physiol Heart Circ Physiol*. 2007;292:H776–H785.

110. Neill W, Hattenhauer M. Impairment of myocardial O2 supply due to hyperventilation. *Circulation*. 1975;52:854 –858.

111. Stalder AF, Schmidt M, Greiser A, Speier P, Guehring J, Friedrich MG, Mueller E. Robust cardiac BOLD MRI using an fMRI-like approach with repeated stress paradigms. *Magn Reson Med*. 2015;73:577–85.

112. Guensch DP, Fischer K, Flewitt JA, Friedrich MG. Myocardial oxygenation is maintained during hypoxia when combined with apnea – a cardiovascular MR study. *Physiol Rep*. 2013;1:e00098.

113. Karmazyn M. Myocardial Ischemia: Mechanisms, Reperfusion, Protection. Birkhäuser; 2013.

114. Schultz HD, Li YL, Ding Y. Arterial Chemoreceptors and Sympathetic Nerve Activity Implications for Hypertension and Heart Failure. *Hypertension*. 2007;50:6–13.

115. Mouren S, Souktani R, Beaussier M, Abdenour L, Arthaud M, Duvelleroy M, Vicaut E. Mechanisms of coronary vasoconstriction induced by high arterial oxygen tension. *Am J Physiol*. 1997;272:H67–75.

116. Jamieson D, Chance B, Cadenas E, Boveris A. The relation of free radical production to hyperoxia. *Annu Rev Physiol*. 1986;48:703–719.

117. Baron JF, Vicaut E, Hou X, Duvelleroy M. Independent role of arterial O2 tension in local control of coronary blood flow. *Am J Physiol*. 1990;258:H1388–1394.

118. Lammerant J, Schryver CD, Becsei I, Camphyn M, Mertens-Strijthagen J. Coronary circulation response to hyperoxia after vagotomy and combined alpha and beta adrenergic receptors blockade in the anesthetized intact dog. *Pflugers Arch*. 1969;308:185–196.

119. McNulty PH, Robertson BJ, Tulli MA, Hess J, Harach LA, Scott S, Sinoway LI. Effect of hyperoxia and vitamin C on coronary blood flow in patients with ischemic heart disease. *J Appl Physiol*. 2007;102:2040–2045.

120. Ramanathan T, Skinner H. Coronary Blood Flow. *Contin Educ Anaesth Crit Care Pain*. 2005;5:61–64.

121. Deussen A, Ohanyan V, Jannasch A, Yin L, Chilian W. Mechanisms of metabolic coronary flow regulation. *Journal of Molecular and Cellular Cardiology*. 2012;52:794–801.

122. Beyer AM, Gutterman DD. Regulation of the human coronary microcirculation. *Journal of Molecular and Cellular Cardiology*. 2012;52:814–821.

123. Shepherd JT. The lungs as receptor sites for cardiovascular regulation. *Circulation*. 1981;63:1–10.

124. Heusser K, Dzamonja G, Tank J, Palada I, Valic Z, Bakovic D, Obad A, Ivancev V, Breskovic T, Diedrich A, Joyner MJ, Luft FC, Jordan J, Dujic Z. Cardiovascular Regulation During Apnea in Elite Divers. *Hypertension*. 2009;53:719–724.

125. Fagius J, Sundlöf G. The diving response in man: effects on sympathetic activity in muscle and skin nerve fascicles. *J Physiol*. 1986;377:429–443.

126. Patel MR, Peterson ED, Dai D, Brennan JM, Redberg RF, Anderson HV, Brindis RG, Douglas PS. Low Diagnostic Yield of Elective Coronary Angiography. *N Engl J Med*. 2010;362:886–895.

127. Pepine CJ, Ferdinand KC, Shaw LJ, Light-McGroary KA, Shah RU, Gulati M, Duvernoy C, Walsh MN, Bairey Merz CN. Emergence of Nonobstructive Coronary Artery DiseaseA Woman's Problem and Need for Change in Definition on Angiography. *J Am Coll Cardiol*. 2015;66:1918–1933.

128. Agrawal S, Mehta PK, Merz CNB. Cardiac Syndrome X – Update 2014. *Cardiol Clin*. 2014;32:463–478.

129. Jespersen L, Hvelplund A, Abildstrøm SZ, Pedersen F, Galatius S, Madsen JK, Jørgensen E, Kelbæk H, Prescott E. Stable angina pectoris with no obstructive coronary artery disease is associated with increased risks of major adverse cardiovascular events. *Eur Heart J*. 2012;33:734–744.

130. Crea F, Camici PG, Bairey Merz CN. Coronary microvascular dysfunction: an update. *Eur Heart J*. 2014;35:1101–1111.

131. Uren NG, Crake T, Lefroy DC, De Silva R, Davies GJ, Maseri A. Delayed recovery of coronary resistive vessel function after coronary angioplasty. *J Am Coll Cardiol*. 1993;21:612–621.

132. Gibson CM, Cannon CP, Murphy SA, Ryan KA, Mesley R, Marble SJ, McCabe CH, Werf FV de, Braunwald E, Group for the T (Thrombolysis IMIS. Relationship of TIMI Myocardial Perfusion Grade to Mortality After Administration of Thrombolytic Drugs. *Circulation*. 2000;101:125–130.

133. Amier RP, Teunissen PFA, Marques KM, Knaapen P, Royen N van. Invasive measurement of coronary microvascular resistance in patients with acute myocardial infarction treated by primary PCI. *Heart*. 2014;100:13–20.

134. Gerber BL, Raman SV, Nayak K, Epstein FH, Ferreira P, Axel L, Kraitchman DL. Myocardial first-pass perfusion cardiovascular magnetic resonance: history, theory, and current state of the art. *J Cardiovasc Magn Reson*. 2008;10:18.

135. Guensch DP, Friedrich MG. Novel Approaches to Myocardial Perfusion: 3D First-Pass CMR Perfusion Imaging and Oxygenation-Sensitive CMR. *Curr Cardiovasc Imaging Rep*. 2014;7:1–6.

136. Guensch DP, Fischer K, Shie N, Lebel J, Friedrich MG. Hyperoxia Exacerbates Myocardial Ischemia in the Presence of Acute Coronary Artery Stenosis in Swine. *Circ Cardiovasc Interv*. 2015;8:e002928.

137. Kahn CM, Line S, Allen DG. The Merck veterinary manual. Merck Whitehouse Station, NJ; 2010.

138. Tanguay J-F, Hammoud T, Geoffroy P, Merhi Y. Chronic Platelet and Neutrophil Adhesion: A Causal Role for Neointimal Hyperplasia in In-Stent Restenosis. *J Endovasc Ther*. 2003;10:968–977.

139. Wilson R, Wyche K, Christensen B, Zimmer S, Laxson D. Effects of adenosine on human coronary arterial circulation. *Circulation*. 1990;82:1595 –1606.

140. Seiler C, Fleisch M, Meier B. Direct Intracoronary Evidence of Collateral Steal in Humans. *Circulation*. 1997;96:4261–4267.

141. Chareonthaitawee P, Kaufmann PA, Rimoldi O, Camici PG. Heterogeneity of resting and hyperemic myocardial blood flow in healthy humans. *Cardiovasc Res*. 2001;50:151–161.

142. Ha J-Y, Lee Y-C, Park S-J, Jang Y-H, Kim J-H. Remifentanil postconditioning has cross talk with adenosine receptors in the ischemic-reperfused rat heart. *J Surg Res*. 2015;195:37–43.

143. Breskovic T, Lojpur M, Maslov PZ, Cross TJ, Kraljevic J, Ljubkovic M, Marinovic J, Ivancev V, Johnson BD, Dujic Z. The influence of varying inspired fractions of O2 and CO2 on the development of involuntary breathing movements during maximal apnoea. *Respir Physiol Neurobiol*. 2012;181:228–233.

144. Taqueti VR, Hachamovitch R, Murthy VL, Naya M, Foster CR, Hainer J, Dorbala S, Blankstein R, Di Carli MF. Global coronary flow reserve is associated with adverse cardiovascular events independently of luminal angiographic severity and modifies the effect of early revascularization. *Circulation*. 2015;131:19–27.

145. Tousoulis D, Antoniades C, Stefanadis C. Evaluating endothelial function in humans: a guide to invasive and non-invasive techniques. *Heart*. 2005;91:553–558.

146. Pries AR, Habazettl H, Ambrosio G, Hansen PR, Kaski JC, Schächinger V, Tillmanns H, Vassalli G, Tritto I, Weis M, Wit C de, Bugiardini R. A review of methods for assessment of coronary microvascular disease in both clinical and experimental settings. *Cardiovasc Res*. 2008;80:165–174.

147. Powers ER, Bannerman KS, Fitz-James I, Cannon PJ. Effect of elevations of coronary artery partial pressure of carbon dioxide (Pco2) on coronary blood flow. *J Am Coll Cardiol*. 1986;8:1175–1181.

148. Farquhar H, Weatherall M, Wijesinghe M, Perrin K, Ranchord A, Simmonds M, Beasley R. Systematic review of studies of the effect of hyperoxia on coronary blood flow. *Am Heart J*. 2009;158:371–377.

149. Reller MD, Morton MJ, Giraud GD, Wu DE, Thornburg KL. Maximal myocardial blood flow is enhanced by chronic hypoxemia in late gestation fetal sheep. *Am J Physiol Heart Circ Physiol*. 1992;263:H1327–H1329.

150. Foster GE, Sheel AW. The human diving response, its function, and its control. *Scand J Med Sci Spor*. 2005;15:3–12.

151. Crystal GJ. Carbon Dioxide and the Heart: Physiology and Clinical Implications. *Anesth Analg*. 2015;121:610–623.

152. Broten TP, Feigl EO. Role of myocardial oxygen and carbon dioxide in coronary autoregulation. *Am J Physiol Heart Circ Physiol*. 1992;262:H1231–H1237.

153. Hardie JA, Vollmer WM, Buist AS, Ellingsen I, Mørkve O. Reference values for arterial blood gases in the elderly. *Chest*. 2004;125:2053–2060.

154. Coleman MD. Chapter 2 - Respiratory and Pulmonary Physiology A2 - Duke, James. In: Anesthesia Secrets (Fourth Edition). Philadelphia: Mosby; 2011. p. 17–23.

155. Ganz W, Donoso R, Marcus H, Swan HJC. Coronary Hemodynamics and Myocardial Oxygen Metabolism during Oxygen Breathing in Patients with and without Coronary Artery Disease. *Circulation*. 1972;45:763–768.

156. Konishi M, Akiyama E, Iwahashi N, Ebina T, Kimura K. Hypercapnia in Acute Heart Failure Patients with or Without Pulmonary Edema. *Journal of Cardiac Failure*. 2014;20:S168.

157. Kety SS, Schmidt CF. The effects of active and passive hyperventilation on cerebral blood flow, cerebral oxygen consumption, cardiac output, and blood pressure of normal young men. *J Clin Invest*. 1946;25:107–119.

158. Moradkhan R, Sinoway LI. Revisiting the Role of Oxygen Therapy in Cardiac Patients. *J Am Coll Cardiol*. 2010;56:1013–1016.

159. Peberdy MA, Callaway CW, Neumar RW, Geocadin RG, Zimmerman JL, Donnino M, Gabrielli A, Silvers SM, Zaritsky AL, Merchant R, Hoek TLV, Kronick SL. Part 9: Post–Cardiac Arrest Care 2010 American Heart Association Guidelines for Cardiopulmonary Resuscitation and Emergency Cardiovascular Care. *Circulation*. 2010;122:S768–S786.

160. Liu Y, Rosenthal RE, Haywood Y, Miljkovic-Lolic M, Vanderhoek JY, Fiskum G. Normoxic Ventilation After Cardiac Arrest Reduces Oxidation of Brain Lipids and Improves Neurological Outcome. *Stroke*. 1998;29:1679–1686.

161. Vereczki V, Martin E, Rosenthal RE, Hof PR, Hoffman GE, Fiskum G. Normoxic resuscitation after cardiac arrest protects against hippocampal oxidative stress, metabolic dysfunction, and neuronal death. *J Cereb Blood Flow Metab*. 2005;26:821–835.

162. Friedrich MG, Karamitsos TD. Oxygenation-sensitive cardiovascular magnetic resonance. *J Cardiovasc Magn Reson*. 2013;15:43.

163. Maroko PR, Radvany P, Braunwald E, Hale SL. Reduction of infarct size by oxygen inhalation following acute coronary occlusion. *Circulation*. 1975;52:360–368.

164. Madias JE, Hood WB. Reduction of precordial ST-segment elevation in patients with anterior myocardial infarction by oxygen breathing. *Circulation*. 1976;53:I198–200.

165. Rawles JM, Kenmure AC. Controlled trial of oxygen in uncomplicated myocardial infarction. *Br Med J*. 1976;1:1121–1123.

166. Loeb HS, Chuquimia R, Sinno MZ, Rahimtoola SH, Rosen KM, Gunnar RM. Effects of low-flow oxygen on the hemodynamics and left ventricular function in patients with uncomplicated acute myocardial infarction. *Chest*. 1971;60:352–355.

167. Burls A, Cabello JB, Emparanza JI, Bayliss S, Quinn T. Oxygen therapy for acute myocardial infarction: a systematic review and meta-analysis. *Emerg Med J*. 2011;28:917–923.

168. Cabello JB, Burls A, Emparanza JI, Bayliss S, Quinn T. Oxygen therapy for acute myocardial infarction. *Cochrane Database Syst Rev*. 2013;8:CD007160.

169. Mak S, Egri Z, Tanna G, Colman R, Newton GE. Vitamin C prevents hyperoxia-mediated vasoconstriction and impairment of endothelium-dependent vasodilation. *Am J Physiol Heart Circ Physiol*. 2002;282:H2414–2421.

170. Nanobashvili J, Neumayer C, Fuegl A, Punz A, Blumer R, Mittlböck M, Prager M, Polterauer P, Dobrucki LW, Huk I, Malinski T. Combined L-arginine and antioxidative vitamin treatment mollifies ischemia-reperfusion injury of skeletal muscle. *J Vasc Surg*. 2004;39:868–877.

171. Welsh DG, Jackson WF, Segal SS. Oxygen induces electromechanical coupling in arteriolar smooth muscle cells: a role for L-type Ca2+ channels. *Am J Physiol*. 1998;274:H2018–2024.

172. Tune JD, Richmond KN, Gorman MW, Feigl EO. Control of coronary blood flow during exercise. *Exp Biol Med (Maywood)*. 2002;227:238–250.

173. Farquhar H, Weatherall M, Wijesinghe M, Perrin K, Ranchord A, Simmonds M, Beasley R. Systematic review of studies of the effect of hyperoxia on coronary blood flow. *Am Heart J*. 2009;158:371–377.

174. Caldeira D, Vaz-Carneiro A, Costa J. Cochrane Corner: What is the clinical impact of oxygen therapy for acute myocardial infarction? Evaluation of a Cochrane systematic review. *Rev Port Cardiol*. 2014;33:641–643.

175. Zwemer CF, Whitesall SE, D'Alecy LG. Cardiopulmonary-cerebral resuscitation with 100% oxygen exacerbates neurological dysfunction following nine minutes of normothermic cardiac arrest in dogs. *Resuscitation*. 1994;27:159–170.

176. Richards EM, Fiskum G, Rosenthal RE, Hopkins I, McKenna MC. Hyperoxic Reperfusion After Global Ischemia Decreases Hippocampal Energy Metabolism. *Stroke*. 2007;38:1578–1584.

177. Bellomo R, Bailey M, Eastwood GM, Nichol A, Pilcher D, Hart GK, Reade MC, Egi M, Cooper DJ, Study of Oxygen in Critical Care (SOCC) Group. Arterial hyperoxia and in-hospital mortality after resuscitation from cardiac arrest. *Crit Care*. 2011;15:R90.

178. Wang C-H, Chang W-T, Huang C-H, Tsai M-S, Yu P-H, Wang A-Y, Chen N-C, Chen W-J. The effect of hyperoxia on survival following adult cardiac arrest: a systematic review and meta-analysis of observational studies. *Resuscitation*. 2014;85:1142–1148.

179. Meyhoff CS, Jorgensen LN, Wetterslev J, Christensen KB, Rasmussen LS, PROXI Trial Group. Increased long-term mortality after a high perioperative inspiratory oxygen fraction during abdominal surgery: follow-up of a randomized clinical trial. *Anesth Analg*. 2012;115:849–854.

180. Tonino PAL, De Bruyne B, Pijls NHJ, Siebert U, Ikeno F, van `t Veer M, Klauss V, Manoharan G, Engstrøm T, Oldroyd KG, Ver Lee PN, MacCarthy PA, Fearon WF. Fractional Flow Reserve versus Angiography for Guiding Percutaneous Coronary Intervention. *N Engl J Med*. 2009;360:213–224.

181. Lindbom L, Tuma RF, Arfors KE. Influence of oxygen on perfused capillary density and capillary red cell velocity in rabbit skeletal muscle. *Microvasc Res*. 1980;19:197–208.

182. Lindbom L, Arfors KE. Mechanisms and site of control for variation in the number of perfused capillaries in skeletal muscle. *Int J Microcirc Clin Exp*. 1985;4:19–30.

183. Reinhart K, Bloos F, König F, Bredle D, Hannemann L. Reversible decrease of oxygen consumption by hyperoxia. *Chest*. 1991;99:690–694.

184. Weaver ME, Pantely GA, Bristow JD, Ladley HD. A quantitative study of the anatomy and distribution of coronary arteries in swine in comparison with other animals and man. *Cardiovasc Res*. 1986;20:907–917.

185. Weaver ME, Pantely GA, Bristow JD, Ladley HD. A quantitative study of the anatomy and distribution of coronary arteries in swine in comparison with other animals and man. *Cardiovasc Res*. 1986;20:907 – 917.

186. Ambrose JA, Singh M. Pathophysiology of coronary artery disease leading to acute coronary syndromes. *F1000Prime Rep* [Internet]. 2015 [cited 2016 Jun 15];7. Available from: http://www.ncbi.nlm.nih.gov/pmc/articles/PMC4311268/

187. Pasotti M, Prati F, Arbustini E. The pathology of myocardial infarction in the pre- and post-interventional era. *Heart*. 2006;92:1552–1556.

188. Rogers T, Lederman RJ. Interventional CMR: Clinical Applications and Future Directions. *Curr Cardiol Rep*. 2015;17:31.

189. Stephan H, Sonntag H, Schenk HD, Kettler D, Khambatta HJ. Effects of propofol on cardiovascular dynamics, myocardial blood flow and myocardial metabolism in patients with coronary artery disease. *Br J Anaesth*. 1986;58:969–975.

190. Kazmaier S, Hanekop G-G, Buhre W, Weyland A, Busch T, O. C. Radke, Zoelffel R, Sonntag H. Myocardial consequences of remifentanil in patients with coronary artery disease. *Br J Anaesth*. 2000;84:578–583.

191. Patel SS, Spencer CM. Remifentanil. *Drugs*. 1996;52:417–427; discussion 428.

192. Diprivan (Propofol) Drug Information: Clinical Pharmacology - Prescribing Information at RxList [Internet]. RxList. [cited 2016 Jun 13];Available from: http://www.rxlist.com/diprivan-drug/clinical-pharmacology.htm

193. Zhang Y, Irwin MG, Wong TM. Remifentanil preconditioning protects against ischemic injury in the intact rat heart. *Anesthesiology*. 2004;101:918–923.

194. Guensch DP. Myocardial blood flow reflects myocardial oxygenation in healthy swine. *Journal of Cardiothoracic and Vascular Anesthesia*. 2015;29:S36.

195. Runsiö M, Bergfeldt L, Rosenqvist M, Owall A, Jorfeldt L. Changes in human coronary sinus blood flow and myocardial metabolism induced by ventricular fibrillation and defibrillation. *Journal of Cardiothoracic and Vascular Anesthesia*. 1998;12:45–50.

196. Vretzakis G, Ferdi E, Papaziogas B, Dragoumanis C, Pneumatikos J, Tsangaris I, Tsakiridis K, Konstantinou F. Coronary sinus venoarterial CO2 difference in different hemodynamic states. *Acta Anaesthesiol Belg*. 2004;55:221–227.

197. Zoghbi GJ, Iskandrian AE. Selective adenosine agonists and myocardial perfusion imaging. *J Nucl Cardiol*. 2012;19:126–141.

198. Posse S, Olthoff U, Weckesser M, Müller-Gärtner HW, Dager SR. Regional dynamic signal changes during controlled hyperventilation assessed with blood oxygen level-dependent functional MR imaging. *AJNR Am J Neuroradiol*. 1997;18:1763–1770.

199. Fieno DS, Shea SM, Li Y, Harris KR, Finn JP, Li D. Myocardial Perfusion Imaging Based on the Blood Oxygen Level–Dependent Effect Using T2-Prepared Steady-State Free-Precession Magnetic Resonance Imaging. *Circulation*. 2004;110:1284–1290.

200. McCommis KS, O'Connor R, Lesniak D, Lyons M, Woodard PK, Gropler RJ, Zheng J. Quantification of global myocardial oxygenation in humans: initial experience. *J Cardiovasc Magn Reson*. 2010;12:34.

201. Kuo L, Davis MJ, Chilian WM. Longitudinal Gradients for Endothelium-Dependent and -Independent Vascular Responses in the Coronary Microcirculation. *Circulation*. 1995;92:518–525.

202. Duling BR. Changes in Microvascular Diameter and Oxygen Tension Induced by Carbon Dioxide. *Circ Res*. 1973;32:370–376.

203. Chilian WM, Eastham CL, Marcus ML. Microvascular distribution of coronary vascular resistance in beating left ventricle. *Am J Physiol*. 1986;251:H779–788.

204. Chilian WM, Layne SM, Klausner EC, Eastham CL, Marcus ML. Redistribution of coronary microvascular resistance produced by dipyridamole. *Am J Physiol Heart Circ Physiol*. 1989;256:H383–H390.

205. Sueda S, Saeki H, Otani T, Ochi N, Kukita H, Kawada H, Matsuda S, Uraoka T. Investigation of the most effective provocation test for patients with coronary spastic angina: usefulness of accelerated exercise following hyperventilation. *Jpn Circ J*. 1999;63:85–90.

206. Cerqueira MD, Nguyen P, Staehr P, Underwood SR, Iskandrian AE. Effects of Age, Gender, Obesity, and Diabetes on the Efficacy and Safety of the Selective A2A Agonist Regadenoson Versus Adenosine in Myocardial Perfusion Imaging - Integrated ADVANCE-MPI Trial Results. *J Am Coll Cardiol Img*. 2008;1:307–316.

207. Hess A, Stiller D, Kaulisch T, Heil P, Scheich H. New insights into the hemodynamic blood oxygenation level-dependent response through combination of functional magnetic resonance imaging and optical recording in gerbil barrel cortex. *J Neurosci*. 2000;20:3328–3338.

208. Kim S-G, Ogawa S. Biophysical and physiological origins of blood oxygenation level-dependent fMRI signals. *J Cereb Blood Flow Metab*. 2012;32:1188–1206.

209. Uren NG, Camici PG, Melin JA, Bol A, de Bruyne B, Radvan J, Olivotto I, Rosen SD, Impallomeni M, Wijns W. Effect of aging on myocardial perfusion reserve. *J Nucl Med*. 1995;36:2032–2036.

210. Danad I, Uusitalo V, Kero T, Saraste A, Raijmakers PG, Lammertsma AA, Heymans MW, Kajander SA, Pietilä M, James S, Sörensen J, Knaapen P, Knuuti J. Quantitative Assessment of Myocardial Perfusion in the Detection of Significant Coronary Artery DiseaseCutoff Values and Diagnostic Accuracy of Quantitative [15O]H2O PET Imaging. *J Am Coll Cardiol*. 2014;64:1464–1475.

211. MacKay CM, Skow RJ, Tymko MM, Boulet LM, Davenport MH, Steinback CD, Ainslie PN, Lemieux CEM, Day TA. Central respiratory chemosensitivity and cerebrovascular CO2 reactivity: a rebreathing demonstration illustrating integrative human physiology. *Advances in Physiology Education*. 2016;40:79–92.

212. Demir OM, Alfakih K, Plein S. Current international guidelines for the investigation of patients with suspected coronary artery disease. *Eur Heart J Cardiovasc Imaging*. 2014;jeu168.

213. Germain P, El Ghannudi S, Jeung M-Y, Ohlmann P, Epailly E, Roy C, Gangi A. Native T1 Mapping of the Heart – A Pictorial Review. *Clin Med Insights Cardiol*. 2014;8:1–11.

214. Malek ŁA, Werys K, Kłopotowski M, Śpiewak M, Miłosz-Wieczorek B, Mazurkiewicz Ł, Petryka-Mazurkiewicz J, Marczak M, Witkowski A. Native T1-mapping for non-contrast assessment of myocardial fibrosis in patients with hypertrophic cardiomyopathy — comparison with late enhancement quantification. *Magn Reson Imaging*. 2015;33:718–724.

215. Kali A, Choi E-Y, Sharif B, Kim YJ, Bi X, Spottiswoode B, Cokic I, Yang H-J, Tighiouart M, Conte AH, Li D, Berman DS, Choi BW, Chang H-J, Dharmakumar R. Native T1 Mapping by 3-T CMR Imaging for Characterization of Chronic Myocardial Infarctions. *JACC Cardiovasc Imaging*. 2015;8:1019–1030.

216. Tonino PAL, Fearon WF, De Bruyne B, Oldroyd KG, Leesar MA, Ver Lee PN, MacCarthy PA, van't Veer M, Pijls NHJ. Angiographic Versus Functional Severity of Coronary Artery Stenoses in the FAME Study: Fractional Flow Reserve Versus Angiography in Multivessel Evaluation. *J Am Coll Cardiol*. 2010;55:2816–2821.

217. Teixeira T, Nadeshalingam G, Fischer K, Marcotte F, Friedrich MG. Breathing maneuvers as a coronary vasodilator for myocardial perfusion imaging. *J Magn Reson Imaging*. 2016;

9 Appendix 1: Scanning protocol for HVBH